AD-A075 277 BOEING WICHITA CO KS F/G 20/1
JET ENGINE CLASS 'C' TEST CELL EXHAUST SYSTEM PHASE. COANDA/REF--ETC(U)
MAY 79 R E BALLARD, D L ARMSTRON N00140-76-C-1229
UNCLASSIFIED D3-11580-1 NAEC-92-113 NL

| OF |
AD
A075277

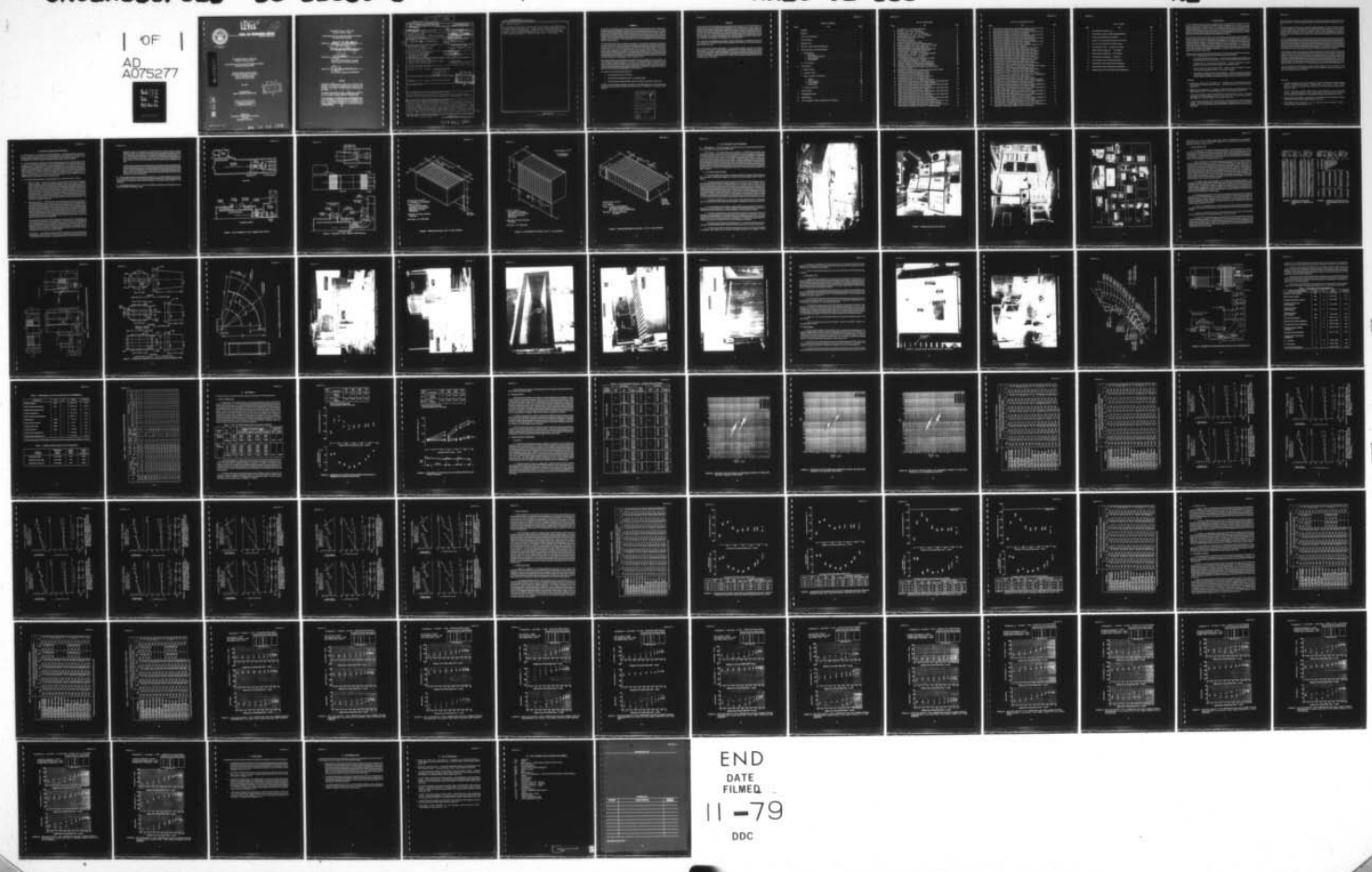

END
DATE FILMED
11-79
DDC

LEVEL II

(12)

NAVAL AIR ENGINEERING CENTER
LAKEHURST, N.J.
08733

REPORT NAEC-92-113

JET ENGINE CLASS "C" TEST CELL EXHAUST SYSTEM PHASE

COANDA/REFRACTION NOISE SUPPRESSION CONCEPT ADVANCED DEVELOPMENT

Propulsion Support Equipment Divison
Ground Support Equipment Department
Naval Air Engineering Center
Lakehurst, New Jersey 08733

May 1979

Technical Report
Airtask A3400000/051C/6WSL57001

Approved for Public Release
Distribution Unlimited

Prepared for:
Commander, Naval Air Systems Command
AIR-340E
Washington D.C. 20361

JET ENGINE CLASS "C" TEST CELL
EXHAUST SYSTEM PHASE

COANDA/REFRACTION NOISE SUPPRESSION CONCEPT
ADVANCED DEVELOPMENT

Prepared by: _____
R. E. Ballard, Boeing Wichita Company

_____
D. L. Armstrong, Boeing Wichita, Company

Reviewed by: _____
D. D. Croce
Advanced Technology Section, Propulsion
Support Equipment Requirements Branch

Approved by: _____
F. E. Evans
Ground Support Equipment Superintendent

NOTICE

12-5-77 AR

(18) NAEC-92

UNCLASSIFIED

SECURITY CLASSIFICATION OF THIS PAGE (When Data Entered)

(19) REPORT DOCUMENTATION PAGE	READ INSTRUCTIONS BEFORE COMPLETING FORM
1 REPORT NUMBER: NAEC-92-113 (7)	2. GOVT ACCESSION NO. (9)
3. RECIPIENT'S CATALOG NUMBER	
4. TITLE (and Subtitle) (6): Jet Engine Class "C" Test Cell Exhaust System Phase · Coanda/Refraction Noise Suppression Concept – Advanced Development ·	5. TYPE OF REPORT & PERIOD COVERED (13): Technical Report · Oct[illegible]976 — Jan[illegible]977
	6. PERFORMING ORG. REPORT NUMBER (14): D3-11580-1
7. AUTHOR(s) (10): R. E. Ballard and D. L. Armstrong	8. CONTRACT OR GRANT NUMBER(s) (15): N00140-76-C-1229
9. PERFORMING ORGANIZATION NAME AND ADDRESS: Boeing Wichita Company, Division of The Boeing Company, Wichita, Kansas 67210	10. PROGRAM ELEMENT, PROJECT, TASK AREA & WORK UNIT NUMBERS: AIRTASK A3400000/051C/6WS-L57001
11. CONTROLLING OFFICE NAME AND ADDRESS (11): Naval Air Systems Command (AIR-340E and AIR-55231B) Washington, D.C. 20361	12. REPORT DATE: May [illegible]979
	13. NUMBER OF PAGES: 81
14. MONITORING AGENCY NAME & ADDRESS (if different from Controlling Office): Naval Air Engineering Center, Ground Support Equipment Department (92623), Lakehurst, New Jersey 08733	15. SECURITY CLASS. (of this report): UNCLASSIFIED
	15a. DECLASSIFICATION DOWNGRADING SCHEDULE: N/A

16. DISTRIBUTION STATEMENT (of this Report)

Approved for public release; distribution unlimited.

(12) 89

17. DISTRIBUTION STATEMENT (of the abstract entered in Block 20, if different from Report)

Approved for public release; distribution unlimited.

DDC RECEIVED OCT 19 1979 A

18. SUPPLEMENTARY NOTES

19. KEY WORDS (Continue on reverse side if necessary and identify by block number)

Coanda jet deflection, ground run up noise suppression, jet engine exhaust noise, test cell acoustic enclosures, aerodynamics, thermodynamics, acoustics.

20. ABSTRACT (Continue on reverse side if necessary and identify by block number)

The successfully demonstrated Coanda/refraction air-cooled exhaust noise suppressor system is applied to the Navy requirement for an effective air-cooled retrofit configuration for the class "C" test cells (concrete enclosure). The technical approach consists of analytically sizing retrofit components to meet both acoustic and aerothermodynamic requirements and then testing at one-sixth scale using simulated afterburning engine exhaust to verify the design configuration. Model variations included exhaust stack height, exhaust stack inner

DD FORM 1 JAN 73 1473 EDITION OF 1 NOV 65 IS OBSOLETE

S/N 0102-LF-014-6601

UNCLASSIFIED

SECURITY CLASSIFICATION OF THIS PAGE (When Data Entered)

059 650

20. Abstract (cont'd.)

flow passage configurations (straight walls and diffuser) and removal of a concrete internal partition wall. Extensive data were recorded and analyzed to identify the aerothermodynamic trends related to these configuration changes. Results present recommendations for an air-cooled Coanda exhaust noise suppression system for retrofit of Navy class "C" test cells.

SUMMARY

A one-sixth scale model test program was conducted in the Boeing-Wichita Acoustic Arena for the purpose of developing a suitable configuration for retrofit of the Navy's existing concrete enclosure class "C" test cells with the air-cooled Coanda exhaust suppressor system. Acoustic and aerothermodynamic analysis and trade studies were accomplished based on techniques developed from previous Coanda suppressor model and full-scale testing to develop compatible inlet and exhaust flow areas with the required acoustic attenuation capability. The scale model testing was accomplished then to verify the aerothermodynamic analysis for the proposed retrofit configuration. Acoustic tests were not run due to the reliability of the acoustic analysis verified in previous testing.

The retrofit configuration was to be adapted to the existing "C" cell without the necessity of modifying the concrete enclosure. The only portion of the existing enclosure that caused concern was a wall that partitioned the old spray chamber from the exhaust chamber. With the existing water-cooling hardware removed, there remained only a nine- by nine-foot opening through which to run the Coanda surface. A three-ejector transition section replaced the old augmenter tube and spray apparatus and an 80-degree turn Coanda surface replaced the existing turning vanes. The existing water-cooled configuration did not provide a large enough secondary air inlet to supply an air-cooled system; therefore, a second air inlet was added just forward of the exhaust stack at the location of a removable roof panel. New acoustic panel designs were provided for the existing secondary air inlet passage and for the primary air inlet.

Flow dynamics testing was accomplished using nozzle flows that reproduced the flow conditions of a TF30-P-408 engine at military rated thrust and J79-GE-10/17/19 engines at MRT and at full afterburning. The model variations included the addition of an exhaust stack extension (needed to obtain the acoustic attenuation required), removal of the wall partition and changes to the exhaust stack inner sidewall angle from vertical. These sidewalls were tested at 0 degree (parallel) and 3.5 degrees and 7 degrees from vertical; the latter two forming a diffuser area progression in the exhaust stack.

The results of the scale model test indicated that:

- The wall partition need not be removed.
- Varying the stack sidewall angle was of no significant benefit.
- The exhaust stack extension actually created an increase in secondary air entrainment.

Therefore, the recommended configuration consisted of the proposed ejector and Coanda configuration, vertical exhaust stack sidewalls, exhaust stack extension and no modification to the existing concrete enclosure.

PREFACE

The development of the Navy Coanda exhaust suppressor system began in 1971 with the awarding of a feasibility study contract to Boeing-Wichita. Existing ground run-up suppressors for military afterburning engines were water-cooled units pumping up to 800 gallons of water per minute into the exhaust plume to cool the 3000°F exhaust gases and reduce the flow velocity. This resulted in excessive maintenance problems due to corrosion and a dirty, sooty exhaust and compounded operational and system complexity with controls, plumbing, pumps, etc. The Navy recognized the life-cycle cost advantages of an air-cooled system and that the Coanda effect may be the key to development of an operationally successful afterburning jet deflector since it requires no components of the suppressor be in the exhaust flow.

The success of the original feasibility study resulted in follow-on development work by Boeing-Wichita, for the Navy, culminating in a full-scale Coanda exhaust suppressor demonstration unit that was successfully demonstrated in late 1975.

Since that successful full-scale demonstration of a demountable suppressor, the Navy has awarded Boeing-Wichita a contract to develop specific adaptations of the Coanda suppressor for improved demountable configurations, retrofit of existing class "C" test cells and "hush-house" (aircraft enclosed) type ground run up suppressors. This document reports the results of the analysis and tests performed to develop a configuration for retrofit of existing Navy class "C" text cells with the air-cooled Coanda/refraction exhaust suppressor system components.

TABLE OF CONTENTS

LIST OF ILLUSTRATIONS

LIST OF ILLUSTRATIONS (CONT'D)

LIST OF TABLES

I. INTRODUCTION

In 1971, Boeing-Wichita was awarded a competitive Navy contract (N00156-72-C-1053) to study the feasibility of utilizing the Coanda effect as an afterburning jet exhaust deflector in an air-cooled ground run-up noise suppressor. Most U.S. Military ground run-up suppressors existing at that time were water-cooled, utilizing up to 800 gallons of water per minute to cool the higher than 3000°F afterburning exhaust plume. This resulted in corrosion problems, a dirty, sooty exhaust, and compounded operational and system complexity with controls, plumbing, pumps, diffusers and water supply. Military suppressor users preferred an air-cooled system but none had been developed that were operationally successful.

The 1971 Navy contract was the first of four Navy Coanda noise suppressor contracts awarded to Boeing-Wichita. The analysis and model tests accomplished under that contract (reported in Reference (a) proved the feasibility of using the Coanda effect for jet deflection and illustrated the advantageous noise directivity change due to refraction. The second contract (N00156-73-C-1974 awarded in 1973) made use of scale-model testing to develop a configuration suitable for full-scale demonstration. The results of that contract were reported in Reference (b). In 1974, the third Navy contract (N00156-74-C-1710) was awarded under which a full-scale Coanda suppressor demonstration unit was built and successfully demonstrated. The full-scale test program was reported in Reference (c). Additional model scale testing included in that program was reported in Reference (d).

The fourth Navy contract, under which the work described in this report was accomplished was awarded in 1976. This contract (N00140-76-C-1229) had the following multiple task objectives:

- Jet Engine Demountable Test Cell Phase – Improve the demountable test cell configuration by increasing exhaust muffler noise suppression to allow a reduction in exhaust system size and cost.
- Jet Engine Class "C" Test Cell Exhaust System Phase – Develop a configuration for retrofit of existing "C" test cells to the Coanda air-cooled exhaust suppressor system.
- Aircraft "Hush-House Exhaust System Phase – Develop a means of adapting the Coanda air-cooled exhaust suppressor system to a "hush-house" application.
- Coanda Exhaust Suppressor System Design Handbook – Develop the necessary procedures and parametric data necessary to provide a comprehensive outline of the method used to make a "first-cut" design of a Coanda exhaust suppressor system with a given set of exhaust conditions.

References

a. Ballard, R.E., Brees, D.W., and Sawdy, D.T., "Feasibility and Initial Model Studies of a Coanda/Refraction Type Noise Suppressor System," The Boeing Company, Wichita, Kansas, D3-9068, January 1973.

b. Ballard, R.E., and Armstrong, D.L., "Configuration Scale Model Studies of a Coanda/Refraction Type Noise Suppressor System," The Boeing Company, Wichita, Kansas, D3-9258, October 1973.

c. "Test Cell Experimental Program Coanda/Refraction Noise Suppression Concept – Advanced Development," Final Technical Report for Navy Contract N00156-74-C-1710, Navy Document Number NAEC-GSED-97, The Boeing Company, Wichita, Kansas, March 1976.

d. "Aircraft System One-Sixth Scale Model Studies, Coanda/Refraction Noise Suppression Concept – Advanced Development," Final Technical Report for Scale Model Portion of Navy Contract N00156-74-C-1710, Navy Document Number NAEC-GSED-98, The Boeing Company, Wichita, Kansas, March 1976.

Each of these tasks are reported in separate final reports. The task results reported in this document are for the jet engine class "C" test cell exhaust system phase. The other tasks are reported in References (e), (f) and (g).

The primary objective of this task was to develop a suitable configuration for retrofit of the Navy's existing concrete enclosure class "C" test cells with the air-cooled Coanda exhaust suppressor system. This was to be accomplished with analytical studies and verified with one-sixth scale model tests. In an attempt to produce a retrofit configuration that is cost effective, a ground rule was established that the concrete enclosure could not be revised with the exception of the removal of those elements that were intended to be removable.

The retrofit configuration that was tested resulted from acoustic and aerothermodynamic analysis and trade studies to develop compatible inlet and exhaust flow areas with the required acoustic attenuation capability. The analyses performed are not presented in this test report but generally follow the outline presented in the Reference (g) design handbook. It was decided that the acoustic analysis necessary to size and locate the acoustic treatment in the exhaust stack and secondary air inlets would be sufficient to allow the model testing to evaluate only the aerodynamic characteristics of the configuration. This confidence in the acoustic analysis was gained from previous scale model and full-scale test results (References (a) through (g)).

The configuration variations that were evaluated included exhaust stack inner wall divergence, exhaust stack height and removal of the partition between the old spray chamber and exhaust chamber. The stack wall divergence variation was to determine if secondary air entrainment could be increased by exhaust stack divergence. The stack height variation was to prove no detrimental effects of adding a stack extension since the acoustic analysis indicated the additional lining area was required to meet acoustic goals. It was felt that the partition may cause some problem with the secondary airflow requirement because of the small existing opening through it. The model tests included the simulation of the TF30-P-408 engine operating at military rated thrust (MRT) and of the J79-GE-10/17/19 engines operating at both MRT and full afterburning (A/B).

This study resulted in the recommended production retrofit configuration outlined in Section II of this document and presented on the configuration control drawings (Reference (h)) that were supplied to the Naval Air Engineering Center in March 1977.

References:

e. "Jet Engine Demountable Test Cell Exhaust System Phase, Coanda/Refraction Noise Suppression Concept – Advanced Development," Technical Report for a portion of Navy Contract N00140-76-C-1229, Navy Document Number NAEC-92-112, the Boeing Wichita Company, Wichita, Kansas, April 1979.

f. "Aircraft Hush-House Exhaust System Phase, Coanda/Refraction Noise Suppression Concept – Advanced Development, Final Technical Report for Navy Contract N00140-76-C-1229, Navy Document Number NAEC-92-114, Boeing Wichita Company, Wichita, Kansas, June 1979.

g. "Design Configuration Handbook, Test Cell System, Coanda/Refraction Noise Suppression Concept," Navy Document Number NAEC Design Data 92-136, April 1979.

h. NAEC-GSED drawing 690AS200, "'C' Cell Installation Noise Suppressor System – Coanda/Refraction," dated January 20, 1977.

II. RETROFIT CONFIGURATION DEFINITION

A. The Navy class "C" test cells have three enclosure sections: the test stand enclosure, including the primary air intake; the spray chamber, including the augmenter tubes and secondary air intake; and the exhaust chamber, including turning vanes and exhaust stack. Figure 1 illustrates the standard class "C" test cell construction and Figure 2 shows the proposed air-cooled Coanda retrofit configuration.

B. The aerothermodynamic properties of the Coanda exhaust suppressor system, as proposed for retrofit of the class "C" test cells were investigated in a one-sixth scale model test. For a realistic evaluation of the aerothermodynamic characteristics of the exhaust suppressor system, the geometry of the acoustic components of the suppressor had to be included in the model design. Acoustic analyses were performed, based on the procedure outlined in Reference (g) and experience from the full-scale Navy demonstrator testing, Reference (c), to determine the location and design of the acoustic components. Trade studies were made to ensure that the flow areas for the acoustic components were compatible with the aerothermodynamic design. For the aerothermodynamic model testing, all acoustic elements were made ineffective (hard wall face sheets rather than perforated plate).

C. The acoustic component designs are discussed below with all dimensions given in full scale.

- Primary Air Intake – The primary air intake is not a component of the exhaust suppressor; however, its design is included to complete the suppressor system retrofit design. It is proposed that this design be used only in the event that the existing primary intake acoustic panels do not perform up to the level of the retrofitted secondary air intakes and exhaust stack, thus causing the primary air intake to become the dominant noise source. The design is shown on Figure 3. The aft wall of the primary air intake shown replaces the original masonry wall between the primary and secondary air intakes. This wall had to be removed to replace the secondary air intake acoustic panels (see Figure 2). The proposed lining design for the acoustic panels consists of a six-inch thickness of 3 pcf Johns-Manville 1000 series Spin-Glas with a 50 percent open area perforated sheet facing. The splitters have this on both sides separated by a solid sheet metal septum. The outer shell is quarter-inch sheet steel.

- Secondary Air Intakes – The secondary air intake was divided into a forward and an aft section to provide the necessary flow area. Since the Coanda retrofit configuration is an air-cooled system, it requires more entrained secondary airflow than the previous water injected configuration. The aft secondary air intake was added by removal of the access panel in the roof of the exhaust chamber (just forward of the exhaust stack). A modular section of acoustic panel was placed on the resulting opening (see Figure 2). The design of this modular section is shown on Figure 4. The proposed design for the aft secondary air inlet acoustic panels consists of six inches of 3 pcf Johns-Manville 1000 series Spin-Glas with 50 percent open area perforated face sheet on each side of a solid sheet metal septum. There are 17 air passages that are 3.88 inches wide and 9 feet, 10 inches long resulting in a flow area of 54.05 square feet.

  The revised forward secondary air intake configuration is shown on Figure 5. The acoustic panels are of the same construction as for the aft secondary air intake. There are 15 flow passages that are 5.2 inches wide and 5 feet long, resulting in a flow area of 32.50 square feet. These acoustic panels replace the existing acoustic panels in the original secondary air intake (see Figure 1). It is necessary to remove the masonry wall between the original primary and secondary intakes to replace these acoustic panels. If it is not deemed necessary to revise the primary intake, as shown previously, then the masonry wall should be replaced.

- Exhaust Stack – The proposed exhaust stack retrofit configuration begins with the removal of the existing acoustic baffles (see Figure 1). The forward and aft walls of the exhaust stack are covered with a one-quarter inch thick sheet of A36 steel attached with two-inch standoffs to keep the high

temperature exhaust from damaging the concrete stack walls. Acoustic panels are inserted between the forward and aft walls to form exhaust stack internal sidewalls (see Figure 2, Section A-A). These panels may be inclined to form a divergent area progression in the exhaust stack. The angle of this internal wall is developed in the model testing. These sidewall acoustic panels are 9 feet, 10 inches wide by 21 feet, 6 inches long. The proposed lining is 18-inch thickness of 3 pcf Johns-Manville 1000 series Spin-Glas material behind a 50 percent open area perforated face sheet.

Acoustic analysis indicates that the sidewall panels do not provide enough acoustic lining area to produce the required suppression. An acoustic exhaust stack extension (see Figure 2) is proposed to obtain the required acoustic levels. The internal dimensions of this extension is 9 feet, 10 inches deep by 12 feet wide. The extension adds 12 feet of height to the exhaust stack (total height is then 55 feet, 6 inches). All four sides of the stack extension are lined with the same 18-inch thick lining design as the internal stack sidewalls.

D. The flow transition ejectors and Coanda surface used for the "C" cell retrofit configuration are the same as those developed in the previous demountable test cell testing, Reference (e), with the exception that the Coanda surface was lengthened to approximately 80 degrees of turning angle to match the internal "C" cell dimensions.

E. A more detailed description of the "C" cell retrofit configuration may be found on the configuration control drawing (Reference (h)) provided to NAEC.

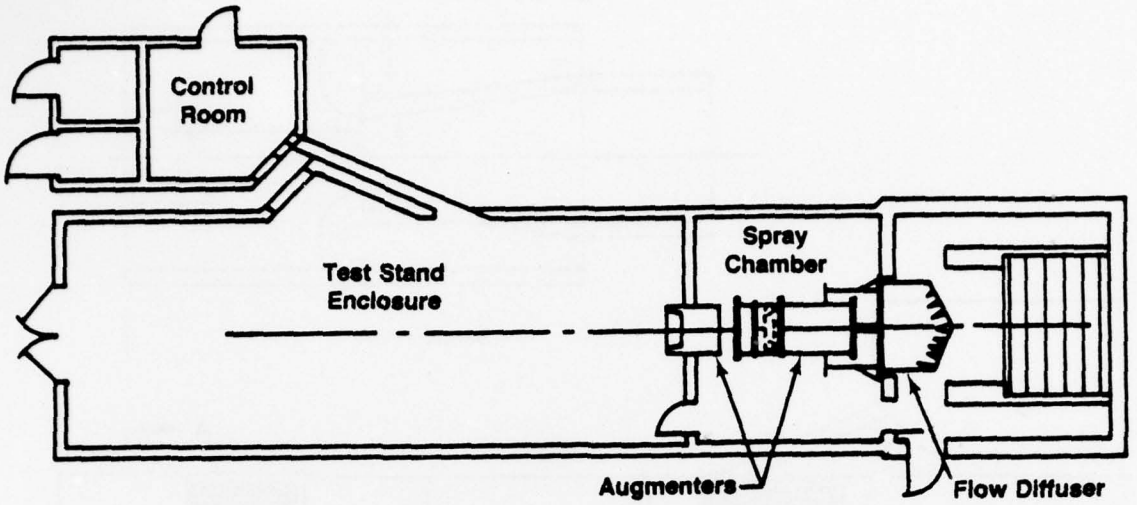

Floor Plan

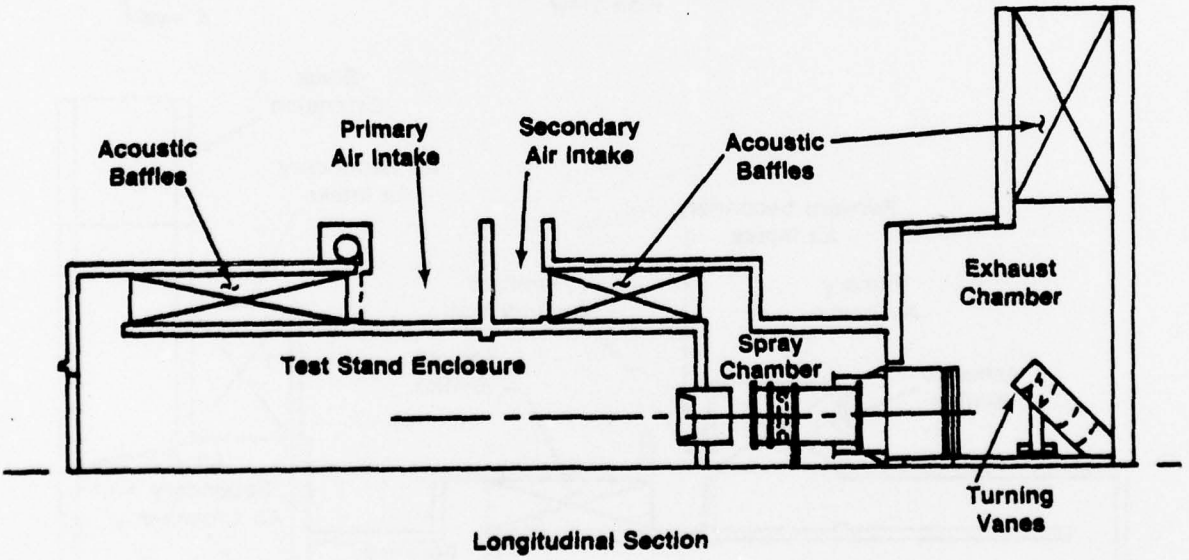

Longitudinal Section

FIGURE 1: NAVY STANDARD "C" CELL TURBOJET TEST FACILITY

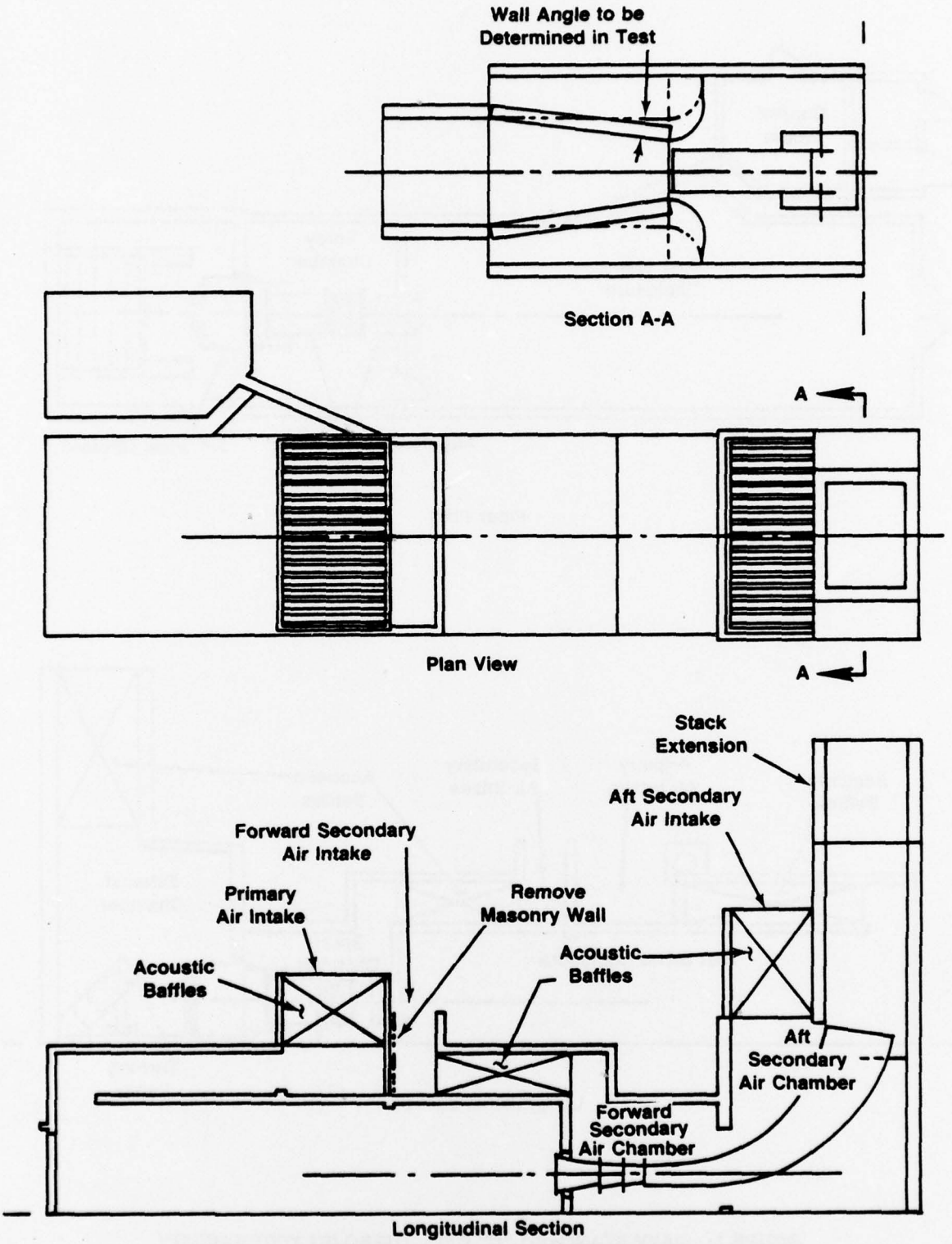

FIGURE 2: PROPOSED "C" CELL RETROFIT CONFIGURATION

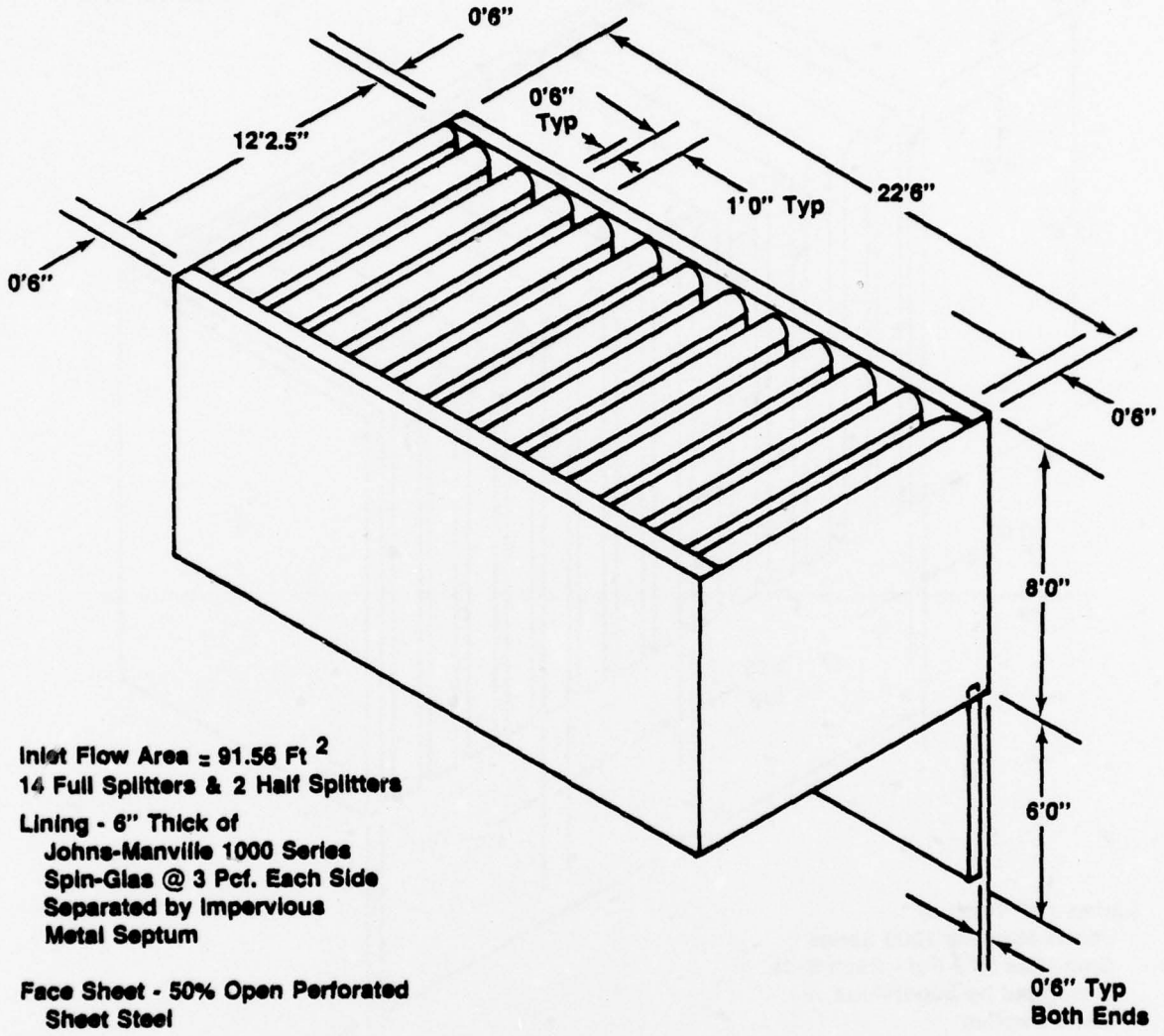

Inlet Flow Area = 91.56 Ft ^{2}
14 Full Splitters & 2 Half Splitters

Lining - 6" Thick of
Johns-Manville 1000 Series
Spin-Glas @ 3 Pcf. Each Side
Separated by Impervious
Metal Septum

Face Sheet - 50% Open Perforated
Sheet Steel

Outer Shell - 1/4 in. Sheet Steel

FIGURE 3: PRIMARY AIR INTAKE - NAVY "C" CELL RETROFIT

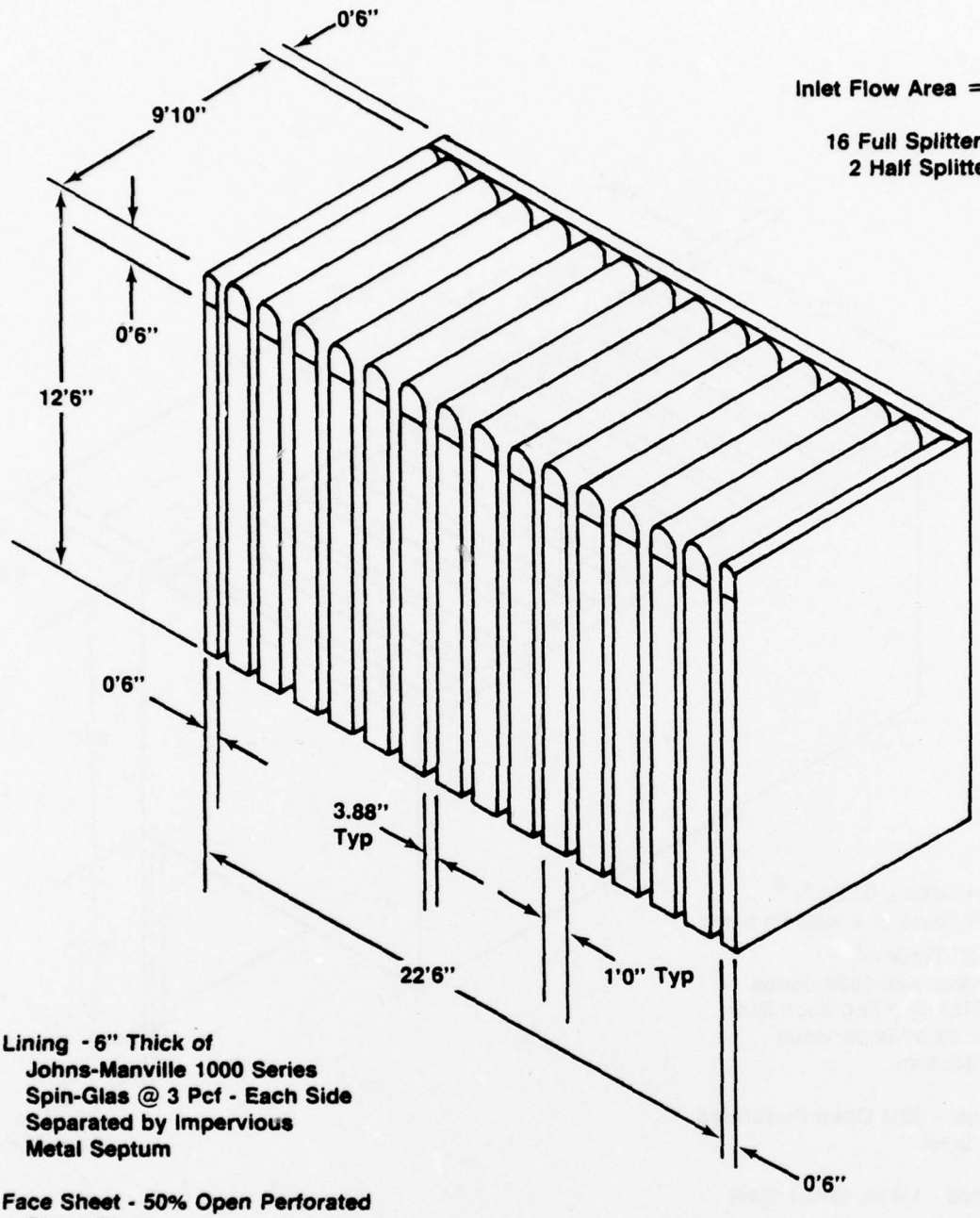

FIGURE 4: AFT SECONDARY AIR INTAKE - NAVY "C" CELL RETROFIT

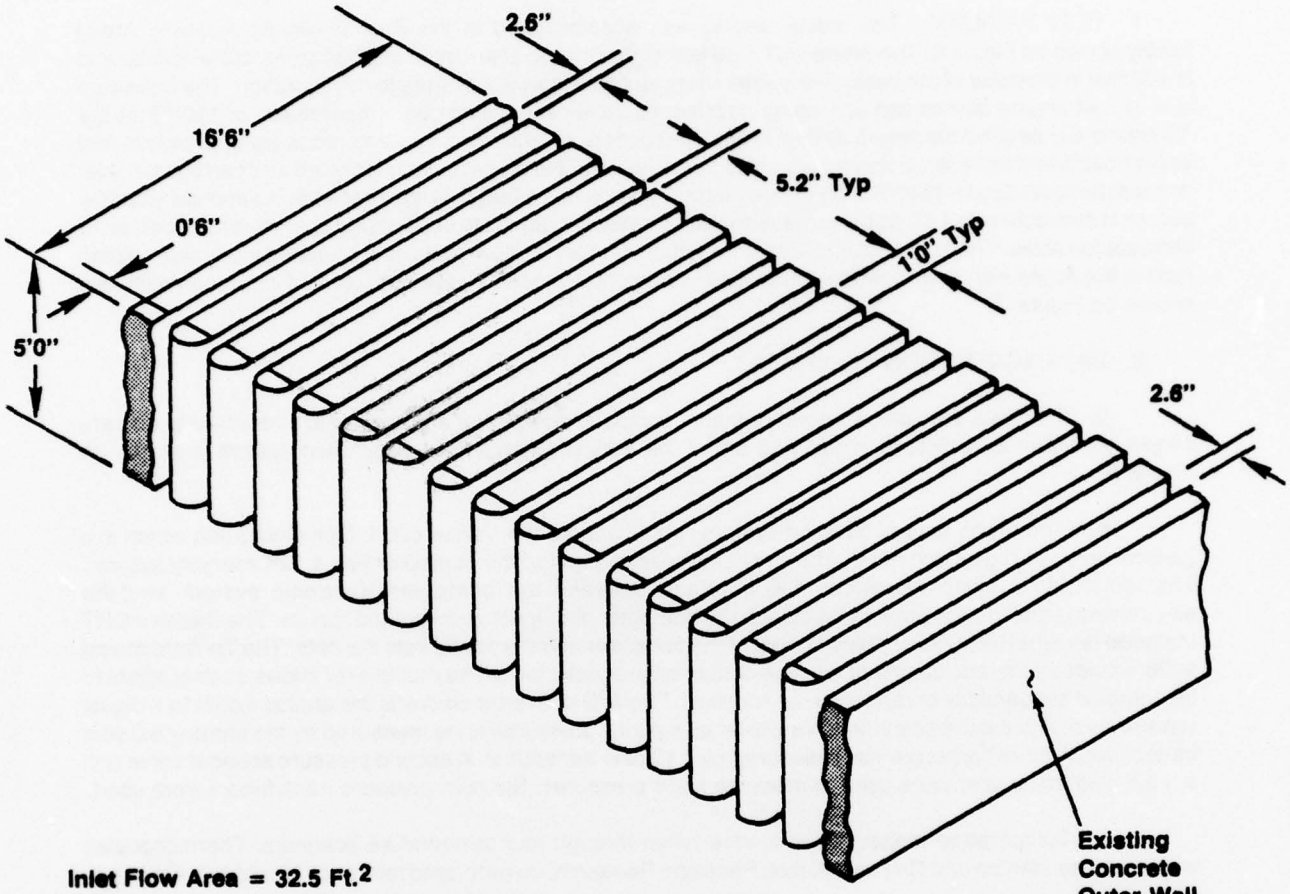

Inlet Flow Area = 32.5 Ft.^{2}

15 Full Splitters

Lining – 6"-Thick of Johns-Manville
1000 Series Spin-Glas @ 3 pcf –
Each Side of Impervious Metal Septum

Face Sheet – 50% Open Perforated
Sheet Steel

FIGURE 5: FORWARD SECONDARY AIR INTAKE – NAVY "C" CELL RETROFIT

III. TEST EQUIPMENT AND PROCEDURES

A. Test Equipment. The following paragraphs describe the test facility, the data acquisition equipment and the test model, including the instrumentation used.

1. TEST FACILITY. The model testing was accomplished in the Boeing-Wichita Acoustic Arena facility shown on Figure 6. The Arena wall is 16 feet high, inclined at an angle of 30 degrees to the vertical and is 100 feet in diameter at the base. The burner (hot gas generator) is a two-stage configuration. The first stage is a J47 jet engine burner can and spray nozzles, capable of reaching gas temperatures of 1500°F at the 15-pound per second maximum airflow rate. The second, or afterburning stage, consists of a central fuel spray nozzle and eight radial spray bars and a flame holder. This stage is water jacketed and can boost the jet exhaust temperature to 3300°F. The primary airflow source has a 300 psia line pressure. A secondary airflow source is available with a 60 psia line pressure with a maximum flow rate of 40 pounds per second of cold air to simulate fan flows. The burner control instrumentation, fuel and airflow controls are housed in a small building next to the Arena with a window for visual observation of the model. These controls and instrumentation are shown on Figure 7.

2. DATA ACQUISITION EQUIPMENT.

a. The data acquisition instrumentation, computer and printer are housed at a remote site and are shown on Figure 8. A pictorial block diagram of the Acoustic Arena data acquisition system is shown on Figure 9.

b. The arena data acquisition system is built around the Varian 620/L Mini-Computer, which is a general purpose digital computer. The central processing unit of the computer has a 12K memory system. The input/output system provides the interface between the computer electronic system and the electromechanical devices that input data to the computer or output the computed results. The Beehive CRT (cathode ray tube) terminal enables control of the computer and the printer lists the data. The Tri-Data model 4036 provides program loading or storage of data on magnetic tape. The multiplexer allows each channel to be sampled sequentially or randomly, as required. The A/D converter converts the analog signal to a digital voltage level. A pressure scanner valve allows all the total pressures to be measured by the same $\pm$5.0 psid transducer. Ambient pressure was measured by a 15 psia transducer. A second pressure scanner valve and a $\pm$2.5 psid transducer were used to measure static pressures. Statham pressure transducers were used.

c. Temperature measurements were taken through four temperature scanners. Thermocouples were Iron-Constantan and Cromel-Alumel; Pace and Research, Incorporated reference junctions were used.

d. For both temperatures and pressures, signal processing was accomplished by use of a B & F Instruments, Inc. signal conditioner and a Dynamics amplifier. The conditioned signal was connected to a monitor panel which permitted manual monitoring capability as well as calibration monitoring.

e. The fuel flow as measured by a 1 gpm turbine type flow transducer in the primary fuel line and a 5 gpm turbine type flow transducer in the afterburner fuel line. The signal was conditioned by a Cox signal conditioner and the signal sent to the monitor panel. The flow rates were also displayed on digital voltmeters in the test control room. The monitor panel inputs were paralleled to the multiplexer input panel where further monitoring was possible. The signals then went into the multiplexer for processing.

f. No acoustic data were recorded during the testing of the "C" cell retrofit configuration; therefore, a discussion of the acoustic data acquisition equipment will not be included but may be found in Reference (e).

g. The performance program provided automatic data acquisition. Once the program was started, all parameters were sampled and the scanners automatically controlled by the computer. The raw

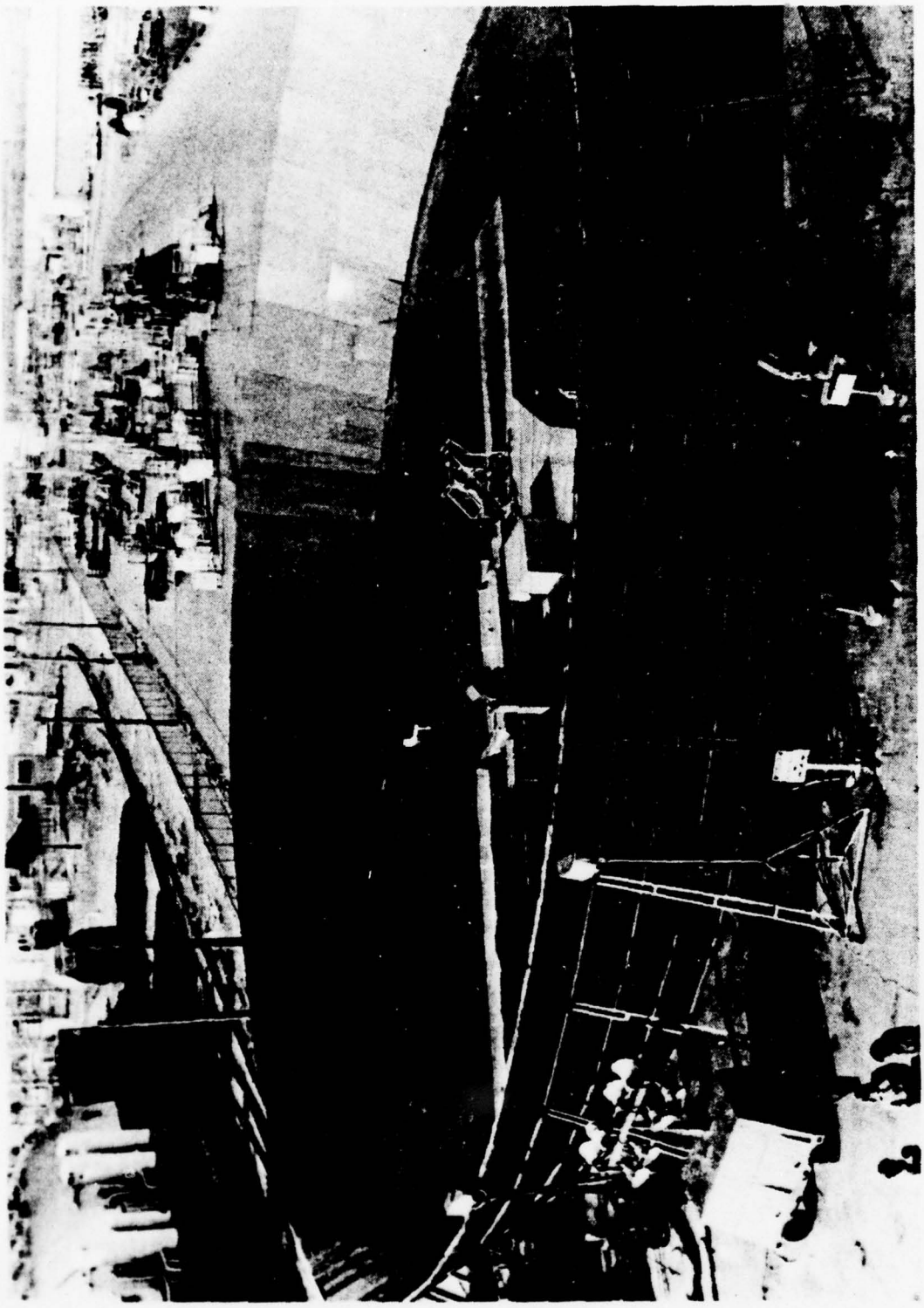

FIGURE 6: BOEING-WICHITA ACOUSTIC ARENA TEST FACILITY

FIGURE 7: BURNER AND AIRFLOW CONTROLS

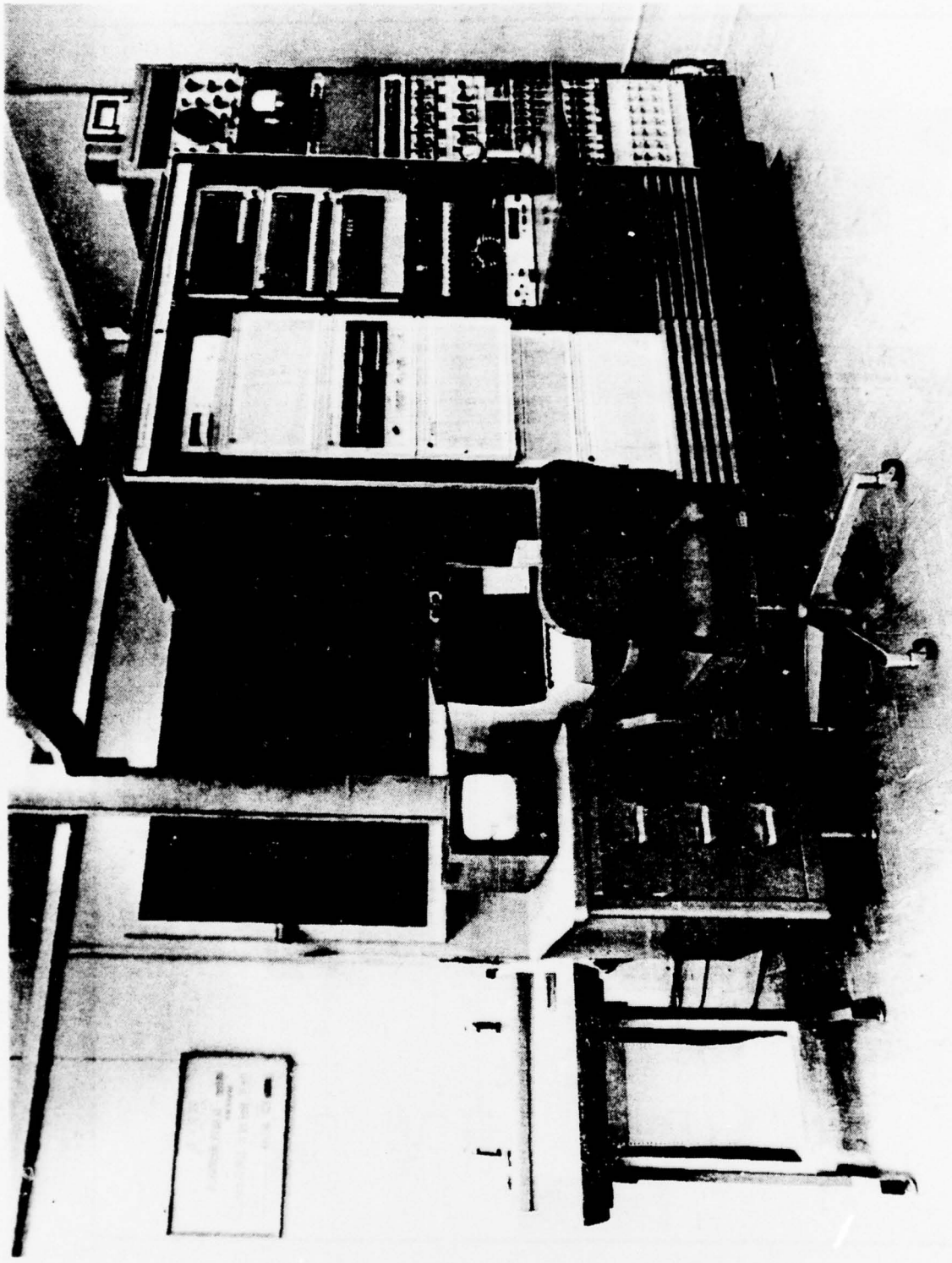

FIGURE 8: DATA ACQUISITION EQUIPMENT

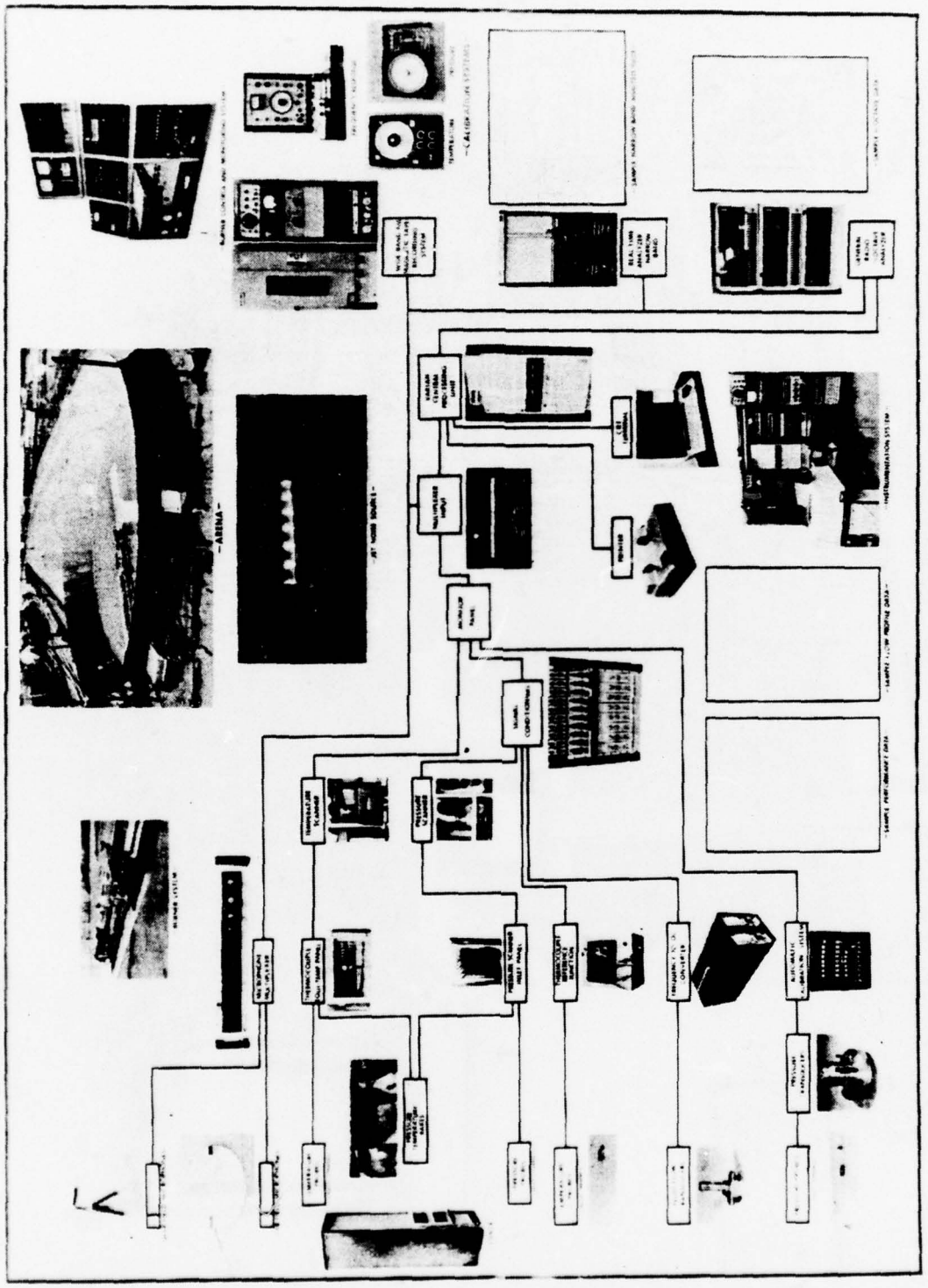

FIGURE 9: ACOUSTIC ARENA DATA ACQUISITION SYSTEM

performance data, in the form of digital voltages, were converted to engineering units and calculation performed in the CPU. The data were then listed in tabulated form. Typical sample performance data output formats are illustrated on Figures 10 and 11.

3. MODEL DESCRIPTION.

a. The Navy class "C" test cells have three enclosure sections: the test stand enclosure, including the primary air intake; the spray chamber, including the augmenter tubes and secondary inlet; and the exhaust chamber, including turning vanes and exhaust stack. Figure 1 illustrates the standard class "C" test cell construction. The aft two enclosures with the proposed Coanda retrofit configuration was simulated in these model tests. The test stand enclosure and primary air intake were not included because the test facility does not have the capability of simulating the engine inlet.

b. Figure 12 presents the "C" cell retrofit configuration of the secondary air inlet, spray chamber and exhaust chamber. The dimensions shown are for the full-scale configuration. The test model was built to simulate the internal lines of the enclosures shown on Figure 12 with dimensions one-sixth those shown. The aft secondary air chamber and exhaust stack were fabricated of steel sheet and angle. The secondary air intakes and forward secondary air chamber (see Figure 2) were fabricated of plywood. The secondary air intake panels were built to one-sixth scale of the configurations shown on Figures 4 and 5. The panels and exterior shell were fabricated of wood. The partition between the forward and aft secondary air chambers was made removable for testing to determine if this wall needs to be removed in the retrofit configuration. The concern was that the 9-foot square (full-scale) opening may not be large enough to disallow any detrimental pressure differential between the two chambers. All walls and acoustic panels were simulated in hard wall (no acoustic treatment) as no acoustic testing was planned.

c. The model exhaust stack configuration was the same as that described in Section II. The simulated stack sidewall acoustic panels were designed to be rotated about the line where their inner surface intersects the top of the existing exhaust stack. These walls are rotated to provide test conditions with 0-degree (vertical), 3.5-degree and 7-degree wall angles. The conditions with the walls inclined creates a throat in the airflow passage near the end of the Coanda surface. The area progression beyond that point is divergent. It was anticipated that the divergent exhaust stack may enhance secondary air pumping, which is beneficial both acoustically and for system cooling.

d. The transition ejector set and Coanda surface models were the same ones used for the previous demountable test cell testing (Reference e). A dimensional schematic of the three model scale ejectors is presented on Figure 13. These model scale ejectors are fabricated from .090 thick stainless steel. The Coanda surface had an additional 15-degree turn extension added to it (total of 80-degree turn) to reach the height of the ceiling in the "C" cell enclosure at the exhaust stack forward wall. A dimensional drawing of the Coanda surface is presented on Figure 14.

e. Figure 15 is a photograph of the "C" cell retrofit model (without the exhaust stack extension) as it was installed in the Acoustic Arena Test Facility. Figure 16 shows the model with the exhaust stack extension in place.

f. Figure 17 is a photograph looking down into the forward secondary air intake. The leading edges of the horizontal acoustic panels may be seen along the aft side of the intake.

g. Figure 18 is a photograph from above (looking aft) which shows the aft secondary air intake and exhaust stack (without extension). The leading edges of the vertical acoustic panels in this air intake are shown. The instrumentation rake that measured the static pressures within each intake passage is shown installed across the aft secondary air intake. The instrumentation rake that measured the total pressure and temperature at the exhaust stack exit is also shown installed. Figure 19 is another photograph showing the exhaust stack exit flow rake installed.

1/6 SCALE NAVY COANDA C-CELL
J-79 A/B-SHORT STACK / 7 0 DEG DIF WALL
RUN NO 90 CONF NO 15
PA(PSIA) 14 166 TA(DEGF) 20 23
TWI(DEGF) 48 82 TWO(DEGF) 87 60
PS1(PSIG) 51 49 DP1(PSID) 26 90
WFP(LB/SEC) 0664 WFAB(LB/SEC) 2532
TNE(DEGF) 3258 4 WAF(LB/SEC) 4 887

DATE 10 JAN77
TIME 16 30 10
RAKE POS INLET1/EXIT 1
PTN(PSIA) 48 799
QPMW(QPM) 81 610
FT1(DEGF) 38 16
TBP(DEGF) 1000 3
NPR 2 8000

LOC	PRESS (PSIA)	LOC	TEMP (DEGF)	LOC	PRESS (PSIA)	LOC	TEMP (DEGF)
01EJ01	13 620	01EJ01	75 0	41NZ01	14 166	SPARE	25 9
02EJ02	13 461	02EJ02	48 3	42NZ02	13 876	65TNE1	17 2
03EJ03	14 092	03EJ03	531 5	43NZ03	14 166	BADRS	-491 1
04EJ04	13 854	04EJ04	81 6	44NZ04	14 166	SPARE	-494 5
05EJ05	13 479	05EJ05	259 7	SPARE	14 165	BADRS	-492 0
06EJ06	13 625	06EJ06	108 2	SPARE	14 166	25SF01	213 1
07EJ07	14 126	07EJ07	619 0	SPARE	14 166	26SF02	413 3
08EJ08	13 945	08EJ08	188 0	SPARE	14 166	27SF03	431 9
09EJ09	14 247	09EJ09	705 3	45IR01	14 015	28SF04	347 3
10EJ10	13 859	10EJ10	209 0	46IR02	14 053	29SF05	1 5
11EJ11	13 472	11EJ11	864 4	47IR03	14 061	30SF06	3 1
12EJ12	14 025	12EJ12	305 1	48IR04	14 055	31SS01	199 0
SPARE	14 166	2JEJ13	63 9	49IR05	14 057	32SS02	441 6
SPARE	14 166	24EJ14	183 0	50IR06	14 074	33SS03	431 9
13CD01	13 740	SPARE	23 0	51IR07	14 048	34SS04	405 0
14CD02	13 652	SPARE	23 0	52IR08	14 067	35SS05	3 1
15CD03	12 846	SPARE	23 0	53IR09	14 058	36SS06	4 7
16CD04	12 982	SPARE	23 1	54IR10	14 066	37SR01	549 2
17CD05	12 729	13CD01	237 3	55IR11	14 059	38SR02	573 5
18CD06	12 711	14CD02	653 8	56IR12	14 067	39SR03	566 2
19CD07	12 818	15CD03	823 7	57IR13	14 069	40SR04	529 2
20CD08	12 994	16CD04	683 8	58IR14	14 064	41SR05	5 5
21CD09	13 178	17CD05	499 1	59IR15	14 069	42SR06	6 2
22CD10	13 595	18CD06	448 5	60IR16	14 060	SPARE	26 6
SPARE	14 165	19CD07	456 1	61IR17	14 078	SPARE	25 9
SPARE	14 165	20CD08	461 7	SPARE	14 166	SPARE	26 6
23EN01	14 064	21CD09	465 3	SPARE	14 165	SPARE	26 6
24EN02	14 062	22CD10	183 7	62AI01	14 125	SPARE	25 9
25EN03	14 008	SPARE	23 8	63AI02	14 115	CALSU8	901 5
26EN04	14 004	SPARE	23 8	64AI03	14 093	51ER01	750 2
SPARE	14 166	43EN01	140 9	65AI04	14 101	52ER02	772 8
PREF	15 150	44EN02	550 8	66AI05	14 005	53ER03	760 4
27ER01	15 020	45EN03	20 8	67AI06	14 121	54ER04	769 1
28ER02	15 122	46EN04	28 3	68AI07	14 003	55ER05	769 1
29ER03	15 136	47EN05	185 8	69AI08	14 123	56ER06	756 8
30ER04	15 094	48EN06	183 6	70AI09	14 091	57ER07	748 8
31ER05	15 015	49EN07	204 7	71AI10	14 122	58ER08	734 9
32ER06	14 907	SPARE	23 8	72AI11	14 007	59ER09	696 9
33ER07	14 743	SPARE	23 1	73AI12	14 120	60ER10	649 3
34ER08	14 540	SPARE	23 8	74AI13	14 079	61ER11	591 2
35ER09	14 308	SPARE	23 8	75AI14	14 119	SPARE	28 2
36ER10	14 263	SPARE	23 8	76AI15	14 007	SPARE	21 9
37ER11	14 227	SPARE	23 8	77AI16	14 124	SPARE	26 6
SPARE	14 159	SPARE	23 1	SPARE	14 166	SPARE	26 6
SPARE	14 165	TREF	999 6	SPARE	14 166	TREF	1001 8
SPARE	14 165	SPARE	8	PREF	15 157	SPARE	8

FIGURE 10: EXAMPLE OF TABULATED PRESSURE AND TEMPERATURE DATA

1/6 SCALE NAVY COANDA C-CELL
J-79 A/B-SHORT STACK / 7 0 DEG DIF WALL
RUN NO 90 CONF NO 15
PA(PSIA) 14 166 TA(DEGF) 20 23
TWI(DEGF) 48 82 TWO(DEGF) 87 60
PS1(PSIG) 51 49 DP1(PSID) 26 90
WFP(LB/SEC) 0664 WFAB(LB/SEC) 2532
TNE(DEGF) 3258 4 WAF(LB/SEC) 4 887

DATE 10 JAN77
TIME 16 30 10
RAKE POS INLET1/EXIT 1
PTN(PSIA) 48 799
QPMW(QPM) 81 610
FT1(DEGF) 38 16
TBP(DEGF) 1000 3
NPR 2 8000

EXIT RAKE VELOCITY PROFILE

LOC	(FT/SEC)	0 200 0 400 0 600 0 800 0 1000 0
01	490 9	XXXXXXXXXXXXXXXXXXXXXXXXXXXX
02	523 1	XXXXXXXXXXXXXXXXXXXXXXXXXXXXX
03	524 3	XXXXXXXXXXXXXXXXXXXXXXXXXXXXX
04	515 8	XXXXXXXXXXXXXXXXXXXXXXXXXXXXX
05	493 4	XXXXXXXXXXXXXXXXXXXXXXXXXX
06	459 7	XXXXXXXXXXXXXXXXXXXXXXXX
07	405 7	XXXXXXXXXXXXXXXXXXXX
08	326 2	XXXXXXXXXXXXXXXX
09	243 9	XXXXXXXXXXXX
10	161 4	XXXXXXXX
11	124 3	XXXXXX

SECONDARY AFT AIR INLET FLOW PARAMETERS

LOC	PS (PSIA)	MACH NO	TT (DEGF)	VP (FT/SEC)	WAF (LB/SEC)
01	14 015	1238	20 2	132 98	9801
02	14 053	1078	20 2	114 86	7626
03	14 061	1038	20 2	110 50	7340
04	14 055	1060	20 2	113 75	7554
05	14 057	1051	20 2	112 76	7488
06	14 074	0962	20 2	103 27	6864
07	14 048	1093	20 2	117 28	7785
08	14 067	1000	20 2	107 27	7128
09	14 058	1044	20 2	112 01	7439
10	14 066	1007	20 2	108 05	7179
11	14 059	1040	20 2	111 63	7415
12	14 067	1001	20 2	107 40	7136
13	14 069	0987	20 2	105 96	7041
14	14 064	1014	20 2	108 83	7238
15	14 069	0992	20 2	106 48	7076
16	14 068	0993	20 2	106 62	7085
17	14 078	0940	20 2	100 94	6711
				TOTAL FLOW	12 4985

SECONDARY FORWARD AIR INLET FLOW PARAMETERS

LOC	PS (PSIA)	MACH NO	TT (DEGF)	VP (FT/SEC)	WAF (LB/SEC)
01	14 128	0681	20 2	73 17	3264
02	14 097	0831	20 2	89 25	8065
03	14 103	0788	20 2	84 64	7650
04	14 101	0786	20 2	84 48	7626
05	14 106	0768	20 2	82 50	7456
06	14 104	0784	20 2	84 18	7600
07	14 099	0812	20 2	87 13	7877
08	14 105	0773	20 2	83 02	7506
				TOTAL FLOW	5 7056

FIGURE 11: EXAMPLE OF EXHAUST VELOCITY AND SECONDARY AIR INLET FLOW DATA

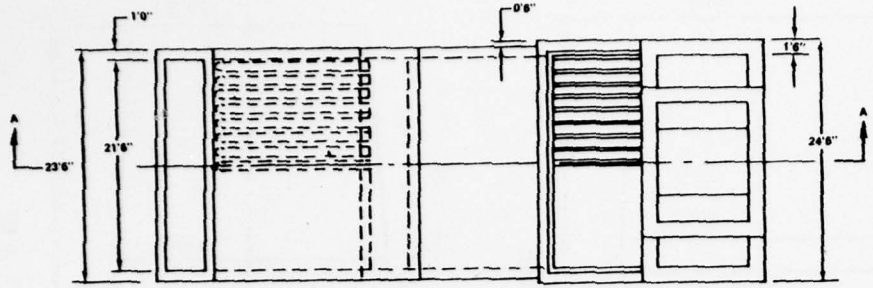

Plan View

Note: Dimensions are Full Scale

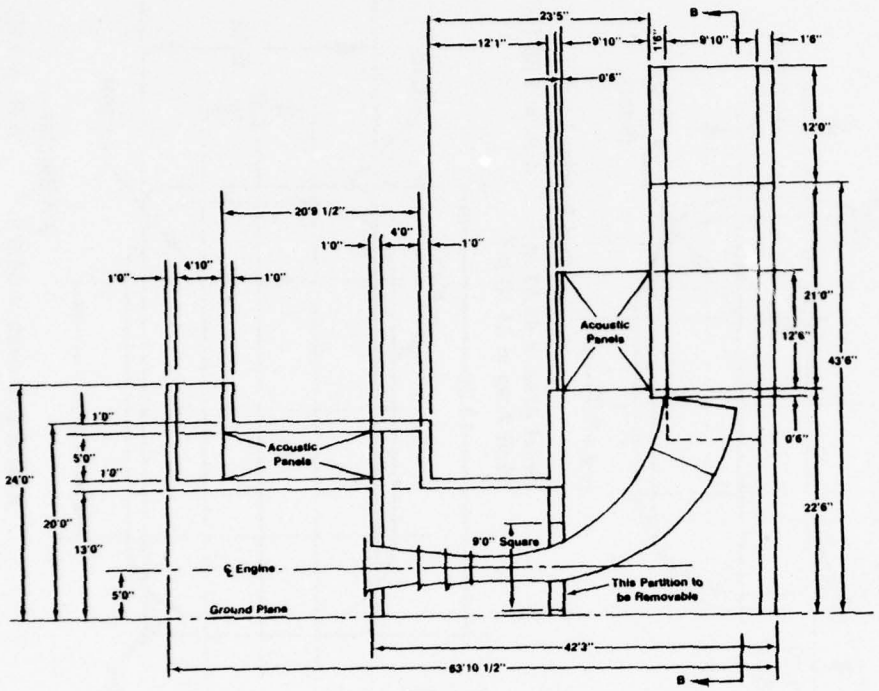

Section A = A

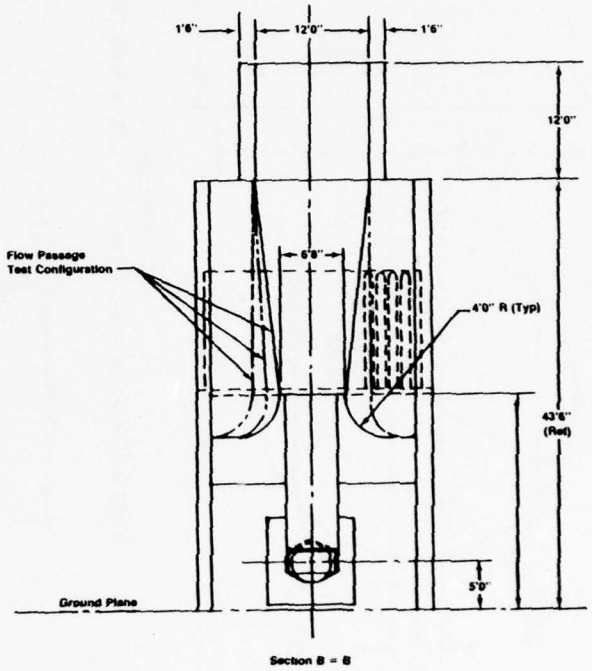

Section B = B

FIGURE 12: RETROFIT CONFIGURATION TO BE TESTED IN MODEL SCALE

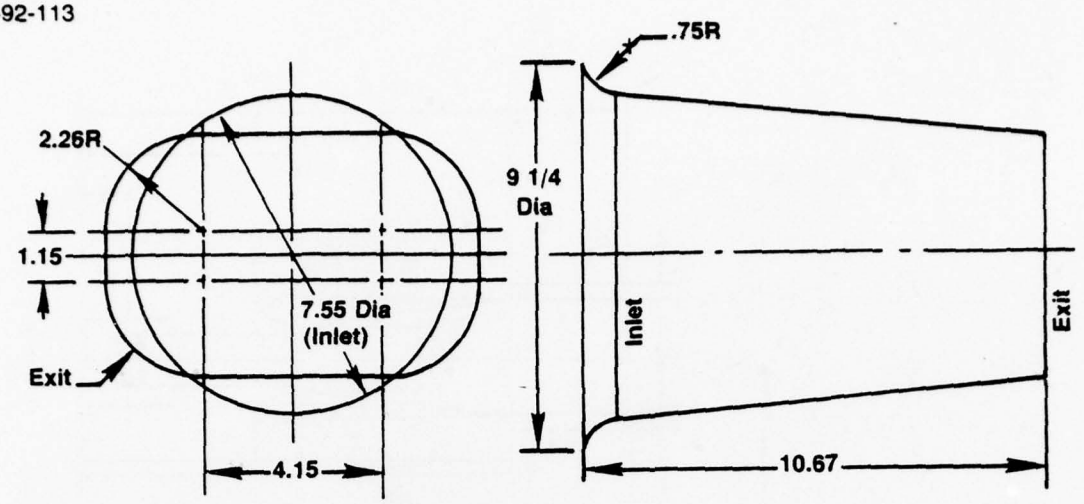

1st Ejector

Inlet & Exit Area = 44.77 in^2 A.R. = 1.49 (TF30 @ A/B)

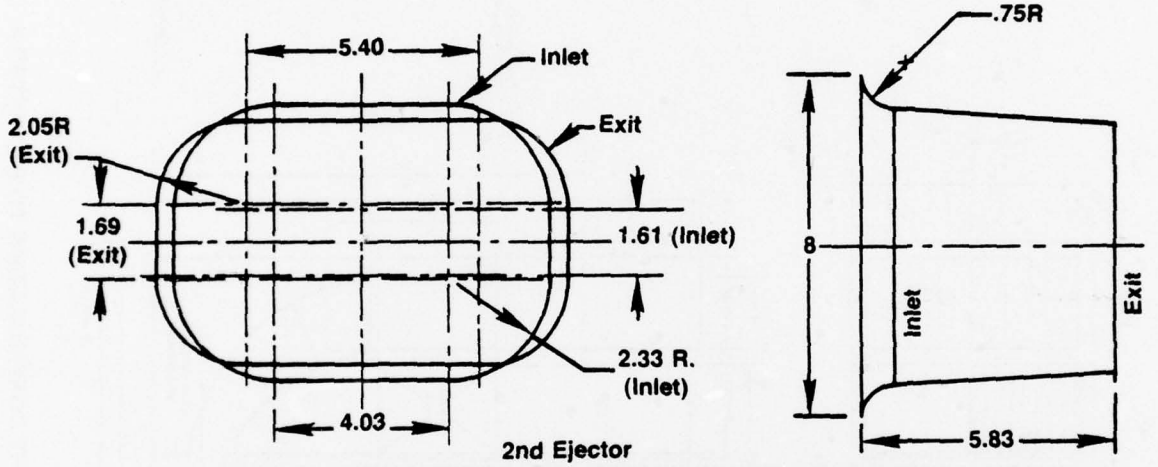

2nd Ejector

Inlet Area = 49.83 in^2 A.R. = 1.66 (TF30 @ A/B)

Exit Area = 51.40 in^2

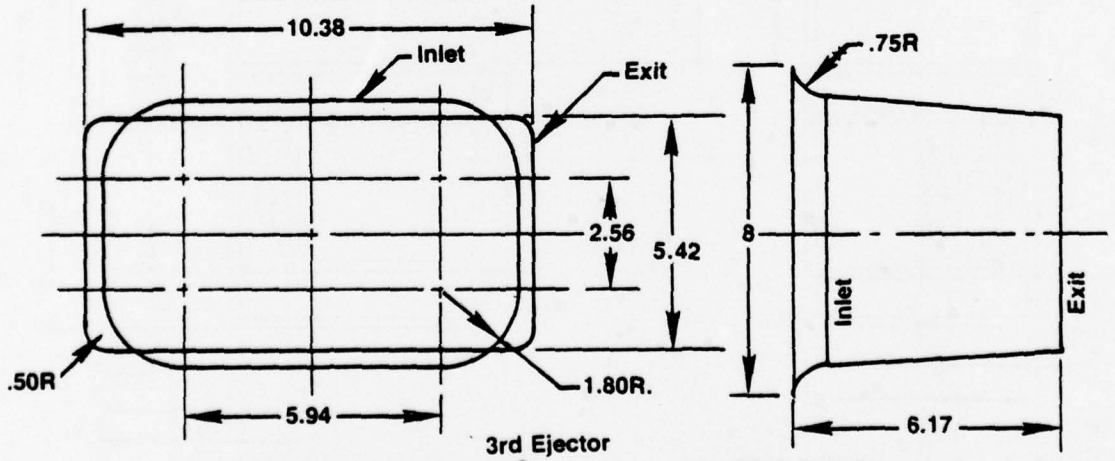

3rd Ejector

Inlet & Exit Area = 56.0 in^2 A.R. = 1.87 (TF30 @ A/B)

FIGURE 13: DIMENSIONAL DRAWING OF SCALE MODEL EJECTORS (INTERNAL LINES)

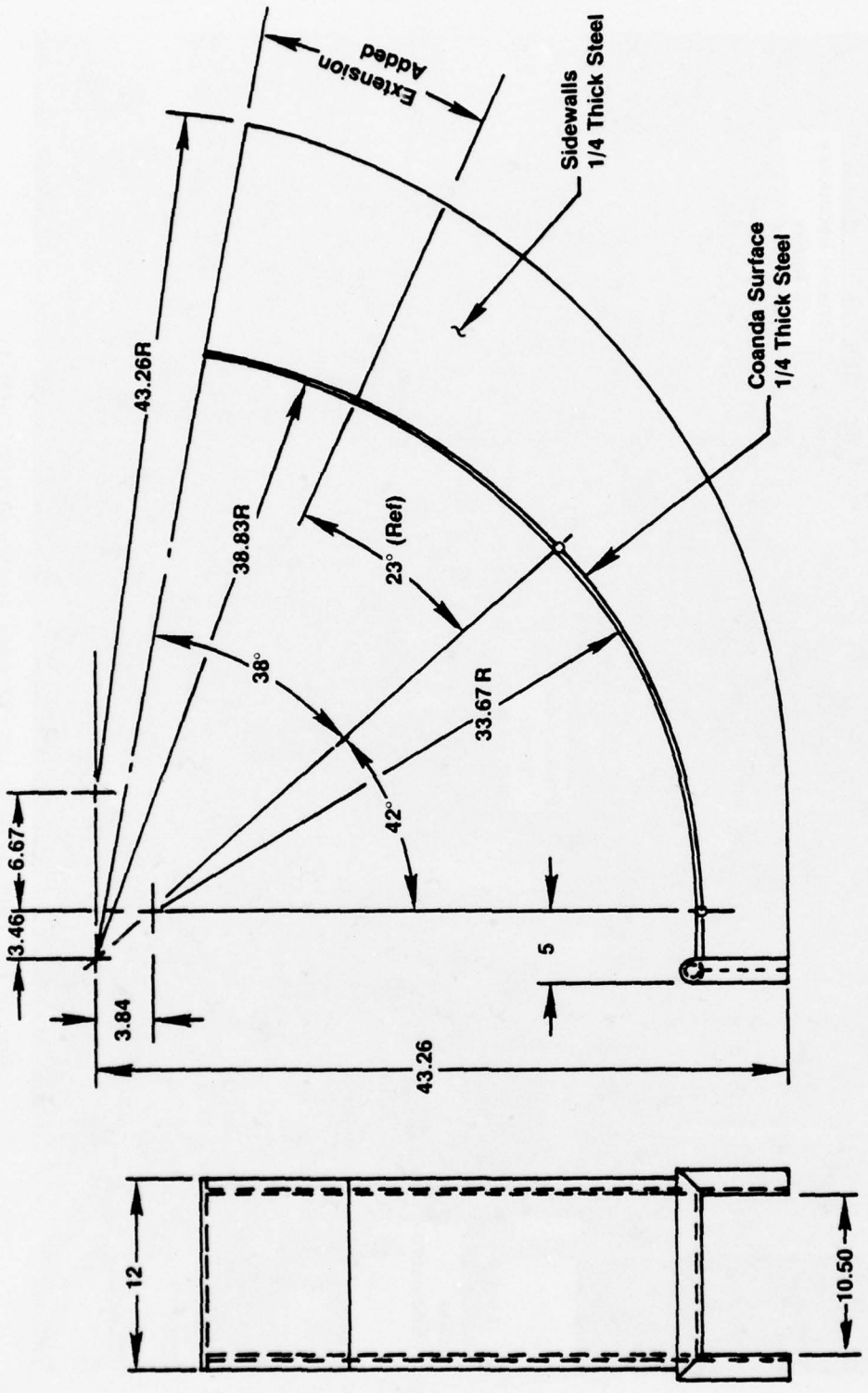

FIGURE 14: DIMENSIONAL DRAWING OF SCALE MODEL COANDA SURFACE

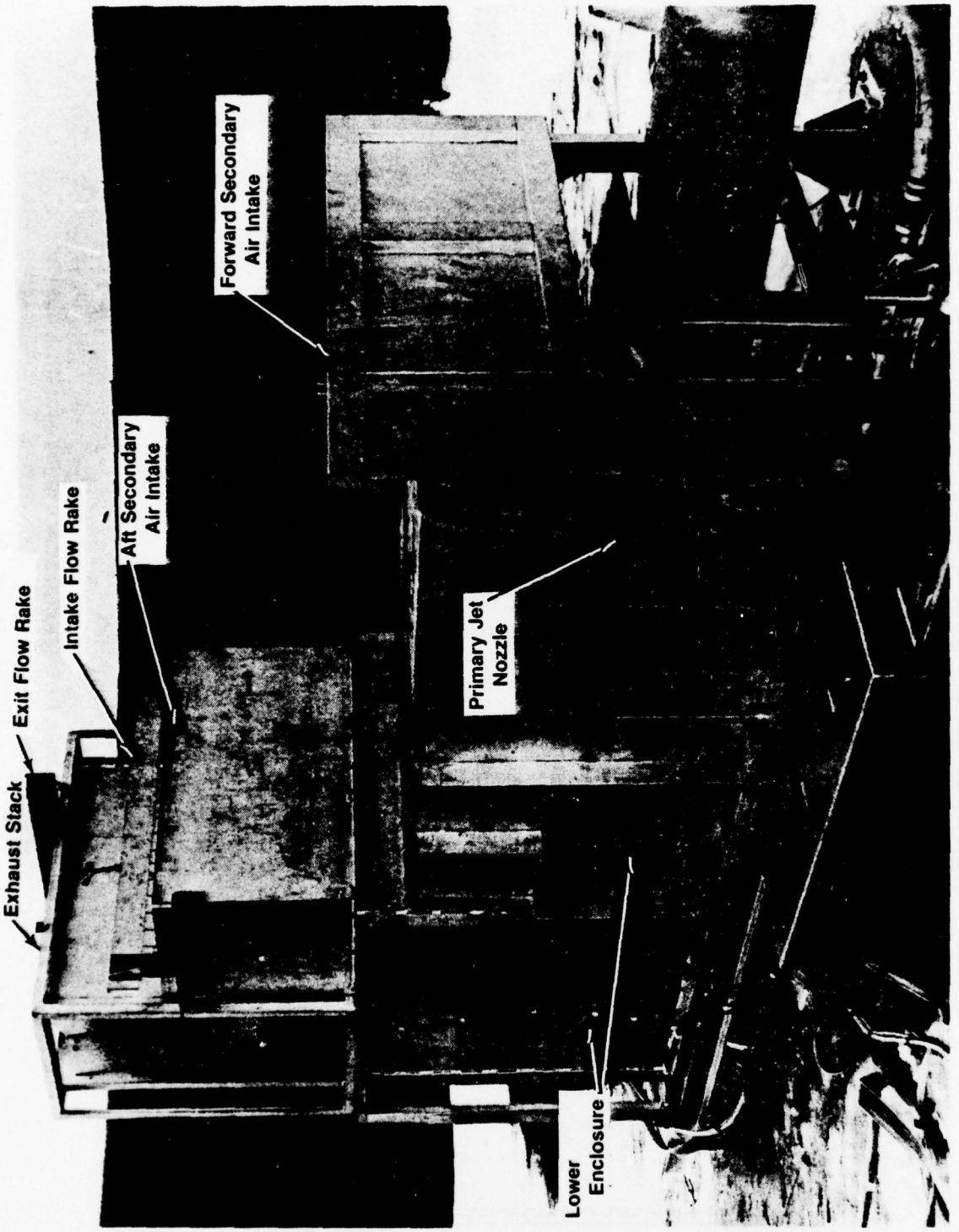

FIGURE 15: ONE-SIXTH SCALE "C" CELL MODEL IN TEST FACILITY

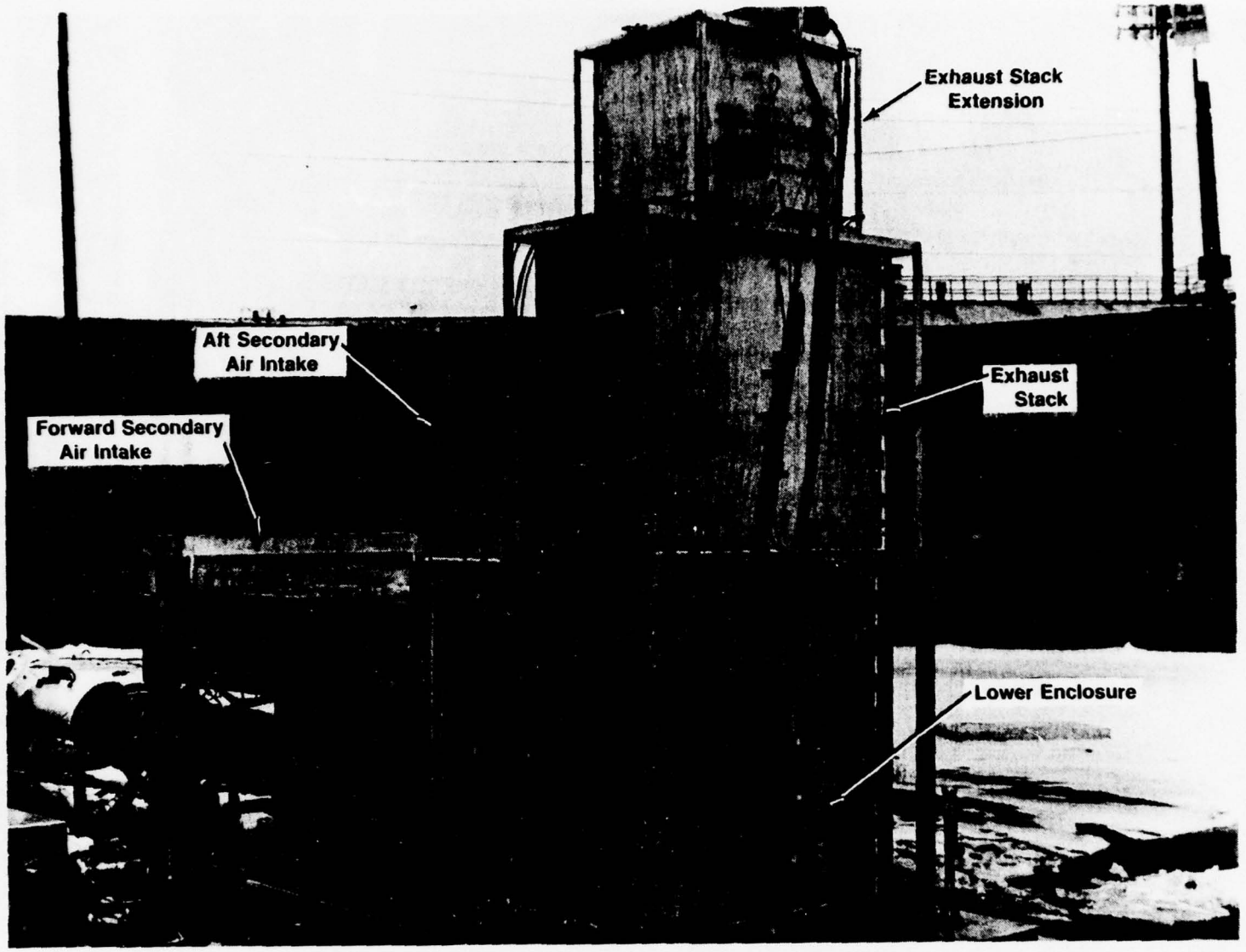

FIGURE 16: ONE-SIXTH SCALE "C" CELL MODEL WITH EXHAUST STACK EXTENSION

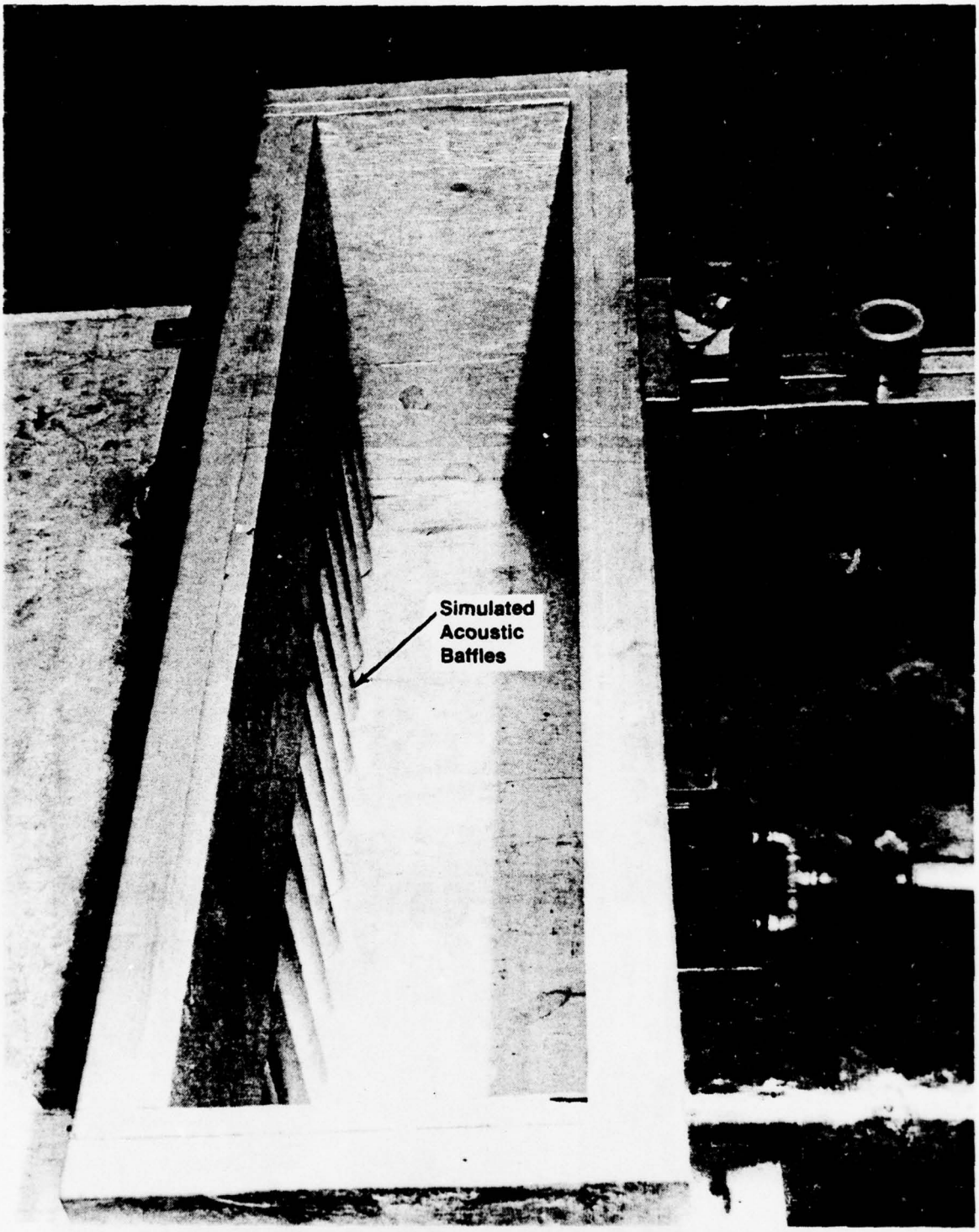

FIGURE 17: FORWARD SECONDARY AIR INTAKE – "C" CELL MODEL

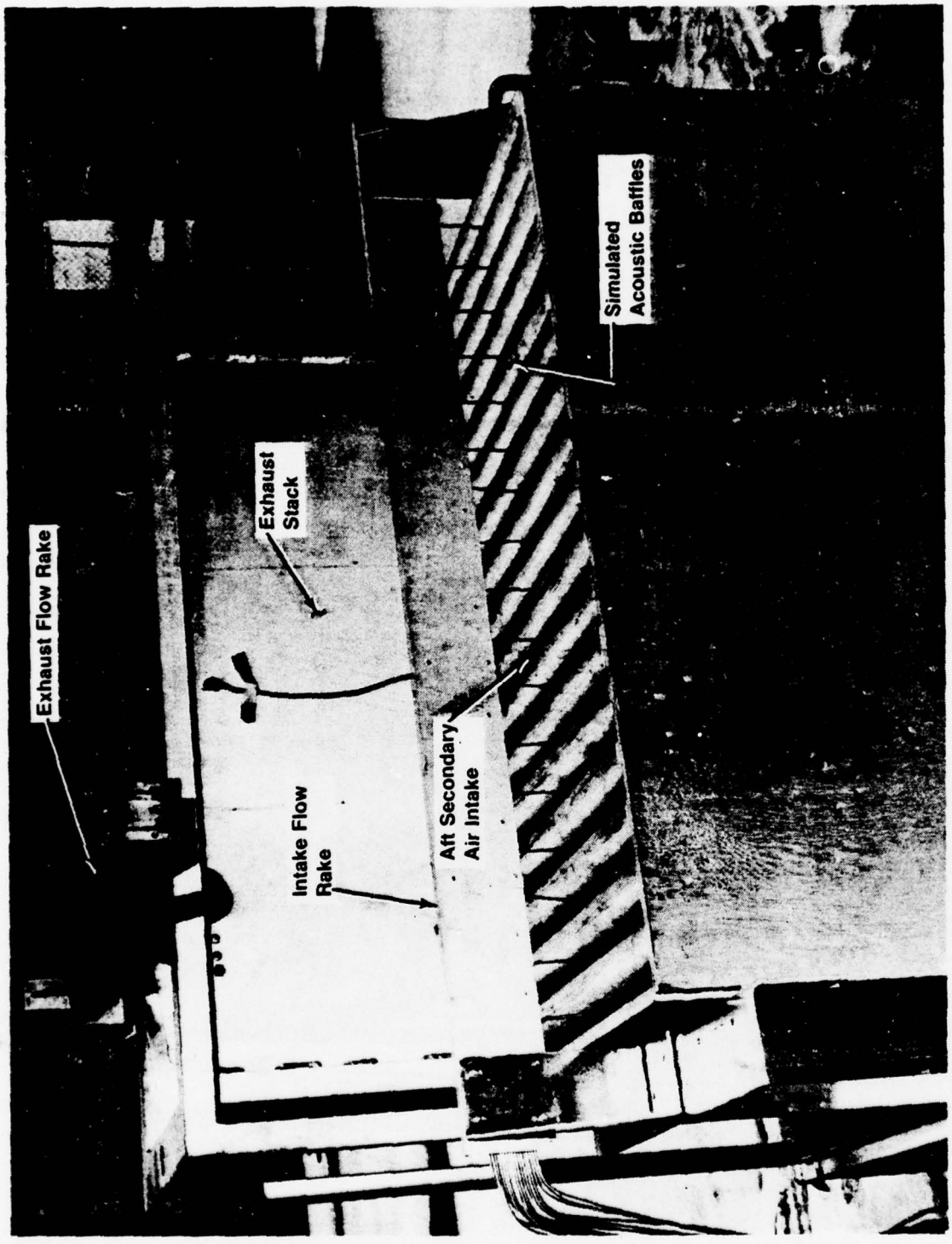

FIGURE 18: AFT SECONDARY AIR INTAKE – "C" CELL MODEL

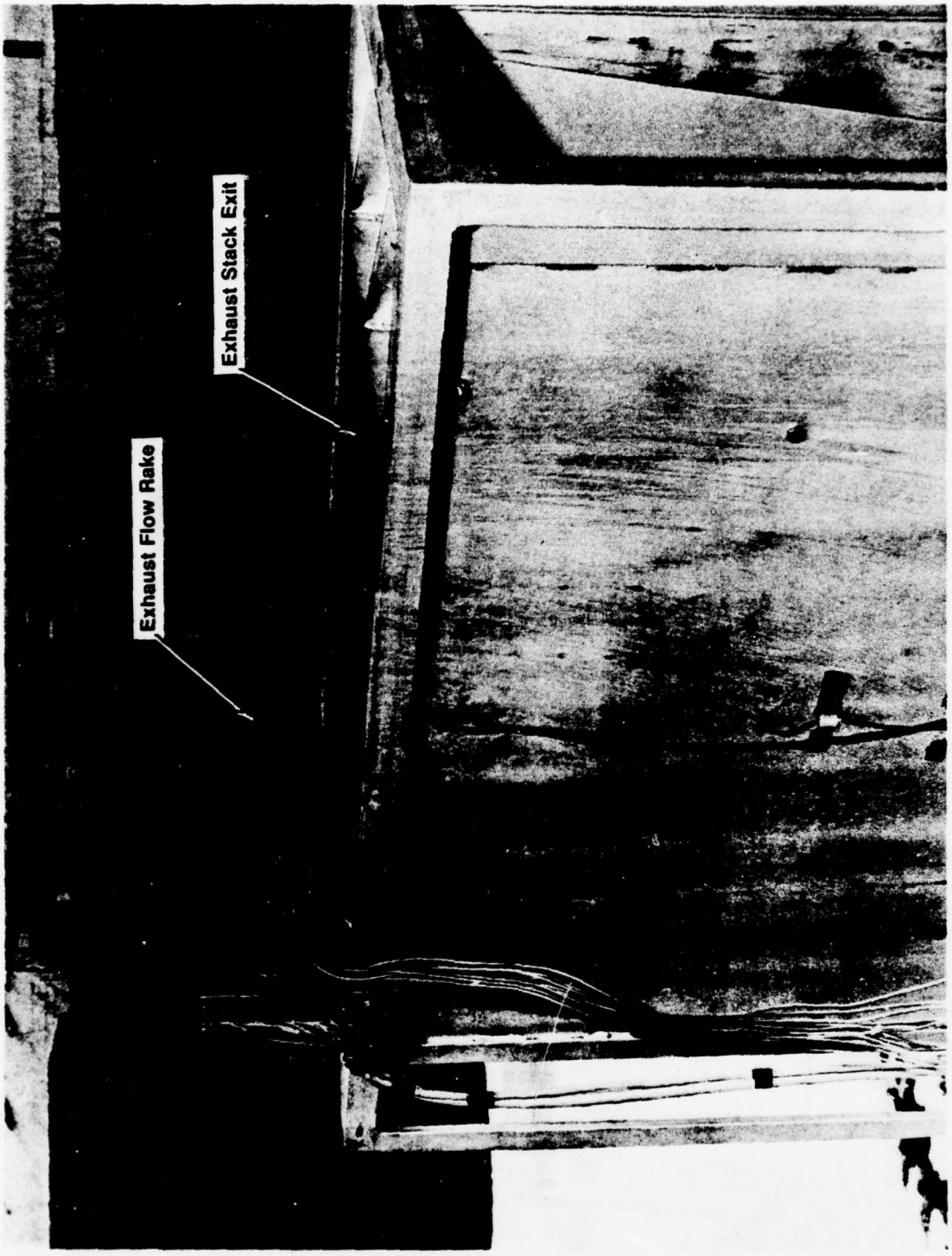

FIGURE 19: "C" CELL MODEL EXHAUST STACK EXIT WITH EXHAUST FLOW RAKE

h. Figure 20 is a photograph from above looking down into the exhaust stack with the stack sidewalls in the 7-degree position, showing the divergence in the exhaust stack for that configuration and the relationship with the Coanda surface sidewalls.

i. Figure 21 shows the afterburning exhaust nozzle and its relationship to the first ejector inlet during the testing.

4. INSTRUMENTATION.

a. Figure 22 shows the relationship of the exhaust nozzle to the ejectors and Coanda surface. The location of the ejector and Coanda surface pressure and temperature instrumentation is also shown. Each of the three ejectors has four static pressure ports and four outside surface temperature thermocouples (two each on the vertical centerline and two each on the horizontal centerline). The Coanda surface has ten each of static pressure ports and outside surface temperature thermocouples at approximately 10-degree intervals along the Coanda centerline, starting at the entrance.

b. The exhaust flow characteristics above the stack exit were measured by an existing exit rake which has fourteen each of total pressure and total temperature probes; however, only eleven of these probes are required to cover the fore-to-aft depth of the "C" cell model exhaust stack. The exit rake was shown installed on the model on Figure 19.

c. Figure 23 shows the locations of the thermocouples and static pressure ports that were added to the enclosures and exhaust stack. The static pressures were to determine cell depression and the thermocouples for determination of internal surface temperatures.

d. The secondary air intakes were instrumented to determine the secondary flow entrainment. Each channel of the inlets had a static pressure port at the centerline approximately 0.75 channel width downstream from the start of the constant area section after the bellmouth. The probes for the aft secondary air intake were on a movable intake rake as shown on Figure 18. The probes for the forward secondary air intake were placed in the channel end plates (upper and lower wall of horizontal passage) as shown on Figure 23. These probes were placed on one side of the enclosure centerline only and symmetry assumed.

e. Table 1 is a list of the instrumentation used and the accuracy requirement placed on that instrumentation.

f. The environmental and flow condition data listed in Table 2 were required in addition to the parameters listed in Table 1.

B. Test Procedure

1. The target values of afterburner nozzle pressure ratio and exhaust gas total temperature for the engines simulated in this test are listed in Table 3. Exit temperature was set for each afterburning data run by setting on a constant value of burner fuel flow at the target afterburner nozzle pressure ratio. This method of setting afterburner exhaust temperature was necessary due to lack of instrumentation capable of measuring the extremely high exhaust gas temperature used for the test. The military rated thrust (MRT) power settings were set by measured exhaust gas temperature and nozzle pressure ratio.

2. A calculation procedure was developed to determine the A/B exhaust gas temperature based on the burner fuel flow, airflow, water jacket heat loss and an assumed burner efficiency of 95 percent. This calculation procedure was outlined in Reference (e), Section II.B. and will not be repeated here.

3. The model configurations tested and the data recorded during those test runs are shown in Table 4. Each test condition was set up as near the desired nozzle pressure and exhaust temperature as was practical.

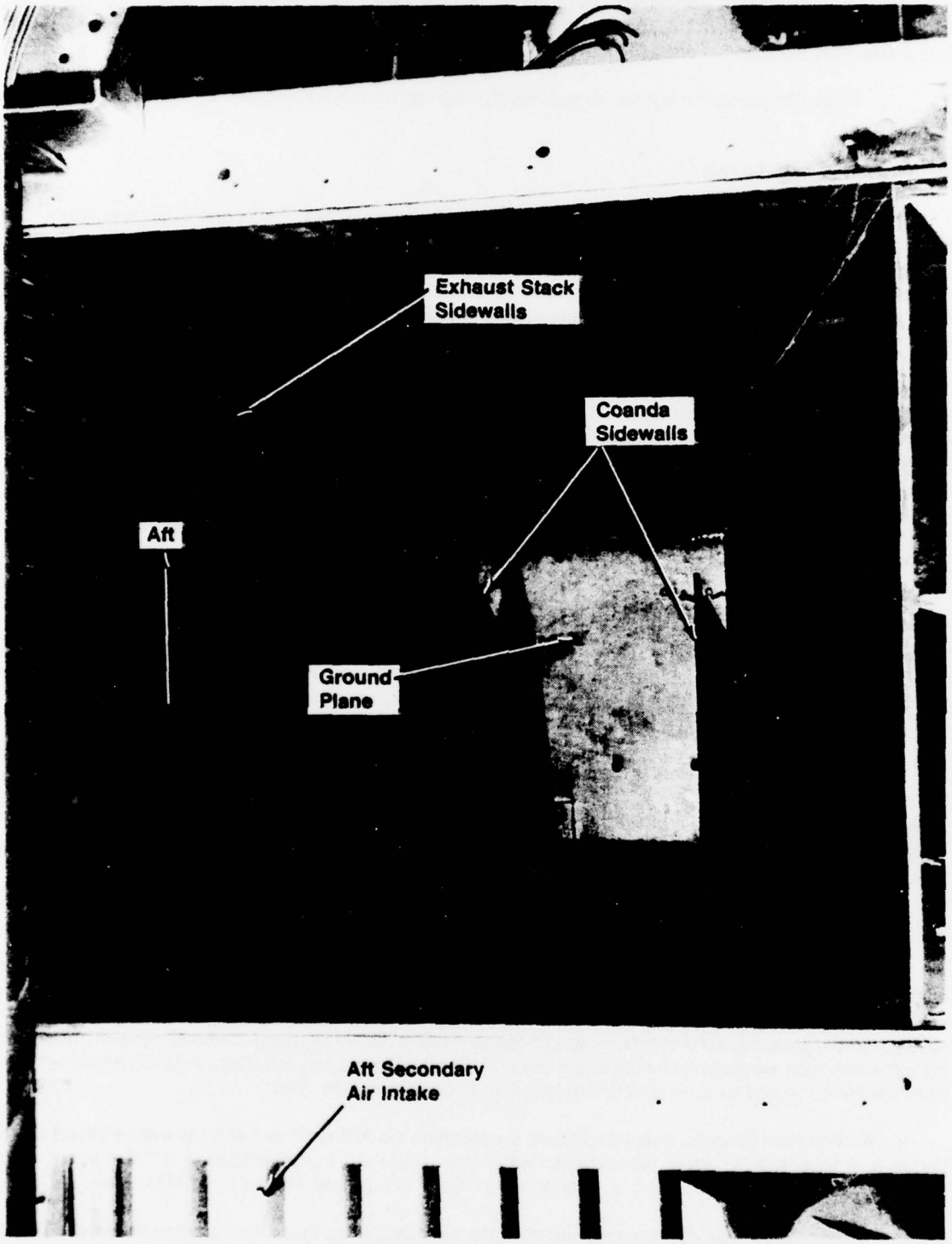

FIGURE 20: EXHAUST STACK FLOW PASSAGE WITH 7° SIDEWALLS

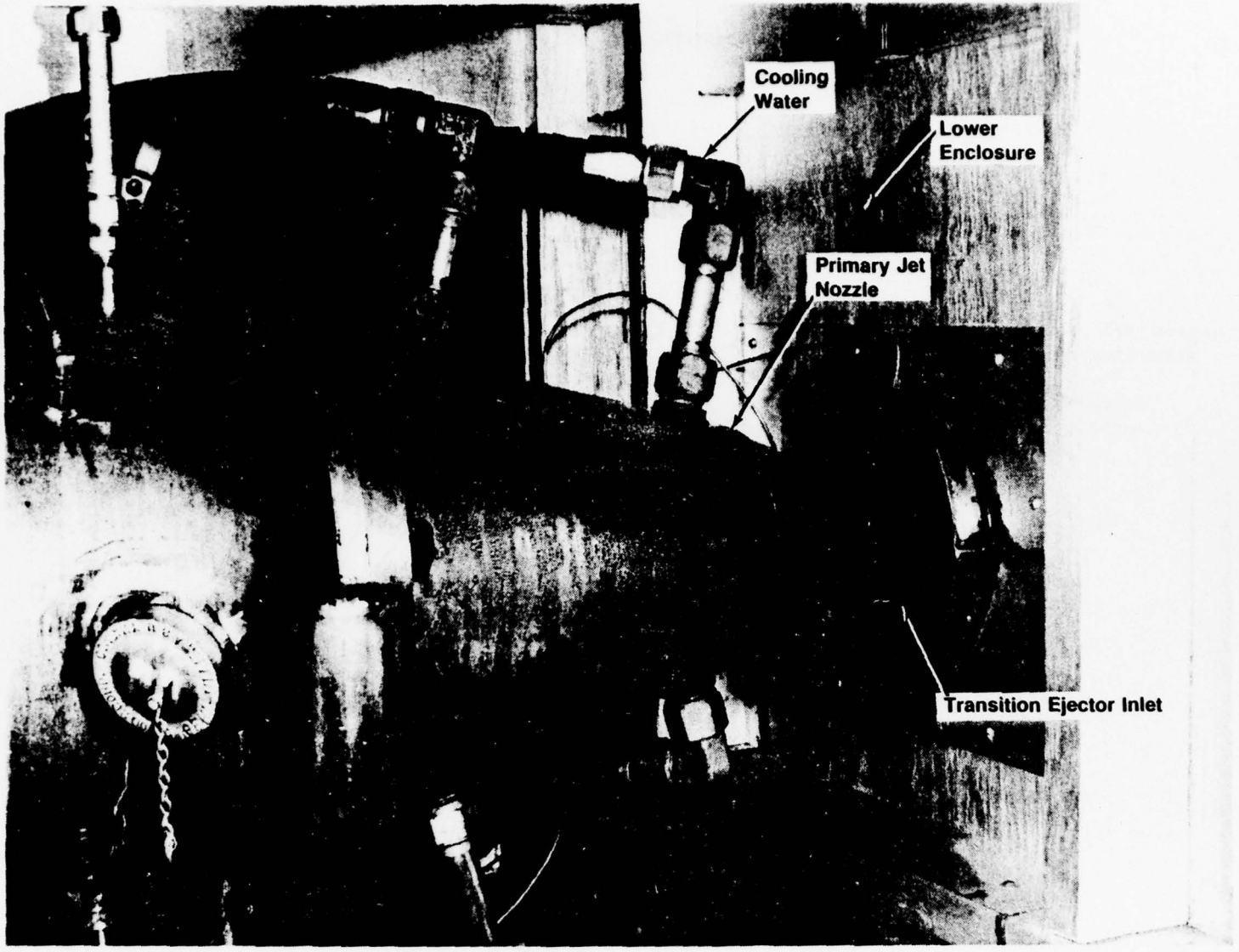

FIGURE 21: PRIMARY JET AFTERBURNING NOZZLE AND TRANSITION EJECTOR INLET

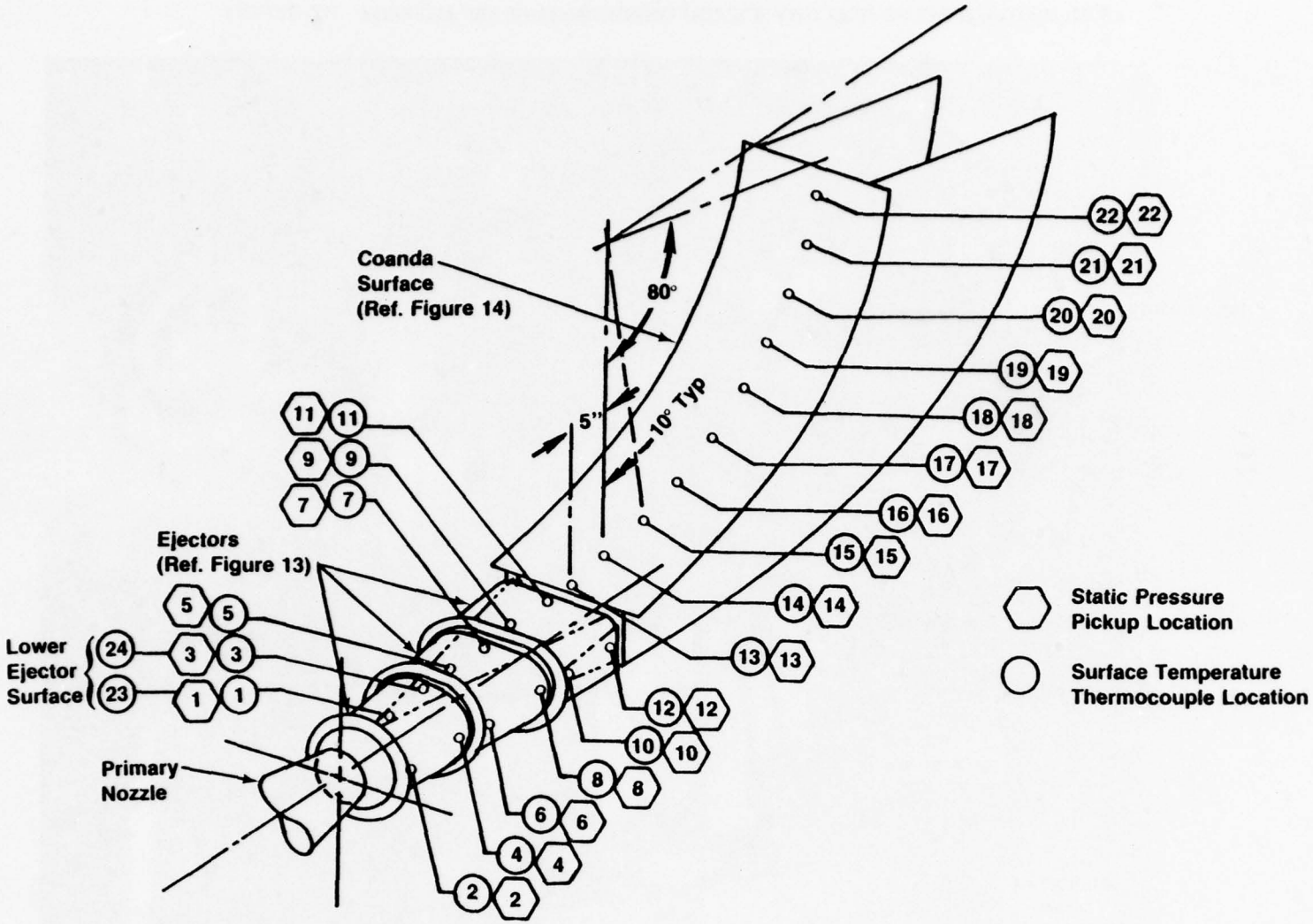

FIGURE 22: SCHEMATIC OF EJECTOR AND COANDA SURFACE INSTRUMENTATION

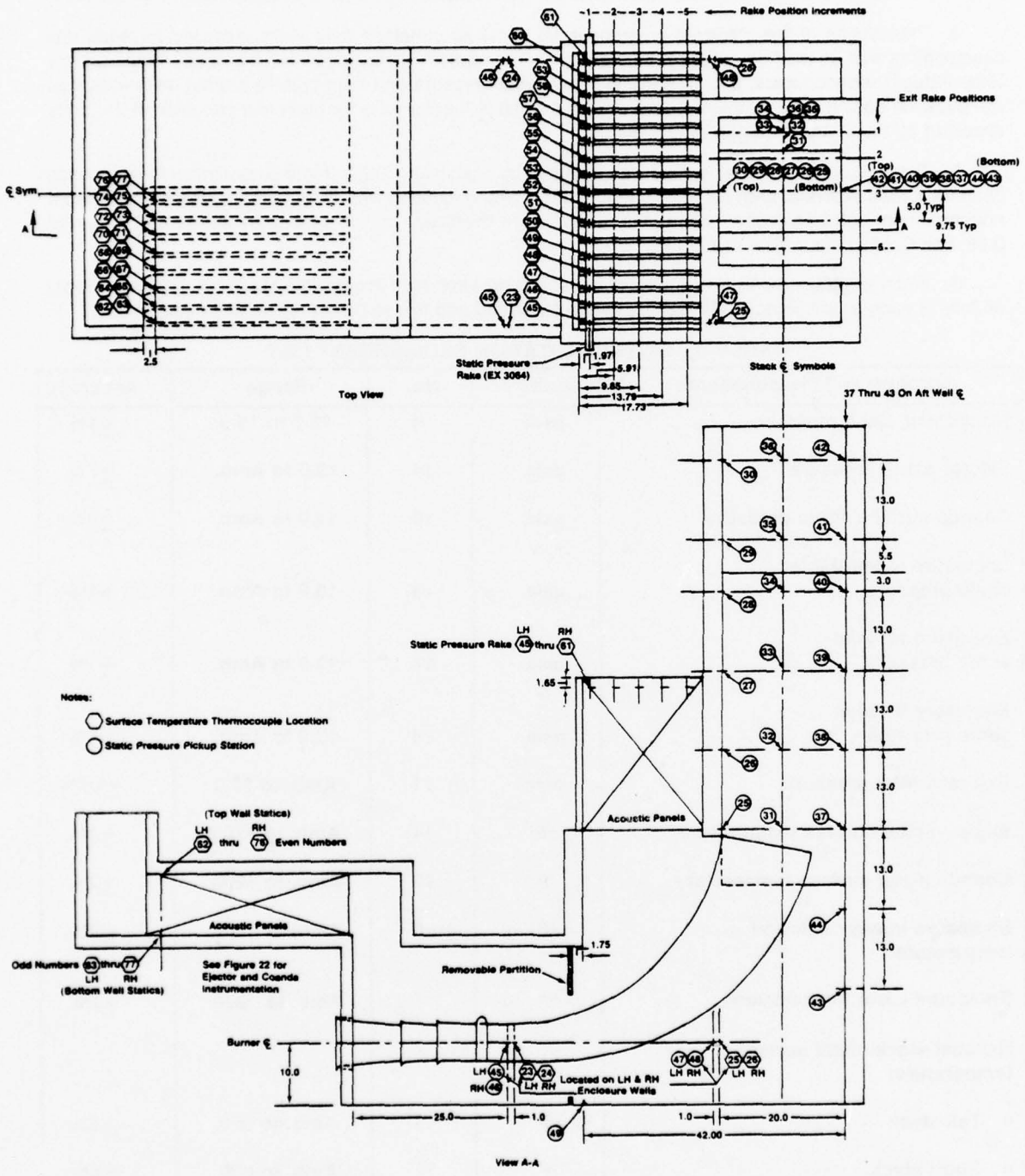

FIGURE 23: SCHEMATIC OF ENCLOSURE AND EXHAUST STACK INSTRUMENTATION

A period of time for thermal stabilization was allowed at each power setting prior to recording data. Measurements were recorded for all instrumentation within each data column checked for each configuration.

4. Tabulations of the standard environmental and flow condition data were recorded for each test condition, as well as model configuration identifying information. All static pressure probes, metal surface temperature thermocouples, and Coanda exit rake total pressure and temperature probes were assigned identification coding. The measured data were recorded in tabular form for each test condition in the units specified by the instrumentation requirements.

5. Total secondary air inlet airflow was obtained by calculating and summing the airflow through each channel. Cross sectional area for each channel at the probe location was determined by the channel width and increment between probe movements. A discharge coefficient for the secondary air inlet bellmouth of 0.98 was used in the airflow calculation.

6. Exit rake total temperature and total pressure data were used to calculate Mach number and velocity of flow at each probe location. These data were tabulated and the velocity profiles computer plotted.

TABLE 1: INSTRUMENTATION REQUIREMENT LIST

Location and Measurements	Units	No.	Range	Accuracy
Nozzle exit static pressure	psia	4	13.0 to 15.0	±1%
Ejector static pressure	psia	14	12.0 to Amb.	±1%
Coanda surface static pressure	psia	10	12.0 to Amb.	±1%
Enclosure forward inlet static pressure	psia	16	13.0 to Amb.	±1%
Enclosure aft inlet static pressure	psia	17	13.0 to Amb.	±1%
Enclosure interior static pressure	psia	4	13.0 to Amb.	±1%
Exit rake total pressure	psia	11	Amb. to 17.0	±1/2%
Ejector metal surface temperature	°F	14	Amb. to 1200	±2%
Coanda metal surface temperature	°F	10	Amb. to 1200	±2%
Enclosure interior sidewall temperature	°F	6	Amb. to 600	±2%
Enclosure Floor temperature	°F	1	Amb. to 300	±2%
Exhaust stack metal surface temperature:				
• Tall stack	°F	18	Amb. to 800	±2%
• Short stack	°F	12	Amb. to 800	±2%
Exit rake total temperature	°F	11	Amb. to 1200	±2%

TABLE 2: ENVIRONMENTAL AND FLOW CONDITION DATA REQUIREMENTS

Measurement	Units	No.	Range	Accuracy
Ambient pressure	psia	1	13.8 to 14.4	±1/2%
Nozzle exhaust total pressure	psia	1	Amb. to 50	±1/2%
Nozzle exhaust pressure ratio	–	1	1.2 to 3.5	±1%
Ambient temperature	°F	1	20 to 100	±2%
Nozzle exhaust gas temperature	°F	1	Amb. to *	±2%
Nozzle airflow	lb/sec	1	0 to 7.5	±1%
Primary burner fuel flow	lb/sec	1	0 to .1	±2%
Afterburner fuel flow	lb/sec	1	0 to .3	±2%
Cooling water flow	gpm	1	0 to 90	±2%
Cooling water temperature in	°F	1	35 to 55	±2%
Cooling water temperature out	°F	1	50 to 190	±2%

* Afterburner temperature is calculated from airflow and fuel flow data used to set up afterburner condition.

TABLE 3: PRIMARY NOZZLE TARGET EXHAUST CONDITIONS

Engine Simulated	Model Scale Nozzle Diameter	Nozzle Pressure Ratio	Exhaust Gas Temperature
TF30-P-408 at MRT	4.31 inches	2.48	1068°F
J79-GE-10/17/19 at MRT	3.40 inches	3.02	1205°F
J79-GE-10/17/19 at A/B	4.29 inches	2.89	3260°F

TABLE 4: COANDA "C" CELL 1/6 SCALE MODEL TEST RUN INDEX

Date	Test Identification				Nozzle Conditions			Enclosure Partition		Exhaust Stack Configuration		Performance Data								
	Config No.	Run Nos.	Rake Pos Nos.									Eject/Coanda		Enclosure		Stack	Inlets		Exhaust Exit	
			Aft Inlet	Exit	Dia-in.	NPR	EGT-°F	With	W/O	Stack Wall Angle	Stack Height	P	T	P	T	T	Fwd P	Aft P	P	T
12/16/76	1	1-2	5,4	1,2	4.31	2.48	1068		X	0°	Tall	X	X	X	X	X	X	X	X	X
12/22/76	2	34-38	5,4,3,2,1	1,2,3,4,5	4.31	2.48	1068	X		0°	Tall	X	X	X	X	X	X	X	X	X
12/17/76 12/20/76	3	12-16	4,5,3,2,1	2,1,3,4,5	4.31	2.48	1068	X		3 1/2°	Tall	X	X	X	X	X	X	X	X	X
12/22/76	4	29-33	2,1,3,4,5	4,5,3,2,1	4.31	2.48	1068	X		7°	Tall	X	X	X	X	X	X	X	X	X
12/21/76	5	22-26	5,4,3,2,1	1,2,3,4,5	4.31	2.48	1068	X		7°	Short	X	X	X	X	X	X	X	X	X
12/21/76	6	17-21	1,2,3,4,5	5,4,3,2,1	4.31	2.48	1068	X		3 1/2°	Short	X	X	X	X	X	X	X	X	X
12/22/76	7	39-43	1,2,3,4,5	5,4,3,2,1	4.31	2.48	1068	X		0°	Short	X	X	X	X	X	X	X	X	X
1/3/77	8	44-48	5,4,3,2,1	1,2,3,4,5	3.40	3.02	1205	X		0°	Short	X	X	X	X	X	X	X	X	X
1/3/77	9	49-53	1,2,3,4,5	5,4,3,2,1	3.40	3.02	1205	X		0°	Tall	X	X	X	X	X	X	X	X	X
1/10/77	10	80-84	1,2,3,4,5	1,2,3,4,5	4.29	2.89	3260	X		7°	Tall	X	X	X	X	X	X	X	X	X
1/7/77	11	75-79	4,5,1,2,3	2,1,5,4,3	4.29	2.89	3260	X		3 1/2°	Tall	X	X	X	X	X	X	X	X	X
1/4/77	12	56-60	5,4,3,2,1	1,2,3,4,5	4.29	2.89	3260	X		0°	Tall	X	X	X	X	X	X	X	X	X
1/5/77	13	61-65	1,2,3,4,5	5,4,3,2,1	4.29	2.89	3260	X		0°	Short	X	X	X	X	X	X	X	X	X
1/5/77	14	66-70	5,4,3,2,1	1,2,3,4,5	4.29	2.89	3260	X		3 1/2°	Short	X	X	X	X	X	X	X	X	X
1/10/77	15	86-90	2,3,4,5,1	2,3,4,5,1	4.29	2.89	3260	X		7°	Short	X	X	X	X	X	X	X	X	X

IV. TEST RESULTS

The pertinent results of the testing previously outlined are discussed in the following paragraphs.

A. Effect of Partition Wall.

1. The Navy class "C" engine test cells have a concrete partition between the spray chamber and the exhaust chamber (see Figure 1). With the existing water spray equipment and augmenter tubes removed, there is a nine-foot square opening in this partition through which the Coanda surface is placed (see Figure 2). The possibility that this restricted passage could affect Coanda flow attachment and create detrimental recirculated flow patterns within the enclosure was examined in the first portion of this test. Test Configuration Number 1 (Runs 1 and 2) was made using an input simulation of the TF30-P-408 at MRT condition with the partition removed. Configuration Number 2 (Runs 34 through 38) was with the same input exhaust nozzle conditions and the same model configuration except the partition was reinstalled. Table 5 presents the enclosure internal static pressures upstream and downstream of the partition for those two configurations. The difference between the upstream (front) and downstream (rear) pressures are listed as ΔP in inches of water for each side (right or left) of the enclosure. The overall average pressure differential is 1.745 in. H2O without the partition and 2.551 in. H2O with it installed. This small increase had an insignificant effect on the Coanda flow and only a small effect on component temperatures.

TABLE 5: CELL ΔP FRONT-TO-REAR WITH AND WITHOUT PARTITION

Configuration		Run No.	P_a	Enclosure Internal Static Pressure				ΔP (Front-Rear) Inches H_2O	
				Front		Rear			
				P_{23} (Left)	P_{24} (Right)	P_{25} (Left)	P_{26} (Right)	Left	Right
1	Without Partition	1	14.048	13.878	13.875	13.815	13.804		
		2	14.052	13.887	13.886	13.818	13.837		
		Average	14.050	13.8825	13.8805	13.8165	13.8205	1.828	1.662
2	With Partition	34	14.073	13.925	12.919	12.838	13.821		
		35	14.073	13.918	13.915	13.836	13.805		
		36	14.076	13.924	13.924	13.841	13.814		
		37	14.082	13.916	13.929	13.844	13.831		
		38	14.084	13.936	13.948	13.860	13.843		
		Average	14.0776	13.9238	13.9270	13.8438	13.8228	2.216	2.886

2. The effect of the partition on Coanda surface temperature and static pressure is presented on Figure 24. The static pressures along the Coanda surface are an indication of the quality of flow attachment to the surface. The data indicate no difference created by presence of the partition. The Coanda surface temperature data shows a decrease in metal temperatures (about 45 degrees off the peak temperature) with the partition in place. This is a desirable condition which is probably the result of a higher secondary flow rate through the nine- by nine-foot (full-scale) opening in the wall caused by the increased ΔP across the wall discussed above.

3. The effect of the partition on the transition ejectors surface temperature is shown on Figure 25. With the partition in place, the highest temperatures recorded (aft upper enclosure surface on centerline) were decreased by about 35 degrees to 40 degrees from those without the partition. The side centerline temperatures were also slightly lower (10 degrees to 15 degrees).

Sym-bol	Configuration		Run No.	Avg. EGT	Avg. NPR	Avg. T_a
⊙	1	Without Partition	1-2	1514°R	2.509	523°R
⊡	2	With Partition	34-38	1530°R	2.483	512°R

TF30-P-408 @ MRT Simulation
Tail Exhaust Stack With 0° Wall Angle

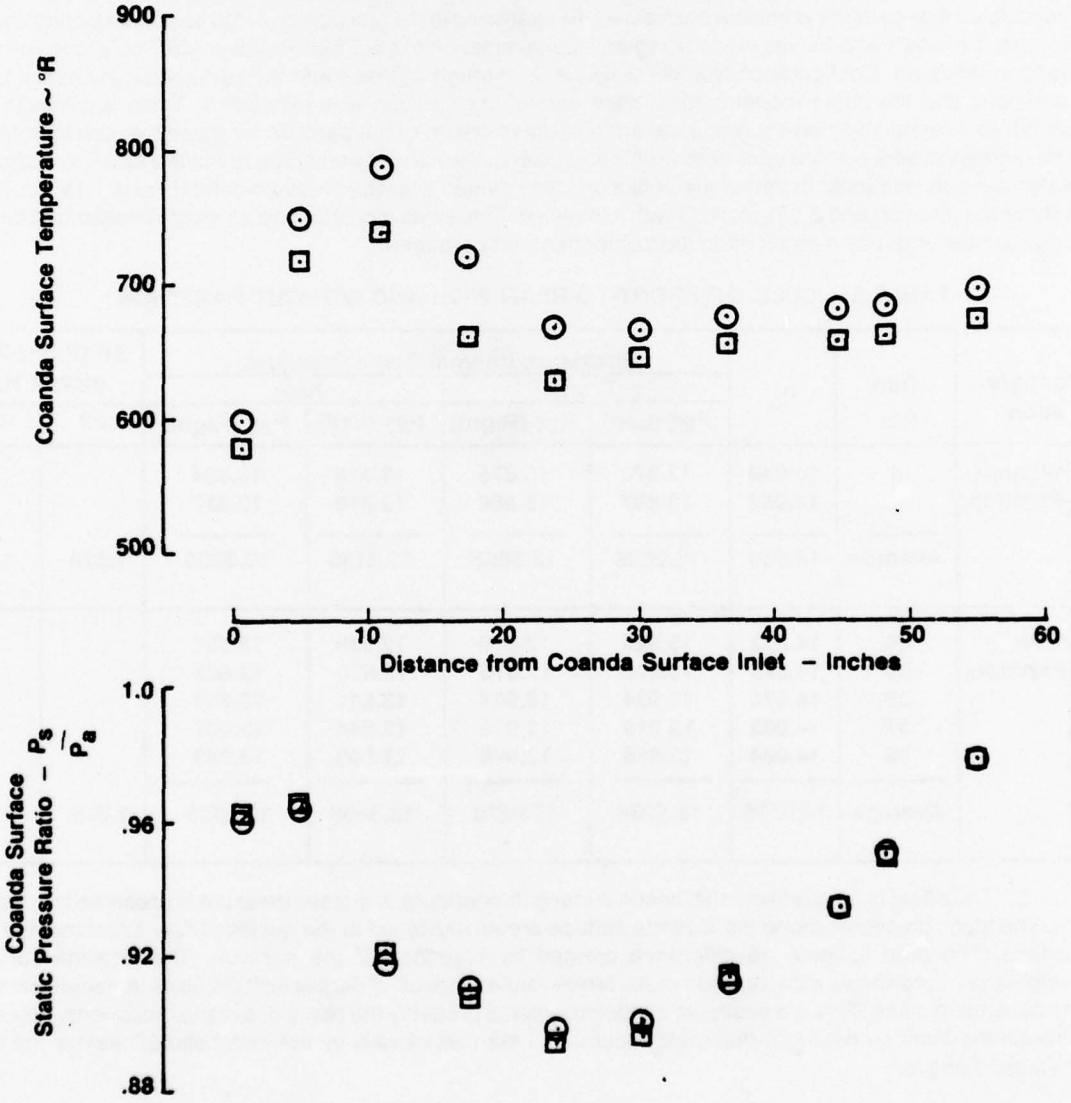

FIGURE 24: COMPARISON OF COANDA SURFACE TEMPERATURE AND STATIC PRESSURE WITH AND WITHOUT PARTITION

Sym-bols	Configuration		Run No.	Avg. EGT	Avg. NPR	Avg. T_a
⊙ ⊡	1	Without Partition	1-2	1514°R	2.509	523°R
● ■	2	With Partition	34-38	1530°R	2.483	512°R

TF30-P-408 @ MRT Simulation
Tail Exhaust Stack With 0° Wall Angle

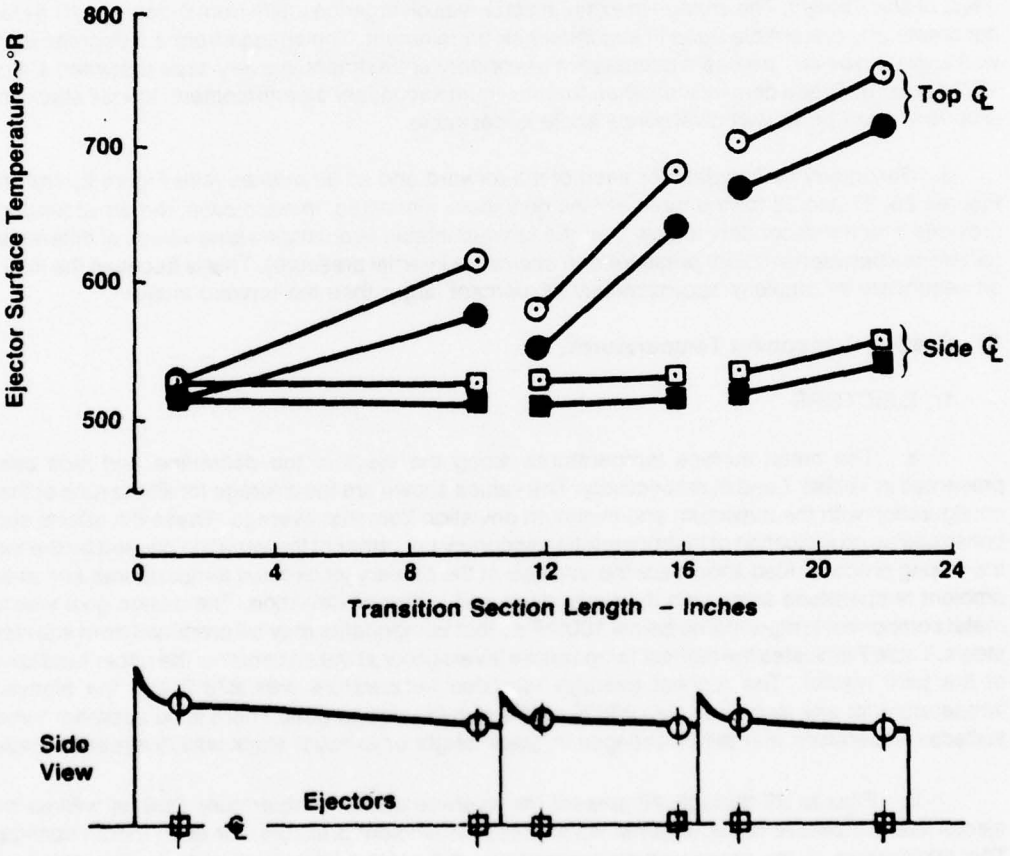

FIGURE 25: COMPARISON OF TRANSITION EJECTOR TEMPERATURES WITH AND WITHOUT PARTITION

4. All the preceding data indicate no detrimental effects due to the presence of the wall between the old spray chamber and exhaust chamber.

B. Secondary Airflow.

1. Table 6 presents the secondary airflow data for all model configurations with the partition in place. These data are for the combined secondary airflow from both the forward and aft secondary air intakes referred to sea level standard day conditions. The secondary flow at the first ejector inlet is omitted as it was not measured. The variation in airflow shown for different runs of the same configurations may not be due to accuracy of recording or of condition setup, but rather to the fact that each of the five runs were made with the aft secondary intake static pressure rake in different positions. Thus, when using the average, the possibility of nonuniform flow throughout the length of a secondary intake passage is accounted for. Using the average data for each configuration, it may be seen that the tall stack creates an increase in secondary airflow from 5.2 percent to 15.7 percent over the similar configuration with the shorter exhaust stack. The tall stack also seems to be the most beneficial for secondary airflow when the engine is at afterburning conditions.

2. The effect of exhaust stack wall angle on secondary flow entrainment is not as obvious as was the effect of stack height. The change in exhaust stack wall divergence angle from 0-degree to 3.5-degrees does not create any discernible trend in secondary air entrainment. The change from 3.5 degrees to 7.0 degrees wall angle, however, creates a decrease in secondary entrainment in every case (between 4.4 percent and 12.7 percent). These data indicate that, for maximum secondary air entrainment, the tall stack configuration with very small or no wall divergence angle is desirable.

3. Secondary airflow data for each of the forward and aft air intakes (see Figure 2) are presented on Figures 26, 27 and 28 for the three engine conditions simulated. In each case, the aft secondary air intake provides a higher secondary airflow than the forward intake, even at the same values of differential pressure (difference between ambient pressure and enclosure internal pressure). This is because the flow area of the aft secondary air intake is approximately 66 percent larger than the forward intake.

C. System Component Temperatures.

1. EJECTORS

a. The metal surface temperatures along the ejectors top centerline and side centerline are presented in Tables 7 and 8, respectively. The values shown are the average for all the runs at that particular configuration with the maximum and minimum deviation from that average. These deviations should not be construed as an indication of instrumentation accuracy but rather of the variation caused by the turbulence of the mixing process. Also shown are the average of the primary jet exhaust temperatures and average of the ambient temperatues along with their maximum and minimum deviation. The design goal was to maintain metal component temperatures below 1000°F so that components may be produced from standard low cost steels. Table 7 indicates the highest temperature levels occur at the aft center of the upper (and lower) surface of the third ejector. The highest average recorded temperature was 878°F and the highest recorded temperature for any single run was 908°F; well within the design goal. There is no apparent trend in ejector surface temperature with either changes in stack height or exhaust stack wall divergence angle.

b. Figures 29 through 42 present the average ejector temperature data as well as the average ejector static pressure ratios (internal static pressure/ambient pressure) for each model configuration run. The relationship of the measurement locations to the ejector inlets and exits is also shown. The static pressure ratios just downstream of the ejector inlet are an indication of the secondary air pumping capability of each ejector. As long as the static pressure ratio is less than unity, there is secondary air entrainment. The ejectors with the lowest static pressure ratios just downstream of their inlet are the most effective at secondary air pumping.

TABLE 6: TOTAL SECONDARY AIRFLOW – FORWARD AND AFT INTAKES

Engine Condition Simulated	Short Stack			Stack Angle (Degrees)	Tail Stack		
	Config No.	Run No.	$\dot{W}_s\sqrt{\theta_a}/\delta_a$ (Lb/Sec)		Config No.	Run No.	$\dot{W}_s\sqrt{\theta_a}/\delta_a$ (Lb/Sec)
TF30-P-408 @ MRT	13	61	20.74	0	12	56	20.97
		62	19.02	0		57	21.00
		63	18.85	0		58	20.57
		64	19.47	0		59	20.57
		65	19.88	0		60	22.58
		Average	19.59				21.14
	14	66	19.29	3.5	11	75	20.10
		67	20.61	3.5		76	21.81
		68	19.81	3.5		77	22.28
		69	20.22	3.5		78	21.54
		70	21.49	3.5		79	20.94
		Average	20.28				21.33
	15	86	18.21	7.0	10	80	18.23
		87	17.99	7.0		81	18.99
		88	16.90	7.0		82	18.45
		89	17.25	7.0		83	19.07
		90	18.16	7.0		84	18.92
		Average	17.70				18.73
J79-GE-10/17/19 @ MRT	8	44	17.35	0	9	49	19.13
		45	15.95	0		50	17.72
		46	17.54	0		51	18.77
		47	17.10	0		52	18.37
		48	18.14	0		53	19.34
		Average	17.22				18.67
J79-GE-10/17/19 @ A/B	7	39	22.85	0	2	34	22.71
		40	21.05	0		35	22.36
		41	20.60	0		36	21.91
		42	20.75	0		37	22.68
		43	21.06	0		38	22.58
		Average	21.26				22.45
	6	17	20.08	3.5	3	12	21.13
		18	20.32	3.5		13	22.52
		19	20.21	3.5		14	22.38
		20	20.74	3.5		15	22.80
		21	21.66	3.5		16	23.74
		Average	20.60				22.51
	5	22	18.01	7.0	4	29	20.95
		23	17.96	7.0		30	22.18
		24	19.20	7.0		31	21.61
		25	18.14	7.0		32	21.50
		26	19.59	7.0		33	21.33
		Average	18.58				21.51

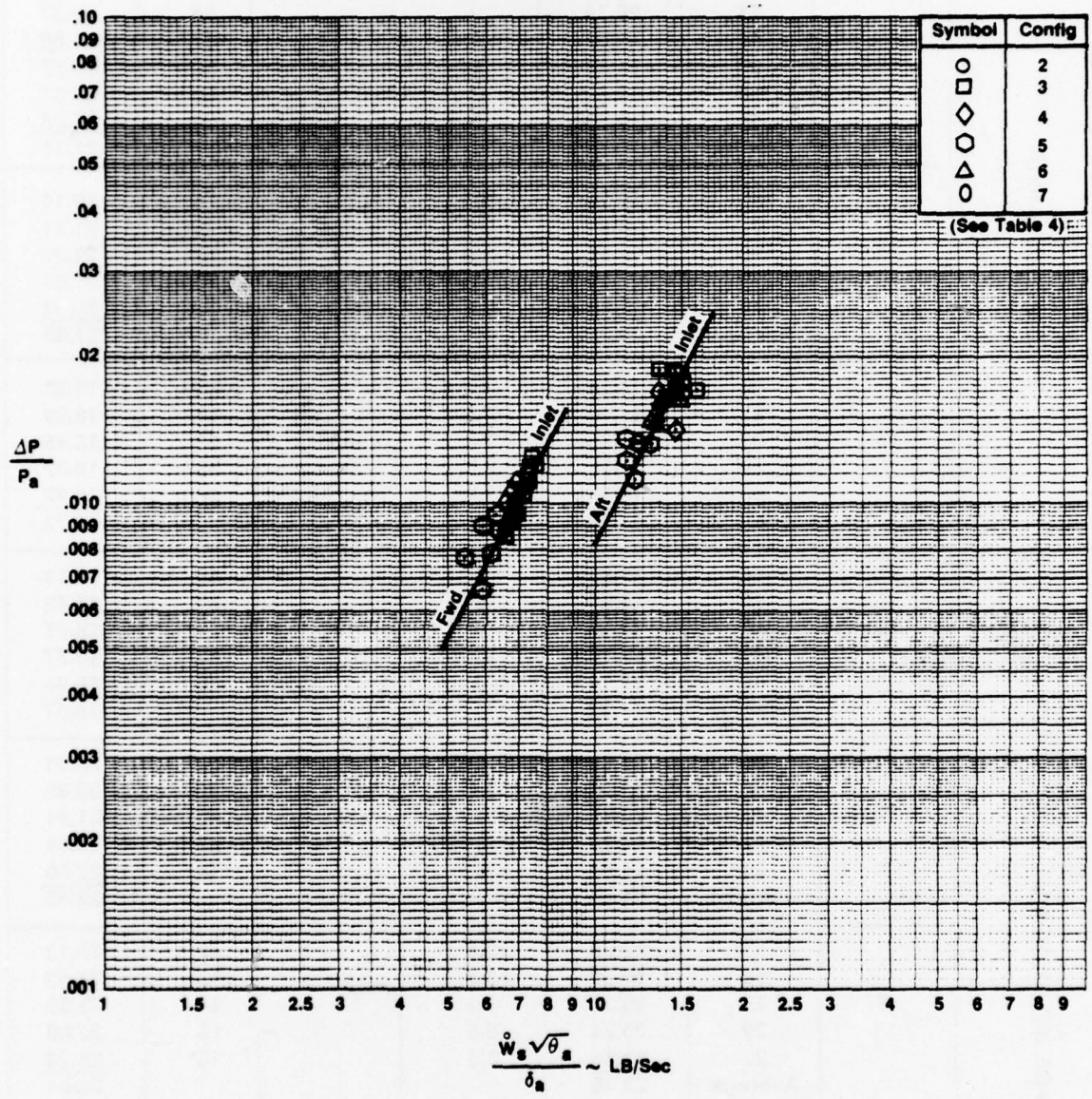

FIGURE 26: SECONDARY AIRFLOW VERSUS CELL DEPRESSION, PRIMARY JET SIMULATING TF30-P-408 AT MILITARY RATED THRUST

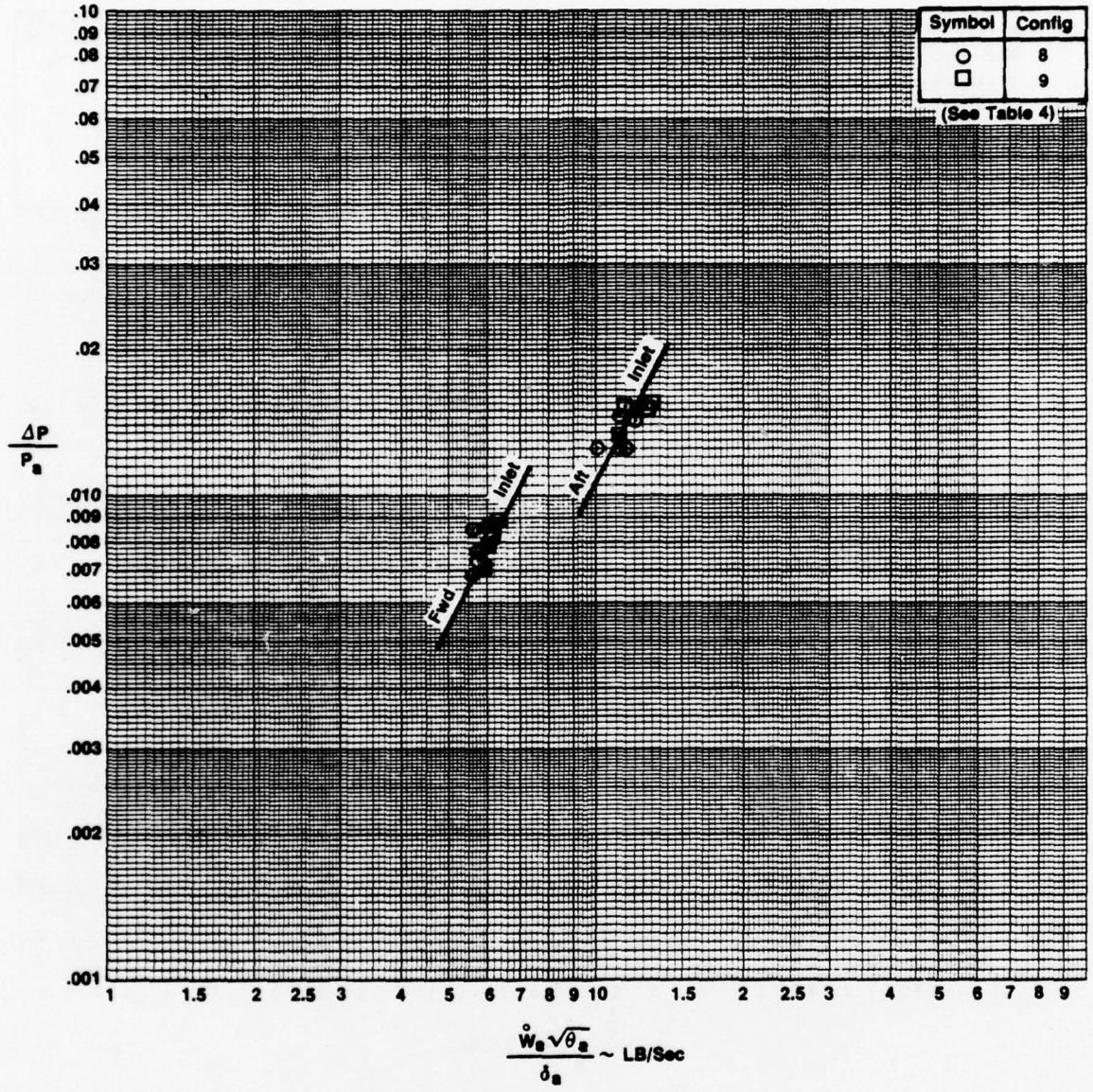

FIGURE 27: SECONDARY AIRFLOW VERSUS CELL DEPRESSION, PRIMARY JET SIMULATING J79-GE-10/17/19 AT MILITARY RATED THRUST

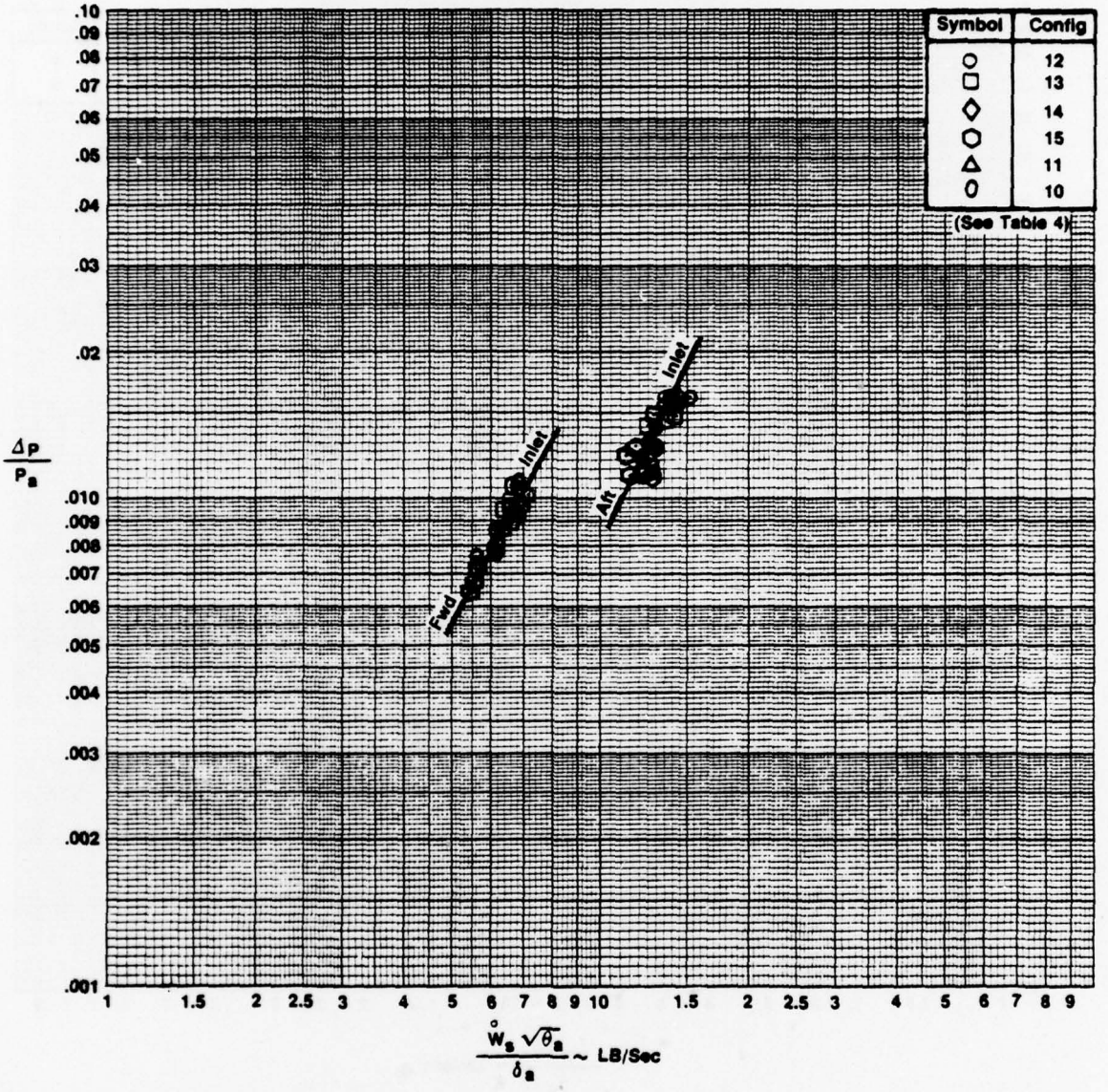

FIGURE 28: SECONDARY AIRFLOW VERSUS CELL DEPRESSION, PRIMARY JET SIMULATING J79-GE-10/17/19 AT AFTERBURNING CONDITIONS

TABLE 7: EJECTOR SURFACE TEMPERATURES – TOP CENTERLINE

Configuration	Average Temperature (°F) with Maximum and Minimum Deviations													
	Thermocouple No. (See Figure 22 for Location)													
	T_{jet}		T_1		T_3		T_5		T_7		T_9		T_{11}		T_a	
1 TF30-P-408, MRT, Tall Stack 0° Wall Angle W/O Partition	1054	+4 −4	69	+1 −1	155	+1 −0	118	+1 −0	221	+0 −0	240	+2 −2	293	+1 −0	63.0	+.1 −.1
2 TF30-P-408, MRT, Tall Stack 0° Wall Angle	1070	+6 −5	54	+1 −1	113	+9 −13	91	+3 −5	179	+9 −13	208	+7 −11	253	+8 −14	51.5	+.6 −.3
3 TF30-P-408, MRT, Tall Stack 3.5° Wall Angle	1066	+7 −8	34	+2 −1	103	+3 −3	75	+1 −2	169	+3 −5	197	+4 −3	247	+3 −3	34.6	+.5 −.8
4 TF30-P-408, MRT, Tall Stack 7° Wall Angle	1067	+4 −5	48	+4 −3	113	+9 −10	90	+6 −3	181	+8 −10	209	+9 −12	256	+6 −8	48.4	+2.2 −2.7
5 TF30-P-408, MRT, Short Stack 7° Wall Angle	1066	+7 −7	39	+1 −1	110	+8 −11	84	+3 −4	175	+8 −11	206	+6 −8	250	+10 −11	38.1	+1.4 −1.0
6 TF30-P-408, MRT, Short Stack 3.5° Wall Angle	1069	+8 −7	31	+2 −2	94	+10 −14	70	+4 −6	161	+8 −12	192	+6 −10	239	+13 −12	32.8	+2.0 −1.0
7 TF30-P-408, MRT, Short Stack 0° Wall Angle	1066	+3 −1	53	+1 −2	107	+4 −2	89	+2 −2	174	+4 −5	203	+4 −5	248	+4 −4	50.5	+.3 −.6
8 J79-GE-10/17/19,MRT,Short Stack, 0° Wall Angle	1202	+2 −2	48	+2 −2	82	+3 −9	81	+5 −8	172	+7 −10	217	+10 −14	262	+8 −11	28.5	+.5 −.5
9 J79-GE-10/17/19,MRT, Tall Stack, 0° Wall Angle	1206	+4 −2	44	+3 −2	76	+1 −3	76	+2 −1	166	+3 −4	206	+4 −3	255	+3 −1	28.9	+.4 −.3
10 J79-GE-10/17/19,A/B,Tall Stack, 7° Wall Angle	*3265	+8 −10	86	+8 −9	527	+39 −21	240	+44 −19	593	+44 −19	638	+68 −29	846	+55 −27	19.1	+2.3 −1.9
11 J79-GE-10/17/19,A/B,Tall Stack, 3.5° Wall Angle	*3262	+4 −5	100	+6 −5	564	+30 −35	252	+8 −8	617	+33 −30	649	+60 −36	842	+66 −118	32.8	+3.9 −3.4
12 J79-GE-10/17/19,A/B,Tall Stack, 0° Wall Angle	*3261	+8 −5	108	+8 −8	574	+18 −15	260	+3 −3	626	+11 −11	652	+10 −12	878	+17 −17	30.9	+.8 −.6
13 J79-GE-10/17/19,A/B, Short Stack, 0° Wall Angle	*3262	+15 −12	98	+16 −9	559	+57 −42	257	+26 −10	612	+45 −19	643	+65 −26	858	+47 −29	22.1	+.6 −.6
14 J79-GE-10/17/19,A/B, Short Stack, 3.5° Wall Angle	*3258	+11 −26	100	+10 −10	522	+22 −24	247	+7 −7	593	+9 −6	626	+7 −9	843	+18 −11	23.9	+.7 −.5
15 J79-GE-10/17/19,A/B, Short Stack, 7° Wall Angle	*3263	+15 −11	80	+7 −5	509	+28 −32	249	+11 −8	594	+25 −28	656	+49 −24	836	+39 −45	18.9	+1.3 −1.3

*Calculated Values Based on Measured Air and Fuel Flow and Burner Efficiency of 95%

TABLE 8: EJECTOR SURFACE TEMPERATURES – SIDE CENTERLINE

	Configuration	Average Temperature (°F) with Maximum and Minimum Deviations													
		Thermocouple No. (See Figure 22 for Location)													
		T_{jet}		T_2		T_4		T_6		T_8		T_{10}		T_{12}		T_a	
1	TF30-P-408, MRT, Tall Stack 0° Wall Angle W/O Partition	1054	+4 −4	67	+1 −0	66	+1 −1	67	+1 −1	70	+0 −0	73	+1 −0	93	+0 −0	63.0	+.1 −.1
2	TF30-P-408, MRT, Tall Stack 0° Wall Angle	1070	+6 −5	53	+1 −1	51	+1 −1	51	+1 −0	54	+1 −1	58	+1 −2	78	+2 −3	51.5	+.6 −.3
3	TF30-P-408, MRT, Tall Stack 3.5° Wall Angle	1066	+7 −8	34	+1 −1	31	+1 −1	31	+1 −1	35	+2 −1	38	+2 −1	58	+6 −3	34.6	+.5 −.8
4	TF30-P-408, MRT, Tall Stack 7° Wall Angle	1067	+4 −5	46	+4 −4	46	+4 −4	46	+4 −3	49	+4 −4	53	+4 −3	74	+5 −4	48.4	+2.2 −2.7
5	TF30-P-408, MRT, Short Stack 7° Wall Angle	1066	+7 −7	39	+1 −1	36	+0 −0	36	+1 −1	41	+2 −1	45	+2 −2	69	+6 −4	38.1	+1.4 −1.0
6	TF30-P-408, MRT, Short Stack 3.5° Wall Angle	1069	+8 −7	31	+3 −4	29	+3 −4	28	+2 −3	33	+2 −2	36	+1 −1	58	+2 −3	32.8	+2.0 −1.0
7	TF30-P-408, MRT, Short Stack 0° Wall Angle	1066	+3 −1	52	+2 −2	51	+0 −1	51	+0 −1	55	+1 −1	58	+1 −1	80	+1 −2	50.5	+.3 −.6
8	J79-GE-10/17/19,MRT,Short Stack, 0° Wall Angle	1202	+2 −2	41	+5 −5	36	+4 −3	33	+2 −2	35	+3 −3	36	+0 −2	44	+2 −4	28.5	+.5 −.5
9	J79-GE-10/17/19,MRT,Tall Stack, 0° Wall Angle	1206	+4 −2	37	+2 −2	34	+1 −1	32	+1 −1	33	+1 −1	33	+1 −1	40	+1 −1	28.9	+.4 −.3
10	J79-GE-10/17/19,A/B,Tall Stack, 7° Wall Angle	*3265	+8 −10	56	+6 −7	81	+10 −9	86	+9 −8	142	+12 −12	161	+8 −11	245	+12 −15	19.1	+2.3 −1.9
11	J79-GE-10/17/19,A/B,Tall Stack, 3.5° Wall Angle	*3262	+4 −5	70	+2 −2	94	+3 −4	99	+4 −5	154	+6 −8	174	+8 −8	258	+10 −11	32.8	+3.9 −3.4
12	J79-GE-10/17/19,A/B,Tall Stack, 0° Wall Angle	*3261	+8 −5	74	+4 −5	96	+4 −6	100	+4 −6	155	+7 −8	173	+9 −7	259	+12 −11	30.9	+.8 −.6
13	J79-GE-10/17/19,A/B, Short Stack, 0° Wall Angle	*3262	+15 −12	65	+7 −5	87	+8 −6	91	+6 −4	144	+6 −4	163	+4 −4	247	+6 −6	22.1	+.6 −.6
14	J79-GE-10/17/19,A/B, Short Stack, 3.5° Wall Angle	*3258	+11 −26	67	+5 −5	88	+7 −7	92	+6 −8	144	+11 −14	163	+11 −13	245	+16 −18	23.9	+.7 −.5
15	J79-GE-10/17/19,A/B,Short Stack, 7° Wall Angle	*3263	+15 −11	53	+4 −5	83	+8 −7	101	+8 −12	173	+15 −19	192	+18 −20	284	+21 −23	18.9	+1.3 −1.3

* Calculated Values Based on Measured Air and Fuel Flow and Burner Efficiency of 95%

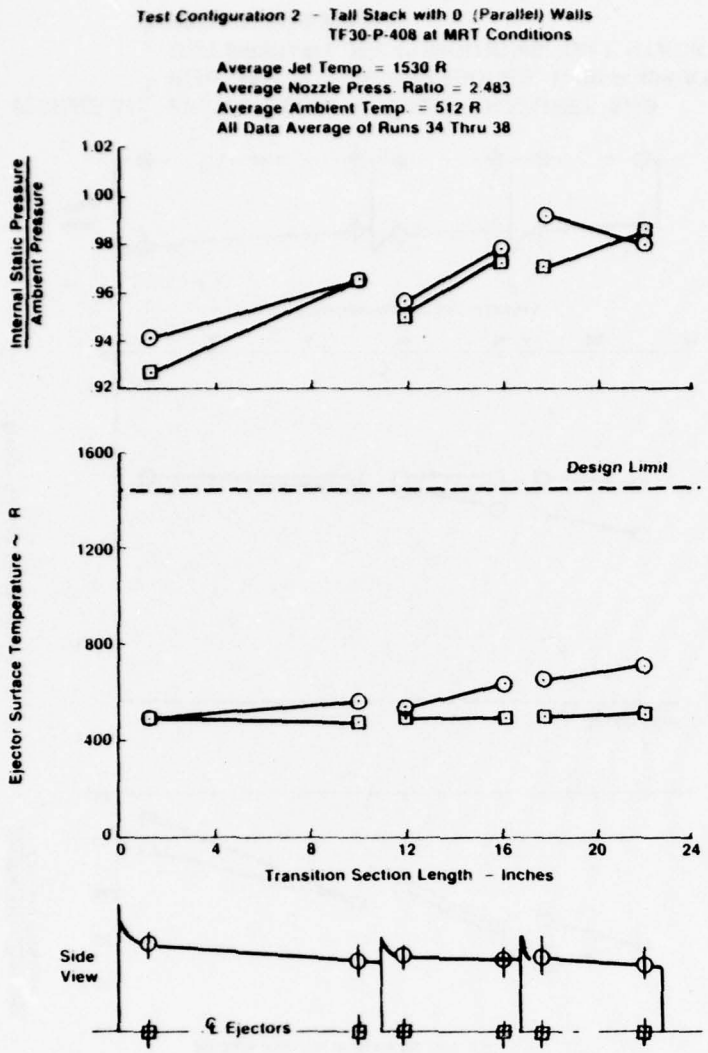

FIGURE 29: EJECTOR SURFACE TEMPERATURES AND INTERNAL STATIC PRESSURES, TF30-P-408 AT MRT PRIMARY JET CONDITIONS, TALL STACK WITH 0° (PARALLEL) SIDEWALLS

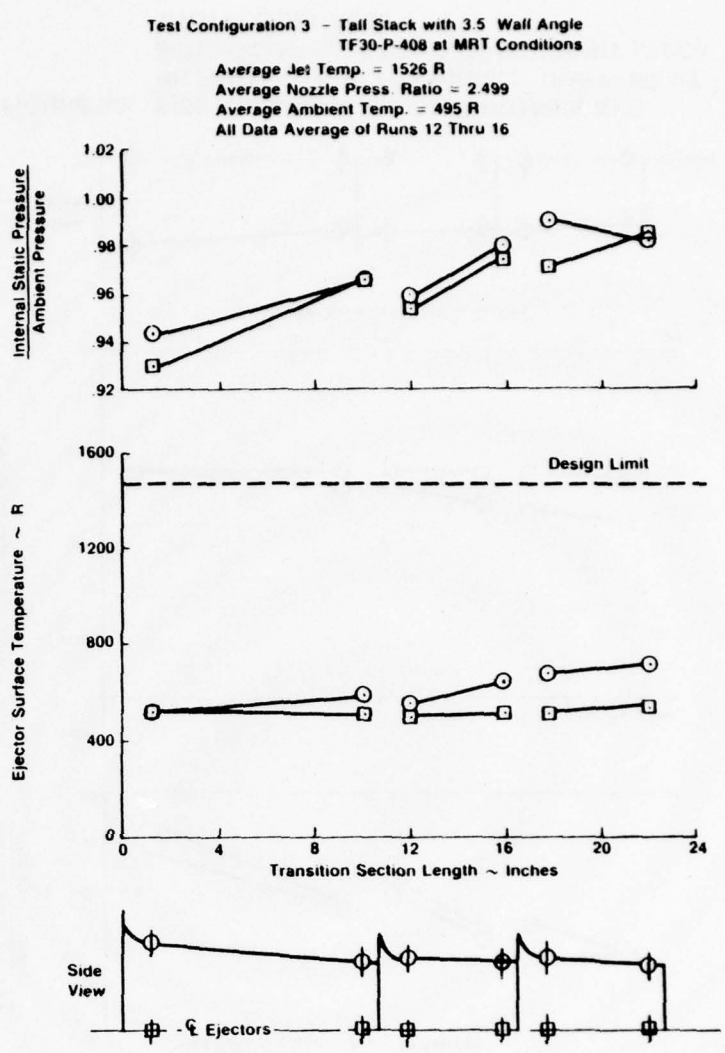

FIGURE 30: EJECTOR SURFACE TEMPERATURES AND INTERNAL STATIC PRESSURES, TF30-P-408 AT MRT PRIMARY JET CONDITIONS, TALL STACK WITH 3.5° SIDEWALLS

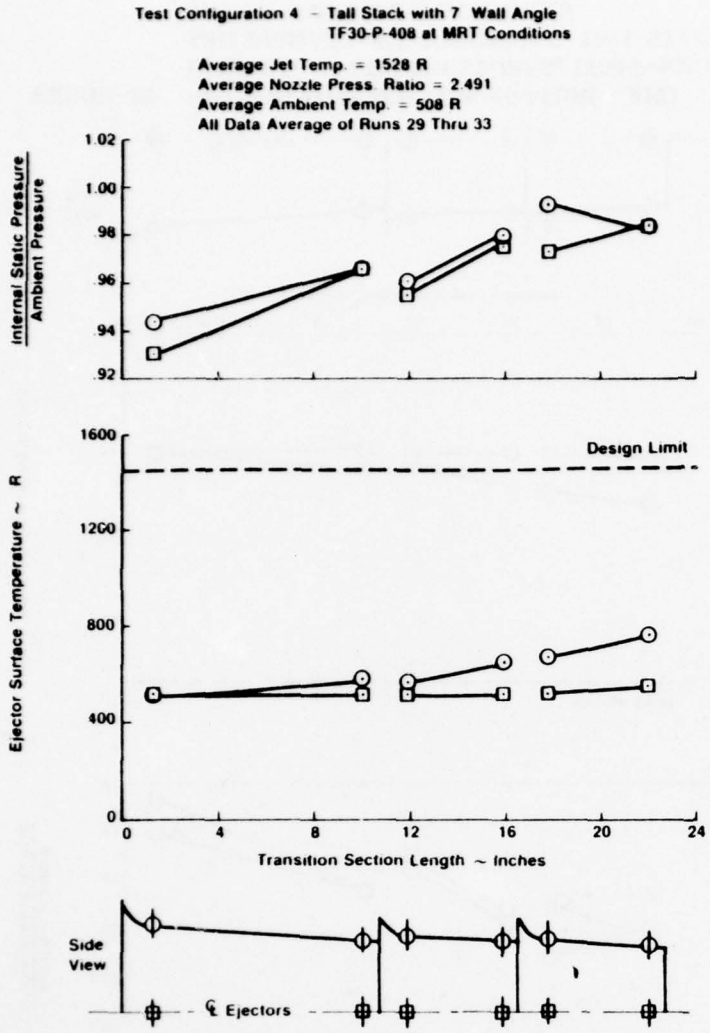

FIGURE 31: EJECTOR SURFACE TEMPERATURES AND INTERNAL STATIC PRESSURES, TF30-P-408 AT MRT PRIMARY JET CONDITIONS, TALL STACK WITH 7° SIDEWALLS

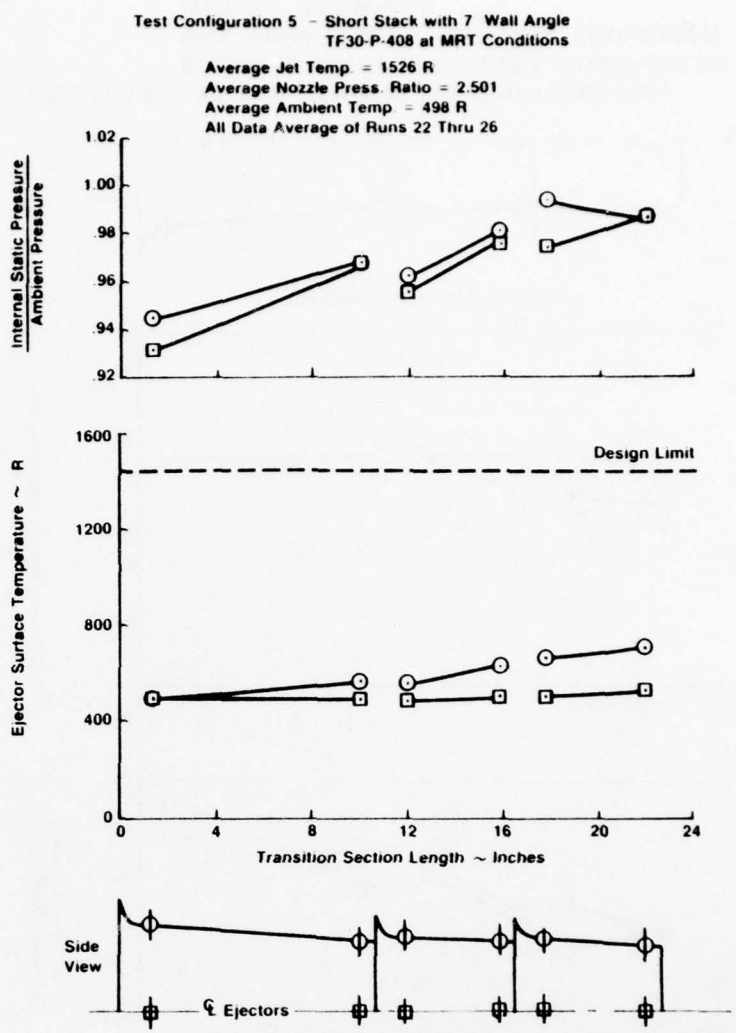

FIGURE 32: EJECTOR SURFACE TEMPERATURES AND INTERNAL STATIC PRESSURES, TF30-P-408 AT MRT PRIMARY JET CONDITIONS, SHORT STACK WITH 7° SIDEWALLS

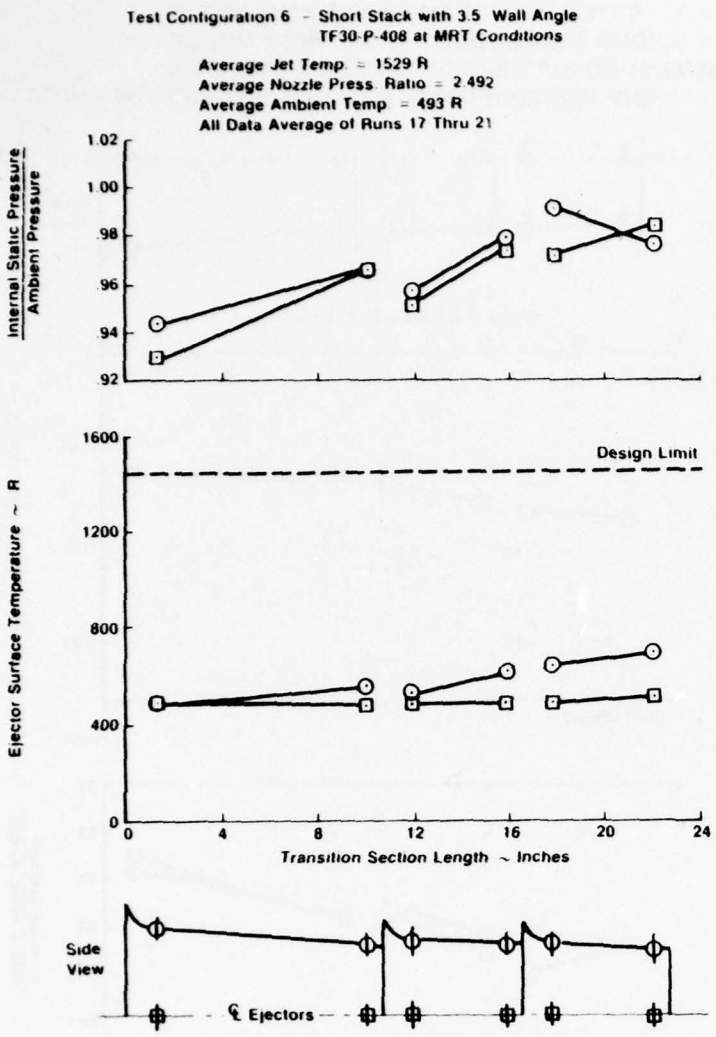

FIGURE 33: EjECTOR SURFACE TEMPERATURES AND INTERNAL STATIC PRESSURES, TF30-P-408 AT MRT PRIMARY JET CONDITIONS, SHORT STACK WITH 3.5° SIDEWALLS

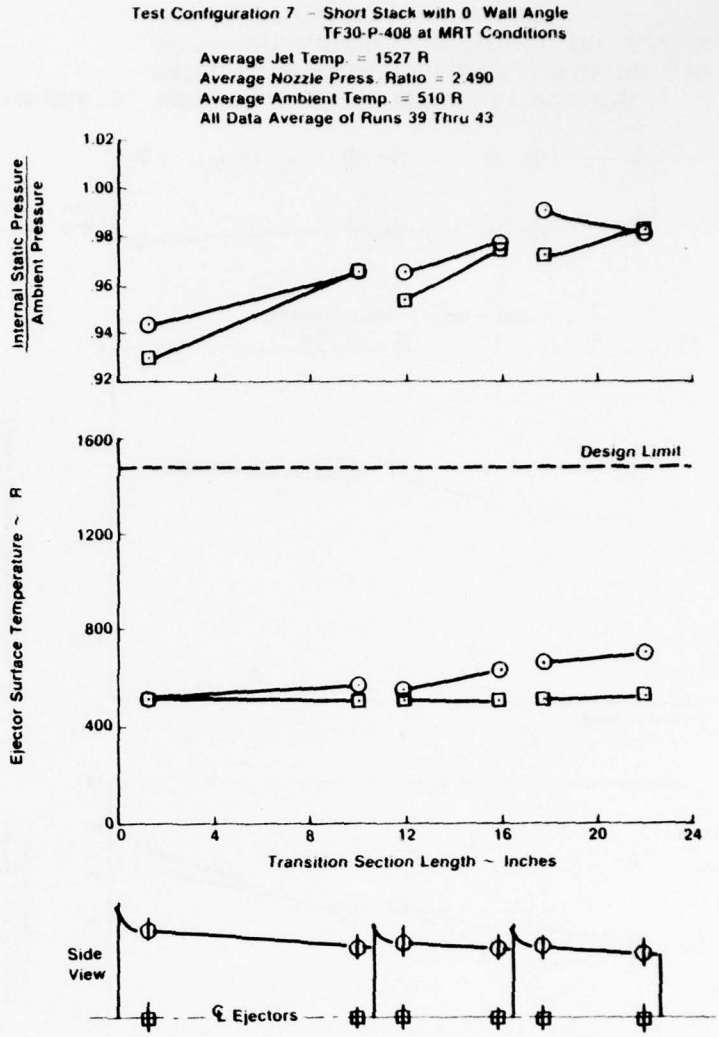

FIGURE 34: EjECTOR SURFACE TEMPERATURES AND INTERNAL STATIC PRESSURES, TF30-P-408 AT MRT PRIMARY JET CONDITIONS, SHORT STACK WITH 0° (PARALLEL) SIDEWALLS

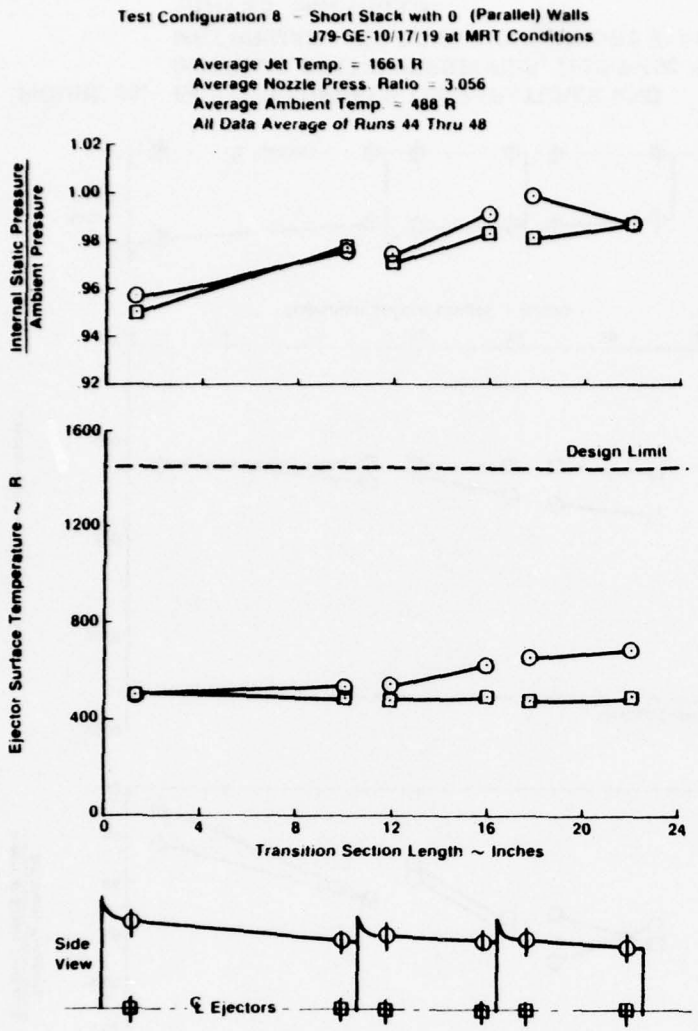

FIGURE 35: EJECTOR SURFACE TEMPERATURES AND INTERNAL STATIC PRESSURES, J79-GE-10/17/19 AT MRT PRIMARY JET CONDITIONS, SHORT STACK WITH 0° (PARALLEL) SIDEWALLS

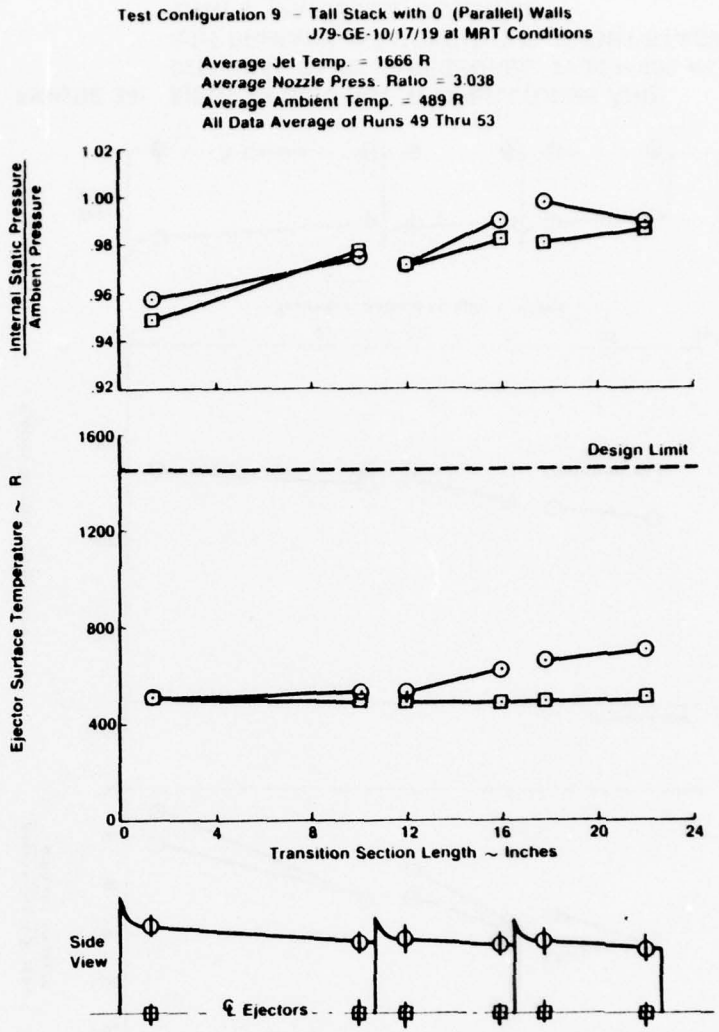

FIGURE 36: EJECTOR SURFACE TEMPERATURES AND INTERNAL STATIC PRESSURES, J79-GE-10/17/19 AT MRT PRIMARY JET CONDITIONS, TALL STACK WITH 0° (PARALLEL) SIDEWALLS

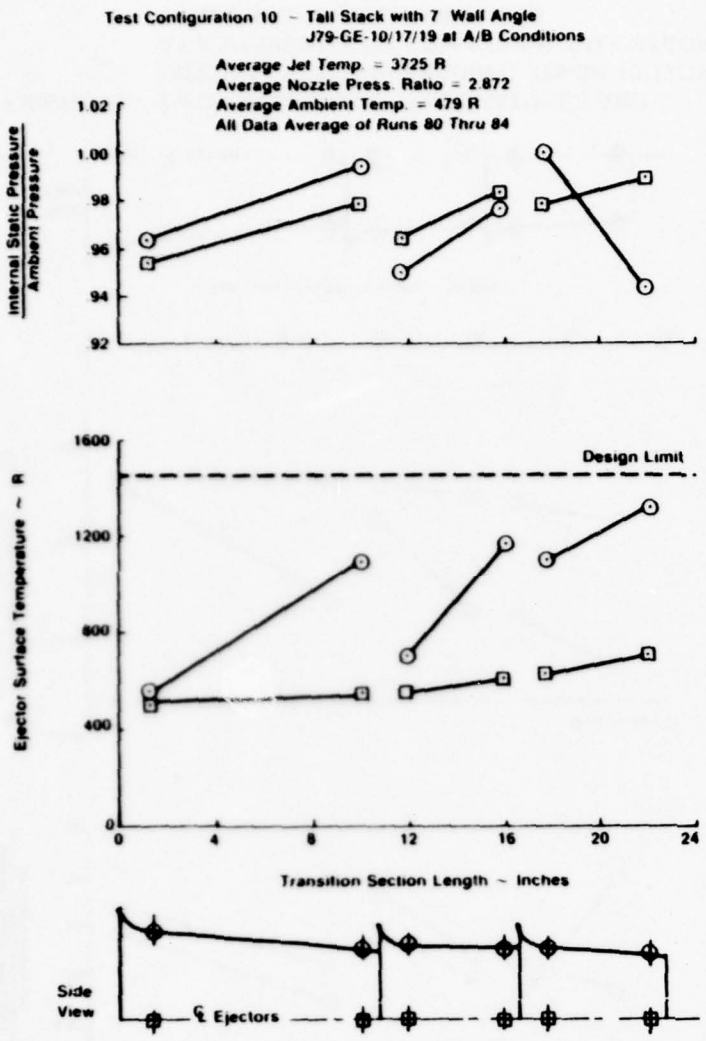

FIGURE 37: EJECTOR SURFACE TEMPERATURES AND INTERNAL STATIC PRESSURES, J79-GE-10/17/19 AT A/B PRIMARY JET CONDITIONS, TALL STACK WITH 7° (PARALLEL) SIDEWALLS

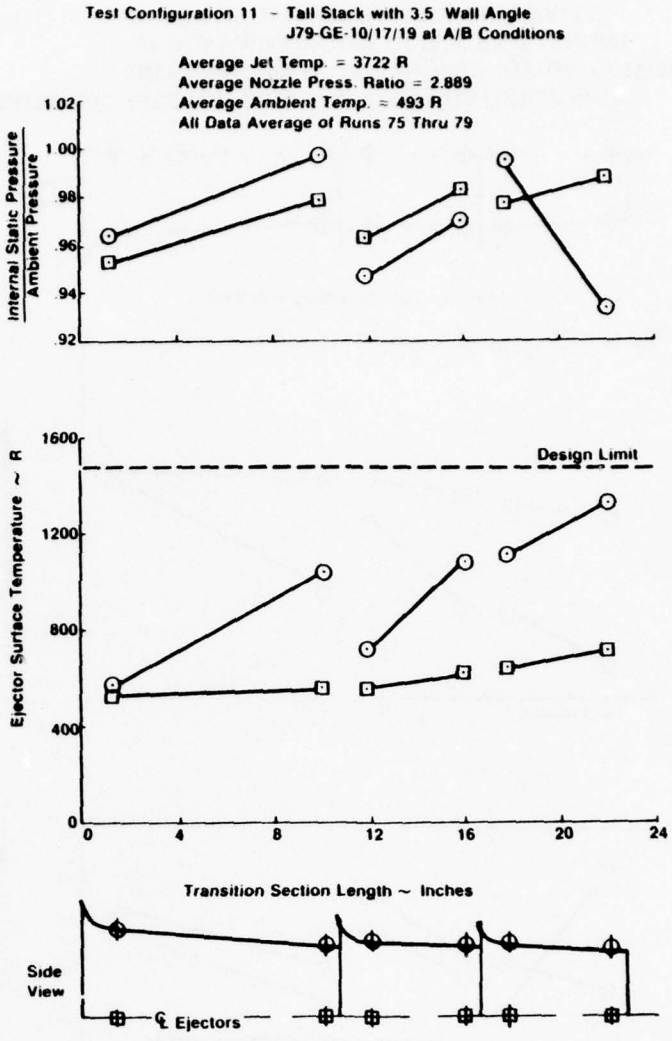

FIGURE 38: EJECTOR SURFACE TEMPERATURES AND INTERNAL STATIC PRESSURES, J79-GE-10/17/19 AT A/B PRIMARY JET CONDITIONS, TALL STACK WITH 3.5° SIDEWALLS

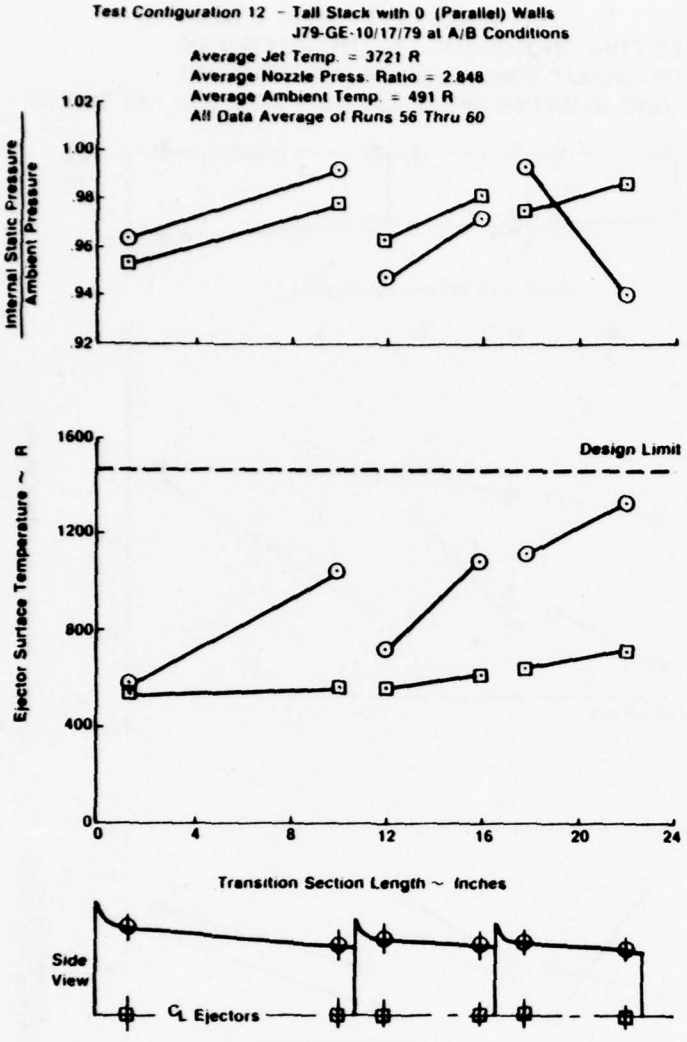

FIGURE 39: EJECTOR SURFACE TEMPERATURES AND INTERNAL STATIC PRESSURES, J79-GE-10/17/19 AT A/B PRIMARY JET CONDITIONS, TALL STACK WITH 0° (PARALLEL) SIDEWALLS

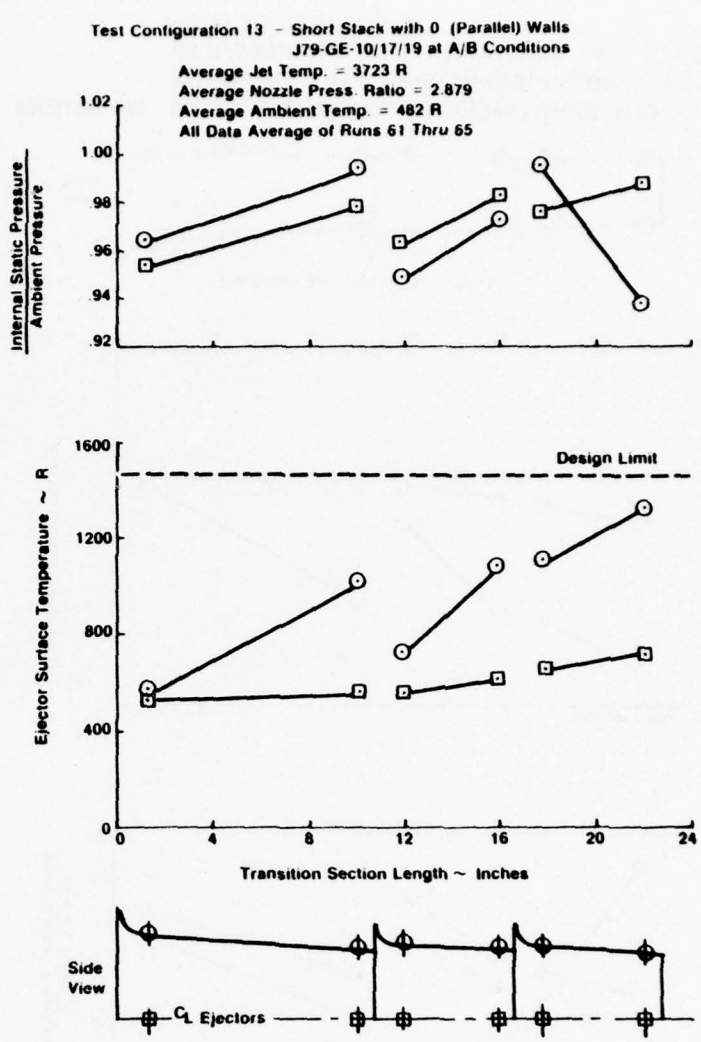

FIGURE 40: EJECTOR SURFACE TEMPERATURES AND INTERNAL STATIC PRESSURES, J79-GE-10/17/19 AT A/B PRIMARY JET CONDITIONS, SHORT STACK WITH 0° (PARALLEL) SIDEWALLS

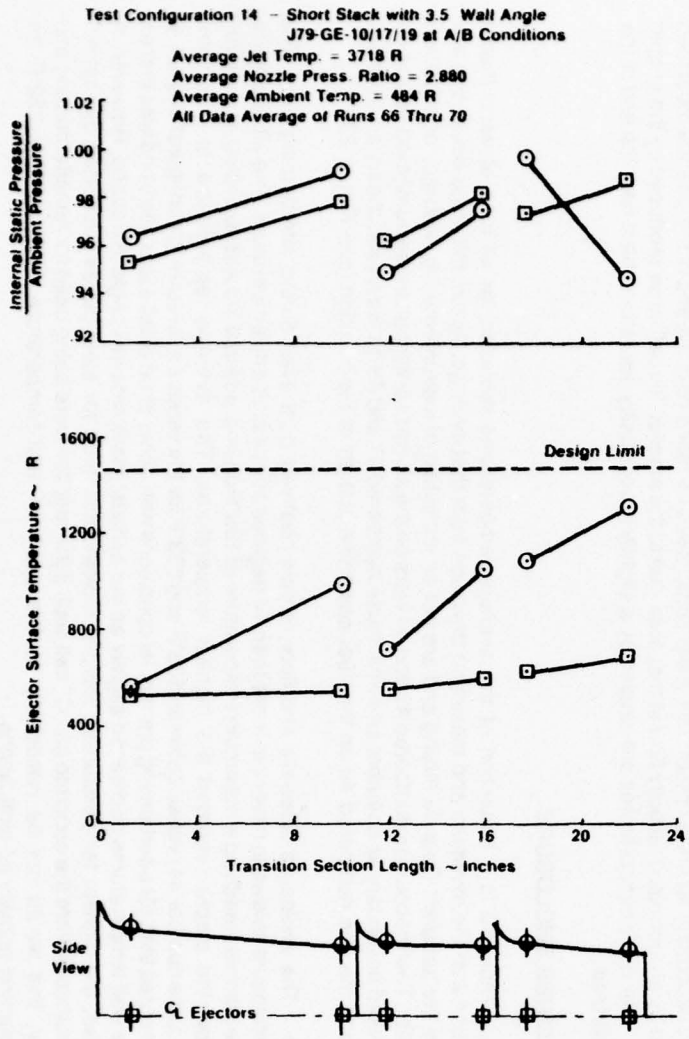

FIGURE 41: EJECTOR SURFACE TEMPERATURES AND INTERNAL STATIC PRESSURES, J79-GE-10/17/19 AT A/B PRIMARY JET CONDITIONS, SHORT STACK WITH 3.5° SIDEWALLS

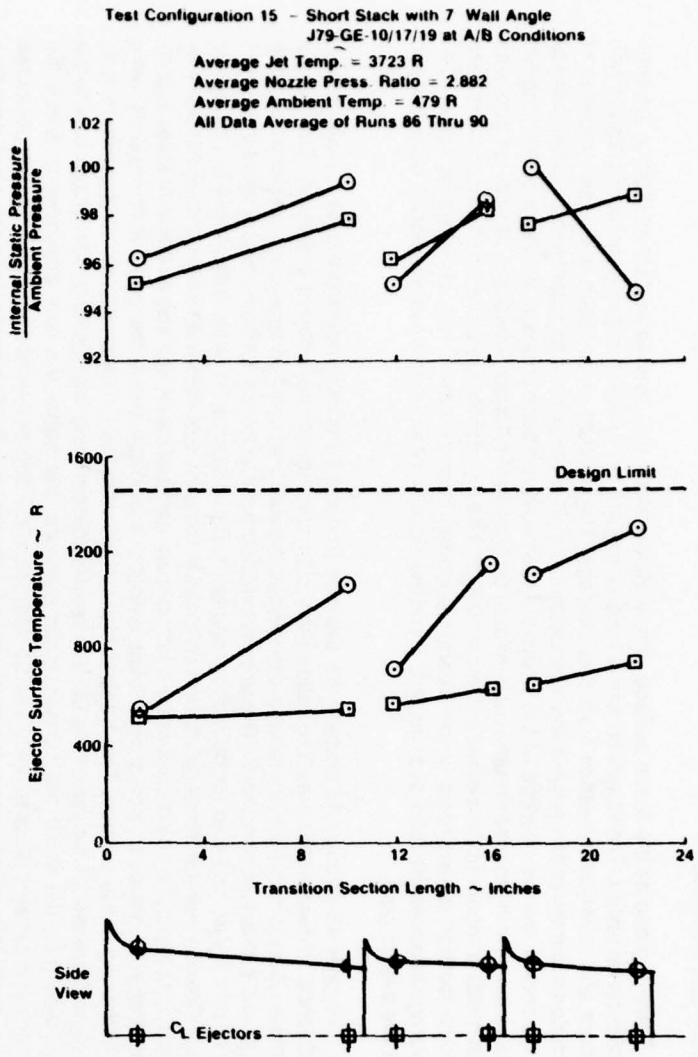

FIGURE 42: EJECTOR SURFACE TEMPERATURES AND INTERNAL STATIC PRESSURES, J79-GE-10/17/19, PRIMARY JET CONDITIONS, SHORT STACK WITH 7° SIDEWALLS

2. COANDA SURFACE.

a. Table 9 presents the metal surface temperatures along the Coanda surface centerline for each model configuration tested. The values shown are the average for all runs at that particular configuration with the maximum and minimum deviation from that average. The amount of deviation is not an indication of instrumentation accuracy or of repeatability of condition setup, but rather of the turbulent nature of the Coanda mixing. Also shown are the average of the primary jet exhaust temperatures and average of the ambient temperatures along with their maximum and minimum deviations. As stated previously, the design goal was to maintain metal component temperatures below 1000°F. The highest temperature levels occur at the third thermocouple location downstream of the Coanda entrance (approximately 12 inches model scale). The highest average temperature recorded was 912°F and the highest for any single run was 956°F, both of which are within the design goal.

b. Figures 43 through 46 present the average Coanda surface temperature data, as well as the average Coanda surface static pressure ratios (flow side static pressure/ambient pressure). The figures compare these data for model configurations with various exhaust stack wall divergence angles and the same stack height and primary jet conditions. These data exhibit the same trends for both military rated thrust and afterburning primary jet and also for both short and tall exhaust stacks. In each case, there is virtually no difference in Coanda surface temperature with changes in exhaust stack sidewall angle until about half way up the surface. At that point, the configurations with diffuser exhaust stack wall angles begin to show slightly lower temperatures; however, not a significant amount, especially since the peak temperatures were recorded further down the surface. This trend is also observed in the Coanda surface static pressure ratio data. These data are one of the yardsticks usually used for determining the quality of flow attachment to the Coanda surface (i.e., the lower the surface static pressure, the better the flow attachment). Since the configurations with exhaust stack sidewalls at 3.5 degrees and 7 degrees exhibit lower surface temperatures with lower surface static pressure ratios, one might conclude that the Coanda mixing is improved and the flow attachment better than with the 0 degree sidewalls. However, the secondary air entrainment data shown previously belies that conclusion since the configurations with higher angled stack sidewalls produced decreased secondary air entrainment. The lower static pressure ratios near the end of the Coanda must then be caused by an increased velocity flow in that area due to the smaller "throat" area produced by the angled sidewalls. The lower temperatures are caused by a slightly lower quality flow attachment near the end of the Coanda surface.

3. LOWER ENCLOSURE.

a. Table 10 is a tabulation of the average temperatures recorded for all runs at each model configuration with the minimum and maximum deviation from that average. Again, the large deviations are caused by the turbulent Coanda mixing and are not an indication of instrumentation accuracy or condition repeatability. Thermocouples numbered 43 and 44 were on the aft wall centerline, those numbered 45 and 46 on the forward secondary air chamber sidewall, those numbered 47 and 48 on the aft secondary air chamber sidewall and the one numbered 49 on the floor centerline just aft of the partition (see Figure 23).

b. The enclosure sidewalls and floor remain relatively cool even during afterburning runs. The forward enclosure sidewalls never got more than 14 degrees above ambient temperature. The aft enclosure was a little warmer, reaching a maximum temperature of 189°F on one sidewall. As was expected, the aft wall (just below the stack) recorded the highest temperatures. The average temperature at that point (thermocouple number 44) varied between 553°F and 633°F for the various afterburning configurations run. It should be noted that, for afterburning primary jet conditions with either short of tall stack, the trend was that aft enclosure wall temperatures decreased slightly as the exhaust stack sidewall angle increased. However, in either case, the highest temperatures recorded indicate the need for steel plates supported by thermal isolated standoffs from the concrete aft "C" cell wall. If the test cell were being used for nonafterburning test runs only, this would not be necessary as the peak aft wall temperature reached only 252°F for nonafterburning primary jet simulations.

TABLE 9: COANDA SURFACE TEMPERATURES – CENTERLINE

	Configuration	Average Temperature (°F) with Maximum and Minimum Deviations										
		Thermocouple No. (See Figure 22 for Location)										
		T_{jet}	T_{13}	T_{14}	T_{15}	T_{16}	T_{17}	T_{18}	T_{19}	T_{20}	T_{21}	T_{22}
1	TF30-P-408, MRT, Tall Stack 0° Wall Angle W/O Partition	1054 +4 −4	138 +1 −1	290 +0 −0	329 +0 −1	262 +0 −1	209 +1 −1	206 +2 −2	217 +1 −1	222 +0 −0	225 +1 −1	238 +1 −1
2	TF30-P-408, MRT, Tall Stack 0° Wall Angle	1070 +6 −5	118 +5 −5	258 +6 −9	280 +8 −6	204 +7 −9	171 +4 −4	186 +10 −7	197 +10 −6	200 +10 −5	203 +11 −7	216 +11 −9
3	TF30-P-408, MRT, Tall Stack 3.5° Wall Angle	1066 +7 −8	94 +8 −5	244 +12 −8	276 +10 −8	200 +5 −5	158 +3 −5	164 +8 −5	172 +9 −6	170 +11 −5	172 +11 −6	170 +17 −9
4	TF30-P-408, MRT, Tall Stack 7° Wall Angle	1067 +4 −5	112 +7 −6	262 +5 −6	288 +7 −3	209 +7 −6	171 +4 −3	182 +8 −4	190 +10 −6	188 +11 −7	190 +11 −9	162 +9 −6
5	TF30-P-408, MRT, Short Stack 7° Wall Angle	1066 +7 −7	104 +10 −6	254 +9 −7	282 +4 −5	206 +4 −3	170 +8 −6	180 +13 −10	186 +13 −9	183 +14 −10	185 +14 −9	163 +16 −11
6	TF30-P-408, MRT, Short Stack 3.5° Wall Angle	1069 +9 −7	97 +5 −5	245 +5 −11	272 +8 −5	196 +6 −9	158 +2 −3	167 +8 −7	176 +8 −10	176 +9 −9	179 +10 −10	188 +13 −13
7	TF30-P-408, MRT, Short Stack 0° Wall Angle	1066 +3 −1	121 +4 −4	257 +3 −3	275 +3 −2	199 +5 −5	172 +4 −3	190 +5 −3	203 +5 −4	206 +5 −4	209 +5 −4	224 +6 −4
8	J79-GE-10/17/19, MRT, Short Stack, 0° Wall Angle	1202 +2 −2	134 +17 −8	282 +12 −11	289 +15 −15	202 +14 −14	163 +11 −10	168 +13 −12	177 +14 −13	179 +16 −14	183 +18 −15	203 +18 −17
9	J79-GE-10/17/19, MRT, Tall Stack, 0° Wall Angle	1206 +4 −2	122 +7 −4	271 +11 −7	279 +13 −8	187 +11 −5	149 +9 −4	156 +8 −4	163 +9 −5	165 +10 −5	169 +10 −5	185 +14 −6
10	J79-GE-10/17/19, A/B, Tall Stack, 7° Wall Angle	*3265 +8 −10	238 +32 −25	658 +66 −44	842 +93 −52	712 +86 −47	525 +71 −44	466 +55 −42	476 +47 −39	473 +44 −32	479 +48 −35	388 +39 −28
11	J79-GE-10/17/19, A/B, Tall Stack, 3.5° Wall Angle	*3262 +4 −5	238 +11 −21	667 +28 −40	871 +30 −50	749 +32 −31	556 +32 −31	479 +26 −19	482 +20 −22	475 +15 −18	482 +17 −18	428 +21 −25
12	J79-GE-10/17/19, A/B, Tall Stack, 0° Wall Angle	*3261 +8 −5	273 +19 −34	721 +38 −55	912 +44 −63	766 +37 −56	566 +35 −47	498 +40 −41	508 +37 −41	509 +33 −42	515 +33 −43	529 +37 −47
13	J79-GE-10/17/19, A/B, Short Stack, 0° Wall Angle	*3262 +15 −12	244 +32 −23	675 +38 −32	872 +71 −63	742 +88 −77	555 +80 −68	501 +69 −54	518 +68 −54	522 +69 −57	526 +71 −56	538 +98 −66
14	J79-GE-10/17/19, A/B, Short Stack, 3.5° Wall Angle	*3258 +11 −26	249 +28 −25	676 +51 −40	865 +48 −49	729 +55 −50	542 +43 −44	489 +42 −37	501 +46 −37	492 +45 −32	497 +43 −32	445 +37 −37
15	J79-GE-10/17/19, A/B, Short Stack, 7° Wall Angle	*3263 +15 −11	237 +43 −29	649 +86 −58	821 +112 −75	865 +106 −62	504 +72 −41	542 +59 −33	468 +56 −32	471 +54 −35	475 +56 −37	387 +43 −27

* Calculated Values Based on Measured Air and Fuel Flow and Burner Efficiency of 95%

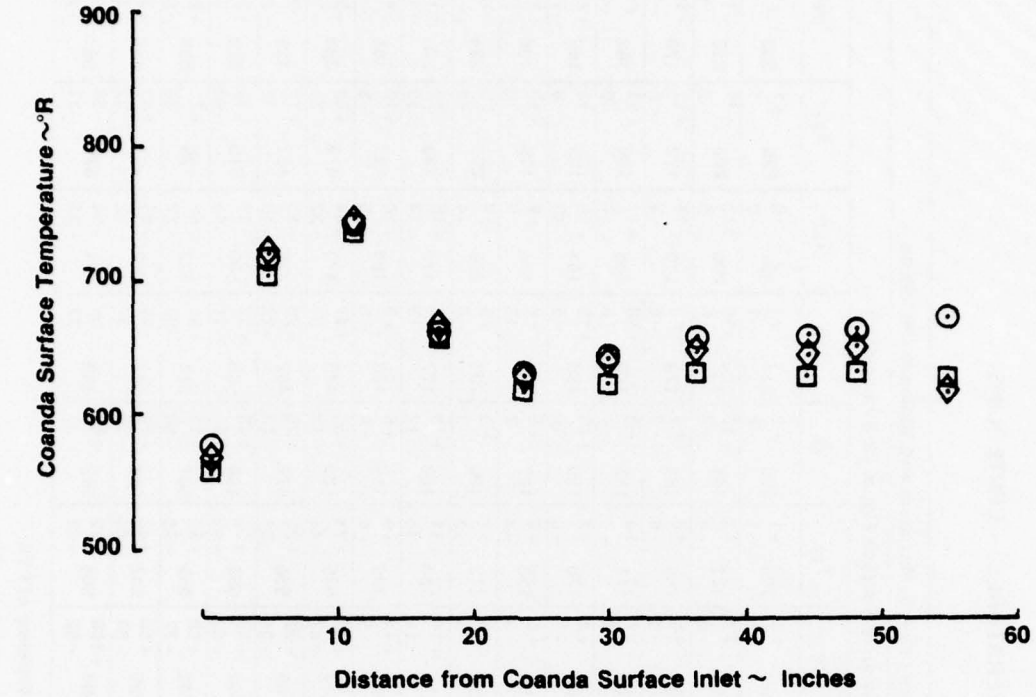

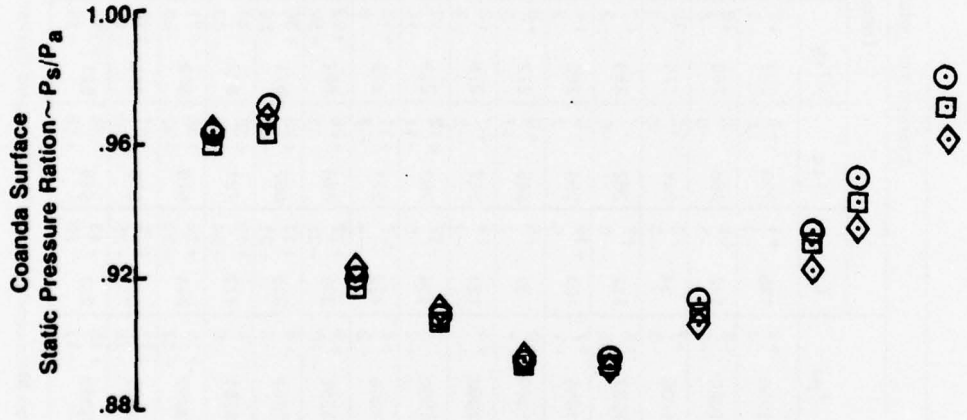

Simulated TF30-P-408 at Military Rated Thrust

Symbol	Config No.	Run No.	Wall Angle	Stack Height	Average Run Conditions			
					EGT ~ (°R)	NPR	Pa ~ (psia)	Ta ~ (°R)
⊙	2	34-38	0°	Tall	1530	2.483	14.078	515
⊡	3	12-16	3.5°	Tall	1526	2.499	14.212	495
◇	4	29-33	7.0°	Tall	1527	2.491	14.078	508

FIGURE 43: COANDA SURFACE TEMPERATURES AND STATIC PRESSURE RATIOS, WITH VARIATION IN EXHAUST STACK WALL ANGLE, MRT ENGINE CONDITIONS AND TALL STACK

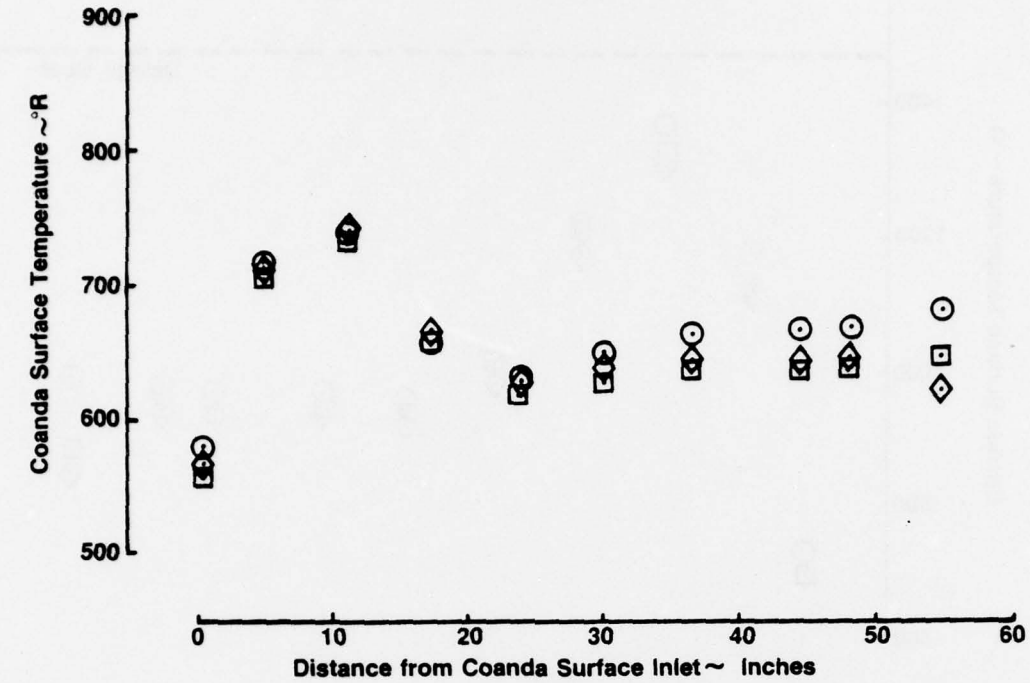

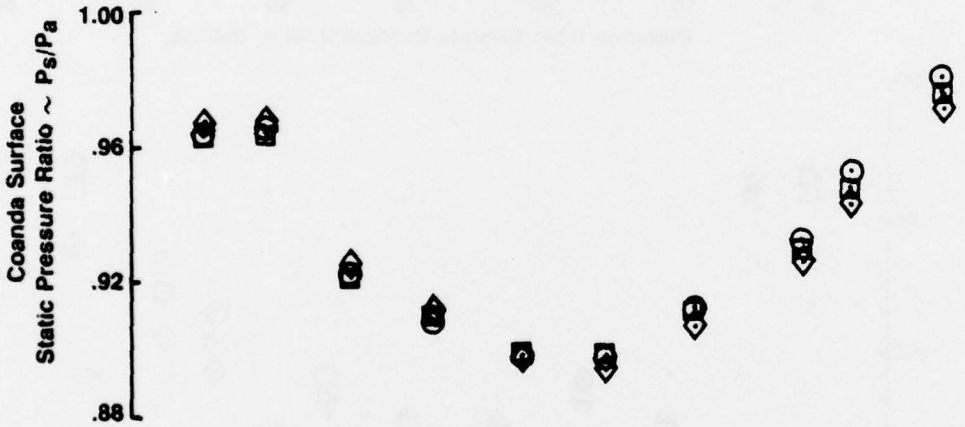

Simulated TF30-P-408 at Military Rated Thrust

Symbol	Config No.	Run No.	Wall Angle	Stack Height	Average Run Conditions			
					EGT ~ (°R)	NPR	Pa ~ (psia)	Ta ~ (°R)
⊙	7	39-43	0°	Short	1526	2.490	14.084	511
⊡	6	17-21	3.5°	Short	1529	2.492	14.171	493
◇	5	22-26	7.0°	Short	1526	2.501	14.015	498

FIGURE 44: COANDA SURFACE TEMPERATURES AND STATIC PRESSURE RATIOS, WITH VARIATION IN EXHAUST STACK WALL ANGLE, MRT ENGINE CONDITIONS AND SHORT STACK

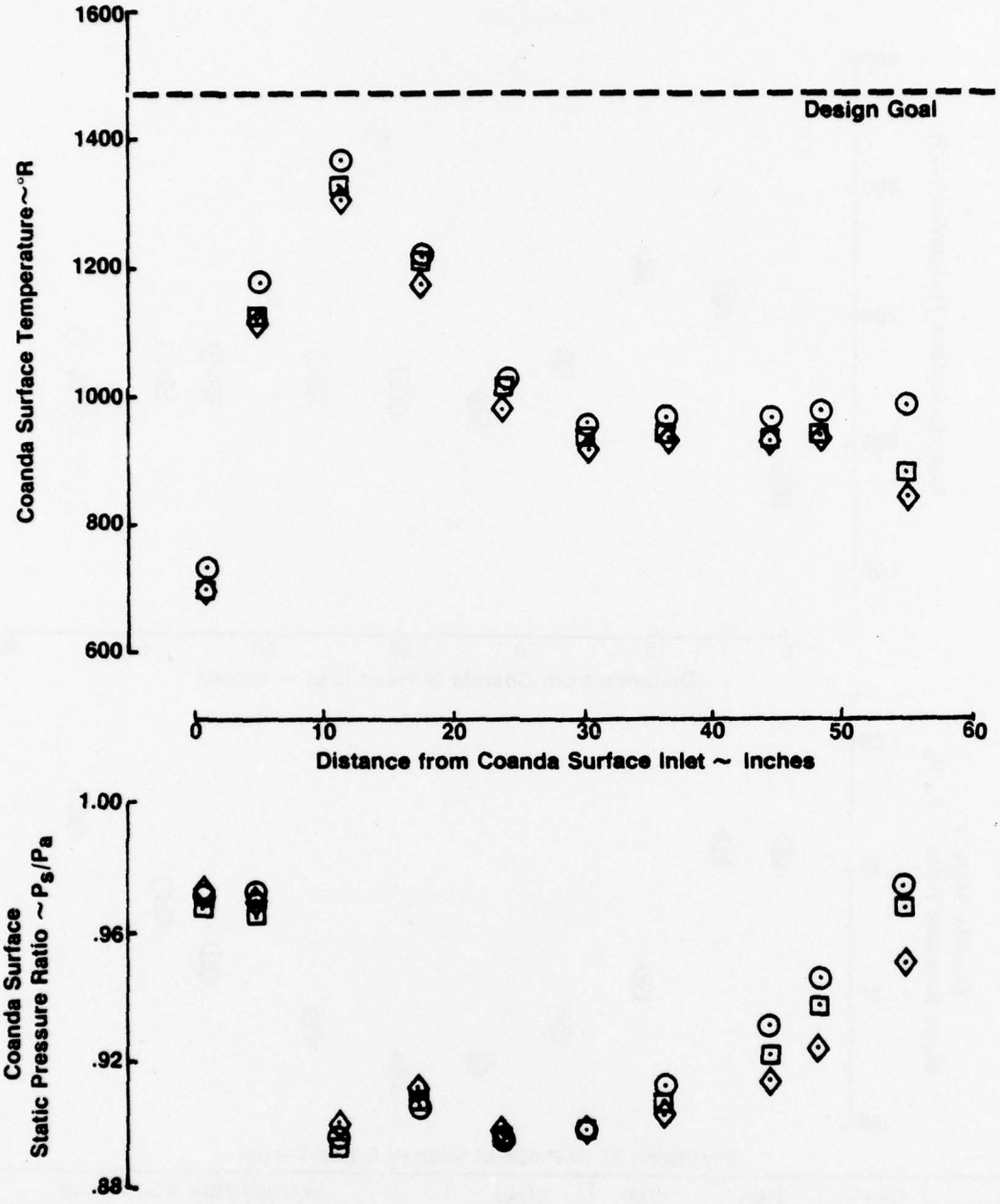

Simulated J79-GE-10/17/19 at Afterburning Conditions

Symbol	Config No.	Run No.	Wall Angle	Stack Height	Average Run Conditions			
					EGT ~ (°R)	NPR	Pa ~ (psia)	Ta ~ (°R)
⊙	12	56-60	0°	Tall	3721	2.848	14.014	491
⊡	11	75-79	3.5°	Tall	3722	2.889	14.004	493
◇	10	80-84	7.0°	Tall	3725	2.872	14.154	479

FIGURE 45: COANDA SURFACE TEMPERATURES AND STATIC PRESSURE RATIOS, WITH VARIATION IN EXHAUST STACK WALL ANGLE, A/B ENGINE CONDITIONS AND TALL STACK

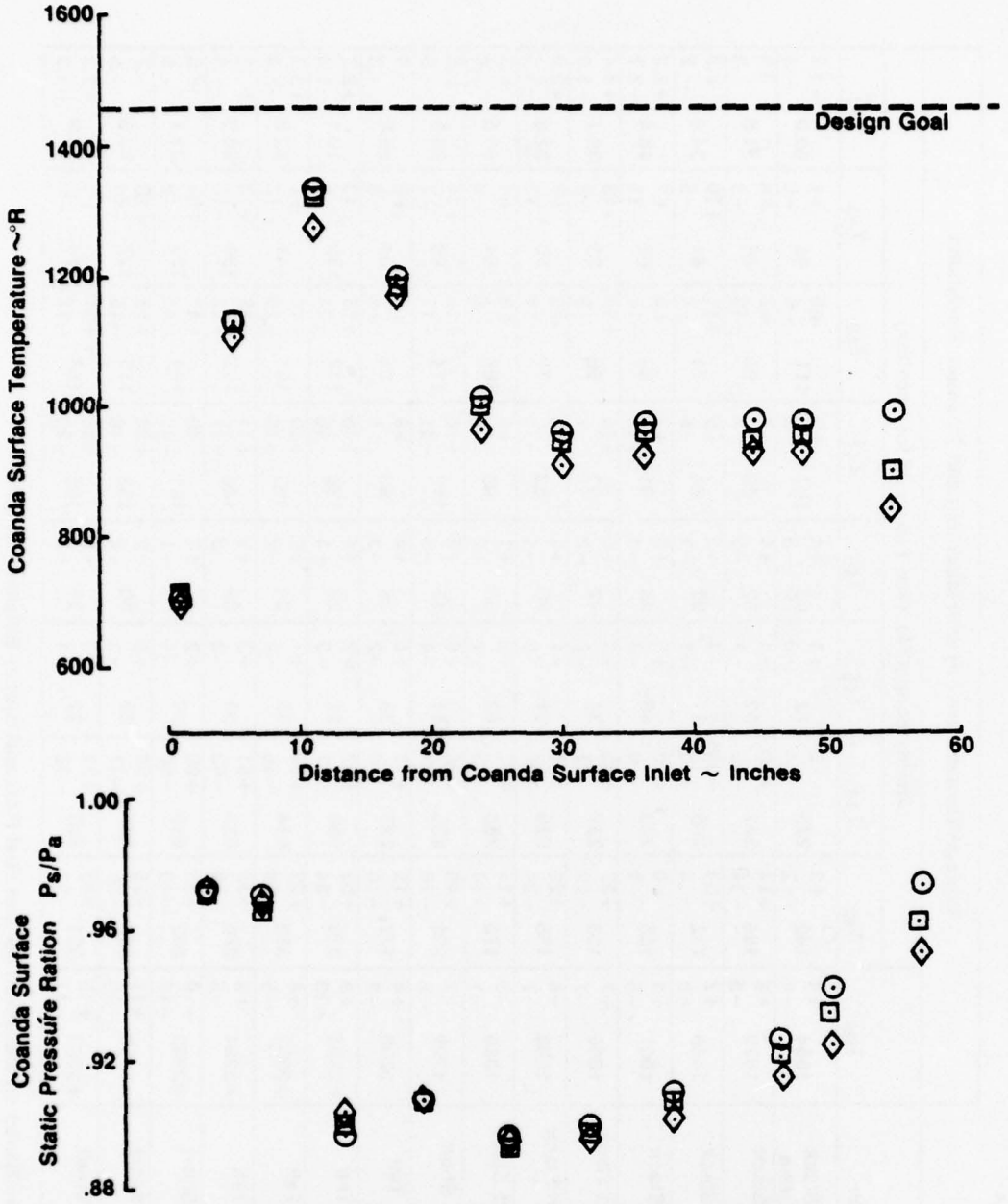

Simulated J79-GE-10/17/19 at Afterburning Conditions

Symbol	Config No.	Run No.	Wall Angle	Stack Height	Average Run Conditions			
					EGT ~ (°R)	NPR	Pa ~ (psia)	Ta ~ (°R)
⊙	13	61-65	0°	Short	3722	2.879	14.178	482
⊡	14	66-70	3.5°	Short	3718	2.880	14.134	484
◇	15	86-90	7.0°	Short	3723	2.882	14.168	479

FIGURE 46: COANDA SURFACE TEMPERATURES AND STATIC PRESSURE RATIOS, WITH VARIATION IN EXHAUST STACK WALL ANGLE, A/B ENGINE CONDITIONS AND SHORT STACK

TABLE 10: LOWER ENCLOSURE INTERNAL SURFACE TEMPERATURES

	Configuration	Average Temperature (°F) with Maximum and Minimum Deviations															
		Thermocouple No. (See Figure 23 for Location)															
		T_{jet}		T_{43}		T_{44}		T_{45}		T_{46}		T_{47}		T_{48}		T_{49}		T_a	
1	TF30-P-408, MRT, Tall Stack 0° Wall Angle W/O Partition	1054	+4 −4	182	+3 −2	265	+5 −4	72	+1 −0	88	+4 −3	107	+2 −2	111	+0 −0	95	+1 −0	63.0	+1.1 −.1
2	TF30-P-408, MRT, Tall Stack 0° Wall Angle	1070	+6 −5	166	+14 −14	241	+18 −19	52	+1 −1	52	+1 −0	89	+7 −8	99	+6 −10	85	+6 −8	51.5	+6 −.3
3	TF30-P-408, MRT, Tall Stack 3.5° Wall Angle	1066	+7 −8	132	+34 −14	206	+33 −14	31	+1 −1	32	+2 −1	64	+9 −5	71	+11 −4	61	+10 −5	34.6	+.5 −.8
4	TF30-P-408, MRT, Tall Stack 7° Wall Angle	1067	+4 −5	155	+8 −9	230	+10 −9	46	+5 −4	46	+6 −4	91	+7 −12	93	+8 −14	82	+7 −11	48.4	+2.2 −2.7
5	TF30-P-408, MRT, Short Stack 7° Wall Angle	1066	+7 −7	166	+37 −19	237	+35 −21	38	+3 −2	42	+6 −2	92	+15 −7	98	+15 −8	83	+13 −8	38.1	+1.4 −1.0
6	TF30-P-408, MRT, Short Stack 3.5° Wall Angle	1069	+8 −7	155	+26 −24	225	+26 −26	31	+1 −0	30	+1 −1	89	+13 −16	79	+9 −11	80	+7 −13	32.8	+2.0 −1.0
7	TF30-P-408, MRT, Short Stack 0° Wall Angle	1066	+3 −1	176	+11 −14	250	+11 −13	52	+2 −1	54	+1 −2	99	+5 −9	106	+3 −5	94	+4 −8	50.5	+.3 −.6
8	J79-GE-10/17/19, MRT, Short Stack, 0° Wall Angle	1202	+2 −2	206	+40 −19	252	+36 −21	41	+4 −4	43	+3 −5	110	+16 −11	114	+18 −11	98	+14 −7	28.5	+.5 −.5
9	J79-GE-10/17/19, MRT, Tall Stack, 0° Wall Angle	1206	+4 −2	177	+15 −10	227	+17 −9	33	+4 −2	36	+4 −3	93	+8 −5	95	+6 −4	84	+6 −3	28.9	+4 −.3
10	J79-GE-10/17/19, A/B, Tall Stack, 7° Wall Angle	*3265	+8 −10	318	+62 −34	559	+87 −57	21	+2 −2	23	+1 −1	138	+16 −16	142	+16 −14	190	+13 −52	19.1	+2.3 −1.9
11	J79-GE-10/17/19, A/B, Tall Stack, 3.5° Wall Angle	*3262	+4 −5	355	+22 −38	614	+34 −35	33	+1 −2	34	+2 −2	150	+10 −16	157	+10 −19	141	+7 −17	32.8	+3.9 −3.4
12	J79-GE-10/17/19, A/B, Tall Stack, 0° Wall Angle	*3261	+8 −5	370	+38 −35	633	+51 −52	39	+2 −3	39	+1 −3	148	+11 −17	152	+13 −22	139	+13 −19	30.9	+ .8 −.6
13	J79-GE-10/17/19, A/B, Short Stack, 0° Wall Angle	*3262	+15 −12	352	+86 −40	616	+92 −56	29	+2 −1	30	+2 −1	141	+40 −45	144	+42 −44	128	+35 −42	22.1	+.6 −.6
14	J79-GE-10/17/19, A/B, Short Stack, 3.5° Wall Angle	*3258	+11 −26	327	+39 −32	581	+50 −47	29	+0 −1	30	+2 −0	133	+24 −16	135	+23 −15	127	+20 −12	23.9	+.7 −.5
15	J79-GE-10/17/19, A/B, Short Stack, 7° Wall Angle	*3263	+15 −11	321	+43 −31	553	+61 −42	22	+2 −1	28	+5 −3	165	+23 −20	168	+21 −17	204	+1 −1	18.9	+1.3 −1.3

*Calculated Values Based on Measured Air and Fuel Flow and Burner Efficienty of 95%.

4. EXHAUST STACK

a. Tables 11, 12 and 13 are tabulations of the average temperatures recorded at the exhaust stack inside aft wall, sidewall and forward wall, respectively, for all runs at each model configuration. Also shown are the minimum and maximum deviation from that average. The large deviations are not an indication of instrumentation accuracy or setup repeatability, but rather of the turbulent nature of the mixing process. Also, once the flow leaves the end of the Coanda surface, the higher energy portion tries to attach to one of the stack walls and not always the same one. This causes that particular wall to record higher surface temperatures than the other three.

b. The data for configurations with military rated thrust (MRT) primary jet conditions indicate very low stack surface temperatures. The configuration without the wall partition between the two secondary air chambers produced slightly higher exhaust stack temperatures. It was shown previously that the presence of the partition created no detrimental flow conditions in the lower enclosure; therefore, the removal of that wall will not be considered further. For configurations with the partition present and MRT engine conditions, the average temperatures recorded ranged from 116°F to 253°F with the highest individual temperature recorded being 271°F.

c. The data for configurations with afterburning (A/B) primary jet conditions show higher stack inside surface temperatures, yet still well below the 1000°F design goal for metal components. The average temperatures within the stack ranged from 203°F to 644°F with the highest individual temperature recorded being 741°F. The aft stack wall was consistently the hottest with some local hot areas appearing on the forward wall. This is due to the narrow (fore-aft) exhaust passage of the existing standard "C" cell. The application of steel plates supported by thermal isolated standoffs to the forward and aft concrete surfaces inside the exhaust passage should keep the concrete at a temperature low enough to prevent damage.

d. At A/B conditions, the configurations with increasing exhaust stack sidewall angles indicate a slightly lower temperature near the top of the stack on all stack walls which would indicate a very slight improvement in mixing within the exhaust stack due to diffuser action. However, the temperature decrease is too small to justify the expense of fabricating the angled sidewall exhaust stack.

D. Exit Airflow Conditions

1. The conditions (velocity, temperature) of the flow as it exits the exhaust stack are an indication of the efficiency of the suppressor in promoting the mixing of primary exhaust and secondary air. In general, the better the mixing (lower exhaust velocity and temperatures) the lower the internal component temperatures and noise level.

2. Figures 47 through 54 present exit flow velocity, total temperature and Mach number profiles at the exhaust stack exit for the configurations at MRT primary jet conditions. The profiles were recorded at five positions across the stack exit, as shown on Figure 23. Rake Positions 1 and 5 were near the sidewalls and Position 3 on the centerline. The velocity profile data indicate a tendency for the flow to attach to both the sidewalls leaving the lower velocity profiles at the center. The temperature profiles, however, indicate a higher temperature flow attached to one sidewall than to the other. The 7-degree angle sidewall configuration seems to aggrevate that trend, especially with the short exhaust stack. The tall exhaust stack tends to produce more uniform exhaust flow conditions and eliminates the small areas of reverse flow seen with the short stack configuration.

3. Figures 55 through 60 present exit flow velocity, total temperature and Mach number profiles at the exhaust stack exit for the configurations at A/B primary jet conditions. These profiles show similar trends to those for data taken at MRT conditions. The flow tends to attach to the sidewalls and aft wall. The tall stack produces more uniform exit flow conditions than the short stack. Temperature profiles across the exhaust stack exit are more uniform for any given configuration than they were at MRT conditions. There seems to be no significant trends in these data due to changes in sidewall angle. However, the 0 degree sidewall configuration does seem to produce more uniform velocity exit profiles (compare Figures 55 to 57 and 58 to 60) as indicated by slightly higher velocities at the forward stack wall. This may also be indicative of a little higher quality Coanda flow attachment with the 0 degree sidewall exhaust stack.

TABLE 11: EXHAUST STACK AFT WALL INSIDE SURFACE TEMPERATURES

Configuration	Average Temperature (°F) with Maximum and Minimum Deviations							
		Thermocouple No. (See Figure 23 for Location)						
	T_{jet}	T_{37}	T_{38}	T_{39}	T_{40}	T_{41}	T_{42}	T_a
1 TF30-P-408, MRT, Tall Stack 0° Wall Angle W/O Partition	1054 +4 −4	250 +1 −0	272 +0 −1	263 +1 −1	247 +2 −3	250 +0 −0	237 +3 −2	63.0 +.1 −.1
2 TF30-P-408, MRT, Tall Stack 0° Wall Angle	1070 +6 −5	231 +21 −10	245 +20 −15	237 +19 −12	222 +18 −8	176 +1 −1	214 +17 −10	51.5 +.6 −.3
3 TF30-P-408, MRT, Tall Stack 3.5° Wall Angle	1066 +7 −8	194 +30 −14	213 +33 −17	207 +30 −15	193 +27 −12	198 +26 −12	187 +29 −12	34.6 +.5 −.8
4 TF30-P-408, MRT, Tall Stack 7° Wall Angle	1067 +4 −5	219 +12 −11	242 +12 −13	237 +13 −12	226 +12 −13	230 +12 −9	227 +8 −9	48.4 +2.2 −2.7
5 TF30-P-408, MRT, Short Stack 7° Wall Angle	1066 +7 −7	222 +27 −17	237 +34 −19	230 +32 −17	213 +27 −14			38.1 +1.4 −1.0
6 TF30-P-408, MRT, Short Stack 3.5° Wall Angle	1069 +8 −7	214 +22 −27	229 +25 −26	224 +22 −26	212 +19 −20			32.8 +2.0 −1.0
7 TF30-P-408, MRT, Short Stack 0° Wall Angle	1066 +3 −1	244 +9 −12	253 +9 −9	244 +9 −9	226 +7 −6			50.5 +.3 −.6
8 J79-GE-10/17/19, MRT, Short Stack, 0° Wall Angle	1202 +2 −2	226 +28 −16	230 +30 −23	222 +29 −22	202 +24 −19			28.5 +.5 −.5
9 J79-GE-10/17/19, MRT, Tall Stack, 0° Wall Angle	1206 +4 −2	203 +13 −12	208 +18 −12	201 +16 −12	184 +12 −16	192 +57 −34	175 +16 −23	28.9 +.4 −.3
10 J79-GE-10/17/19, A/B, Tall Stack, 7° Wall Angle	*3265 +8 −10	535 +70 −42	580 +87 −53	565 +80 −50	540 +72 −43	542 +74 −47	534 +55 −59	19.1 +2.3 −1.9
11 J79-GE-10/17/19, A/B, Tall Stack, 3.5° Wall Angle	*3262 +4 −5	577 +23 −39	604 +39 −37	586 +35 −39	555 +26 −36	552 +33 −32	528 +31 −34	32.8 +3.9 −3.4
12 J79-GE-10/17/19, A/B, Tall Stack, 0° Wall Angle	*3261 +8 −5	593 +42 −56	622 +53 −68	596 +51 −69	558 +48 −65	551 +15 −22	522 +46 −64	30.9 +.8 −.6
13 J79-GE-10/17/19, A/B, Short Stack, 0° Wall Angle	*3262 +15 −12	586 +110 −87	619 +126 −83	594 +125 −89	542 +115 −84			22.1 +.6 −.6
14 J79-GE-10/17/19, A/B, Short Stack, 3.5° Wall Angle	*3258 +11 −26	556 +58 −47	597 +77 −62	579 +78 −63	532 +72 −58			23.9 +.7 −.5
15 J79-GE-10/17/19, A/B, Short Stack, 7° Wall Angle	*3263 +15 −11	541 +66 −38	575 +81 −47	560 +29 −47	527 +74 −42			18.9 +1.3 −1.3

* Calculated Values Based on Measured Air and Fuel Flow and Burner Efficienty of 95%.

TABLE 12: EXHAUST STACK SIDEWALL INSIDE SURFACE TEMPERATURES

	Configuration	Average Temperature (°F) with Maximum and Minimum Deviations							
			Thermocouple No. (See Figure 23 for Location)						
		T_{jet}	T_{31}	T_{32}	T_{33}	T_{34}	T_{35}	T_{36}	T_a
1	TF30-P-408, MRT, Tall Stack 0° Wall Angle W/O Partition	1054 +4 −4	196 +0 −0	216 +1 −1	220 +2 −2	215 +4 −4	242 +1 −0	241 +0 −1	63.0 +.1 −.1
2	TF30-P-408, MRT, Tall Stack 0° Wall Angle	1070 +6 −5	175 +15 −9	194 +18 −8	199 +19 −8	194 +20 −9	219 +18 −13	217 +18 −13	51.5 +.6 −.3
3	TF30-P-408, MRT, Tall Stack 3.5° Wall Angle	1066 +7 −8	146 +27 −14	167 +27 −14	168 +25 −13	160 +26 −13	190 +29 −14	185 +32 −13	34.6 +.5 −.8
4	TF30-P-408, MRT, Tall Stack 7° Wall Angle	1067 +4 −5	173 +11 −15	197 +12 −15	194 +12 −18	188 +14 −21	218 +13 −12	214 +13 −12	48.4 +2.2 −2.7
5	TF30-P-408, MRT, Short Stack 7° Wall Angle	1066 +7 −7	183 +28 −16	194 +23 −14	185 +25 −14	169 +26 −13			38.1 +1.4 −1.0
6	TF30-P-408, MRT, Short Stack 3.5° Wall Angle	1069 +8 −7	161 +24 −28	177 +24 −26	175 +22 −25	165 +22 −23			32.8 +2.0 −1.0
7	TF30-P-408, MRT, Short Stack 0° Wall Angle	1066 +3 −1	187 +7 −11	205 +7 −9	208 +8 −9	199 +8 −8			50.5 +.3 −.6
8	J79-GE-10/17/19, MRT, Short Stack, 0° Wall Angle	1202 +2 −2	183 +26 −17	187 +26 −17	185 +24 −15	176 +22 −13			28.5 +.5 −.5
9	J79-GE-10/17/19, MRT, Tall Stack, 0° Wall Angle	1206 +4 −2	160 +11 −11	166 +12 −13	166 +12 −13	162 +11 −15	181 +16 −19	178 +16 −22	28.9 +.4 −.3
10	J79-GE-10/17/19, A/B, Tall Stack, 7° Wall Angle	*3265 +8 −10	378 +64 −36	422 +62 −40	406 +59 −42	386 +52 −39	477 +82 −46	464 +79 −46	19.1 +2.3 −1.9
11	J79-GE-10/17/19, A/B, Tall Stack, 3.5° Wall Angle	*3262 +4 −5	380 +26 −37	432 +30 −37	439 +27 −36	425 +24 −37	511 +37 −37	497 +37 −36	32.8 +3.9 −3.4
12	J79-GE-10/17/19, A/B, Tall Stack, 0° Wall Angle	*3261 +8 −5	380 +38 −49	439 +42 −58	455 +40 −58	445 +43 −60	524 +51 −63	508 +51 −65	30.9 +.8 −.6
13	J79-GE-10/17/19, A/B, Short Stack, 0° Wall Angle	*3262 +15 −12	367 +95 −77	430 +107 −88	449 +108 −90	427 +104 −86			22.1 +.6 −.6
14	J79-GE-10/17/19, A/B, Short Stack, 3.5° Wall Angle	*3258 +11 −26	358 +51 −30	421 +65 −41	430 +69 −47	406 +71 −48			23.9 +.7 −.5
15	J79-GE-10/17/19, A/B, Short Stack, 7° Wall Angle	*3263 +15 −11	390 +59 −37	438 +64 −37	427 +63 −35	396 +59 −36			18.9 +1.3 −1.3

* Calculated Values Based on Measured Air and Fuel Flow and Burner Efficiency of 95%.

TABLE 13: EXHAUST STACK FORWARD WALL INSIDE SURFACE TEMPERATURES

	Configuration	Average Temperature (°F) with Maximum and Minimum Deviations							
		Thermocouple No. (See Figure 23 for Location)							
		T_{jet}	T_{25}	T_{26}	T_{27}	T_{28}	T_{29}	T_{30}	T_a
1	TF30-P-408, MRT, Tall Stack 0° Wall Angle W/O Partition	1054 +4 −4	220 +4 −4	205 +4 −4	202 +4 −4	191 +5 −4	208 +4 −4	208 +4 −4	63.0 +.1 −.1
2	TF30-P-408, MRT, Tall Stack 0° Wall Angle	1070 +6 −5	198 +16 −9	183 +17 −8	181 +17 −9	174 +19 −9	189 +20 −10	189 +19 −10	51.5 +.6 −.3
3	TF30-P-408, MRT, Tall Stack 3.5° Wall Angle	1066 +7 −8	139 +16 −8	146 +24 −11	141 +26 −10	133 +15 −12	148 +31 −13	147 +31 −14	34.6 +.5 −.8
4	TF30-P-408, MRT, Tall Stack 7° Wall Angle	1067 +4 −5	116 +8 −9	180 +11 −12	176 +12 −14	169 +10 −15	186 +12 −14	185 +12 −15	48.4 +2.2 −2.7
5	TF30-P-408, MRT, Short Stack 7° Wall Angle	1066 +7 −7	116 +13 −8	168 +25 −13	159 +24 −11	139 +23 −10			38.1 +1.4 −1.0
6	TF30-P-408, MRT, Short Stack 3.5° Wall Angle	1069 +8 −7	159 +18 −18	163 +20 −25	159 +23 −29	146 +20 −22			32.8 +2.0 −1.0
7	TF30-P-408, MRT, Short Stack 0° Wall Angle	1066 +3 −1	214 +8 −9	197 +9 −12	193 +10 −12	179 +8 −8			50.5 +.3 −.6
8	J79-GE-10/17/19, MRT, Short Stack, 0° Wall Angle	1202 +2 −2	188 +18 −15	185 +29 −19	176 +27 −17	160 +23 −16			28.5 +.5 −.5
9	J79-GE-10/17/19, MRT, Tall Stack, 0° Wall Angle	1206 +4 −2	165 +4 −12	160 +14 −14	153 +12 −14	141 +11 −17	152 +14 −24	149 +15 −27	28.9 +.4 −.3
10	J79-GE-10/17/19, A/B, Tall Stack, 7° Wall Angle	*3265 +8 −10	203 +21 −16	403 +58 −39	439 +29 −36	353 +46 −32	388 +62 −40	378 +60 −39	19.1 +2.3 −1.9
11	J79-GE-10/17/19, A/B, Tall Stack, 3.5° Wall Angle	*3262 +4 −5	303 +14 −25	380 +20 −34	449 +35 −39	362 +21 −37	401 +32 −39	396 +35 −39	32.8 +3.9 −3.4
12	J79-GE-10/17/19, A/B, Tall Stack, 0° Wall Angle	*3261 +8 −5	422 +34 −55	408 +40 −56	611 +20 −35	390 +44 −60	426 +49 −65	420 +48 −66	30.9 +.8 −.6
13	J79-GE-10/17/19, A/B, Short Stack, 0° Wall Angle	*3262 +15 −12	435 +105 −93	412 +114 −89	422 +98 −113	375 +105 −86			22.1 +.6 −.3
14	J79-GE-10/17/19, A/B, Short Stack, 3.5° Wall Angle	*3258 +11 −26	311 +41 −29	391 +73 −50	644 +96 −128	338 +66 −46			23.9 +.7 −.5
15	J79-GE-10/17/19, A/B, Short Stack, 7° Wall Angle	*3263 +15 −11	221 +57 −22	411 +66 −40	499 +150 −67	343 +57 −33			18.9 +1.3 −1.3

* Calculated Values Based on Measured Air and Fuel Flow and Burner Efficiency of 95%

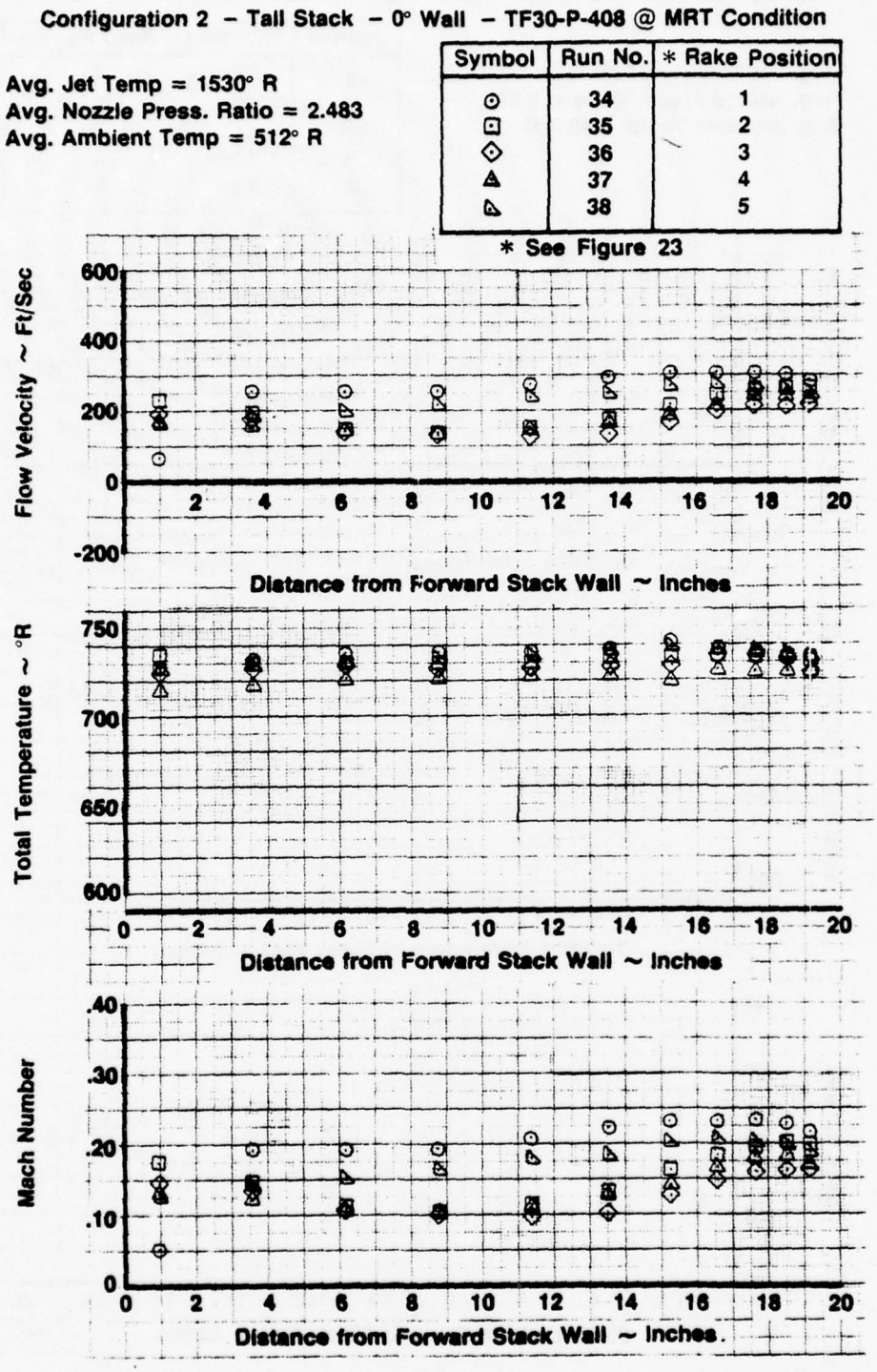

FIGURE 47: EXIT FLOW VELOCITY, TOTAL TEMPERATURE AND MACH NUMBER PROFILES, CONFIGURATION 2, TALL STACK, 0° WALL ANGLE, TF30-P-408 AT MRT CONDITION

Configuration 3 – Tall Stack – 3.5° Wall – TF30-P-408 @ MRT Condition

Avg. Jet Temp = 1526° R
Avg. Nozzle Press. Ratio = 2.499
Avg. Ambient Temp = 495° R

Symbol	Run No.	* Rake Position
⊙	13	1
⊡	12	2
◇	14	3
△	15	4
◺	16	5

* See Figure 23

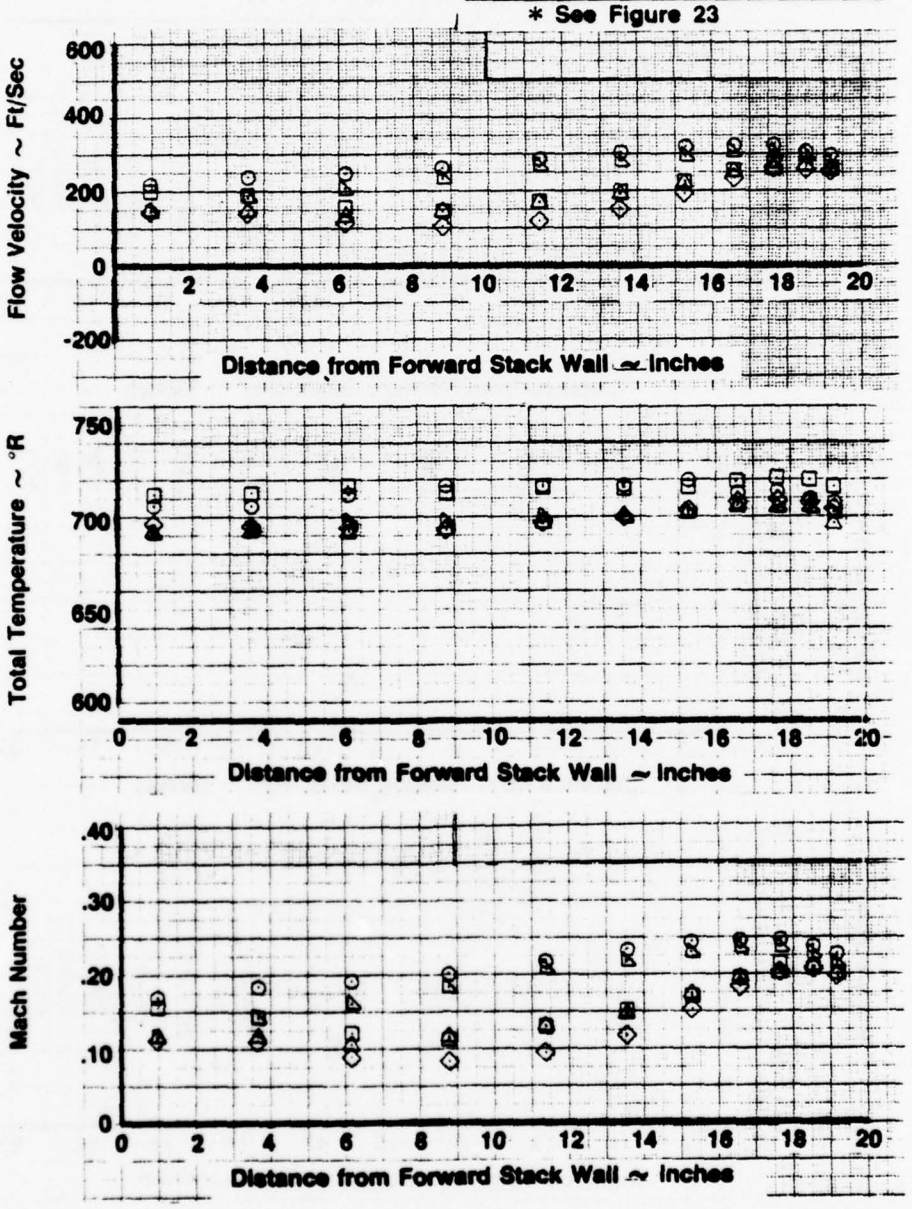

FIGURE 48: EXIT FLOW VELOCITY, TOTAL TEMPERATURE AND MACH NUMBER PROFILES, CONFIGURATION 3, TALL STACK WITH 3.5° SIDEWALL ANGLE, TF30-P-408 AT MRT CONDITION

Configuration 4 – Tall Stack – 7° Wall – TF30-P-408 @ MRT Condition

Avg. Jet Temp = 1528° R
Avg. Nozzle Press. Ratio = 2.491
Avg. Ambient Temp = 508° R

Symbol	Run No.	* Rake Position
⊙	33	1
⊡	32	2
◇	31	3
△	29	4
◺	30	5

* See Figure 23

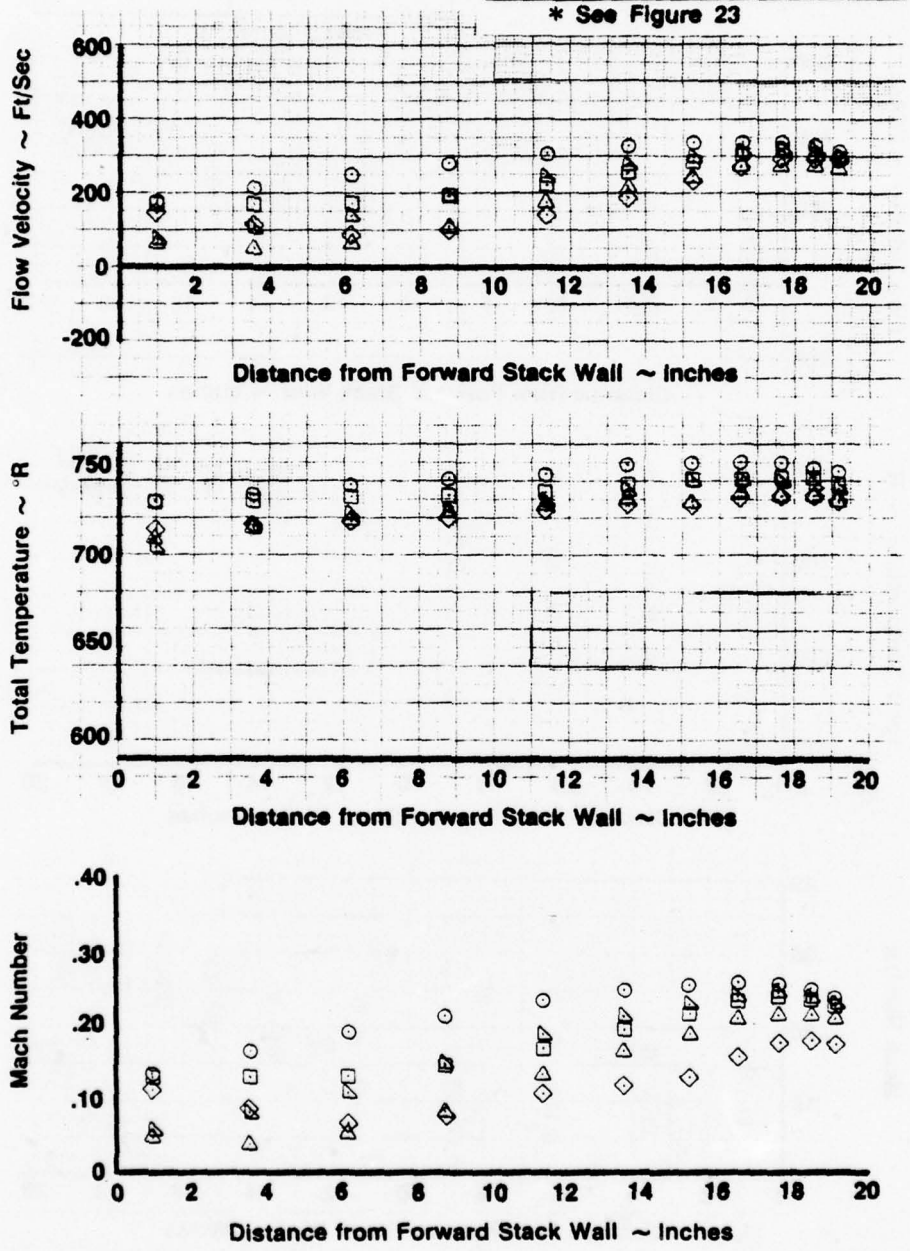

FIGURE 49: EXIT FLOW VELOCITY, TOTAL TEMPERATURE AND MACH NUMBER PROFILES, CONFIGURATION 4, TALL STACK, 7° WALL ANGLE, TF30-P-408 AT MRT CONDITION

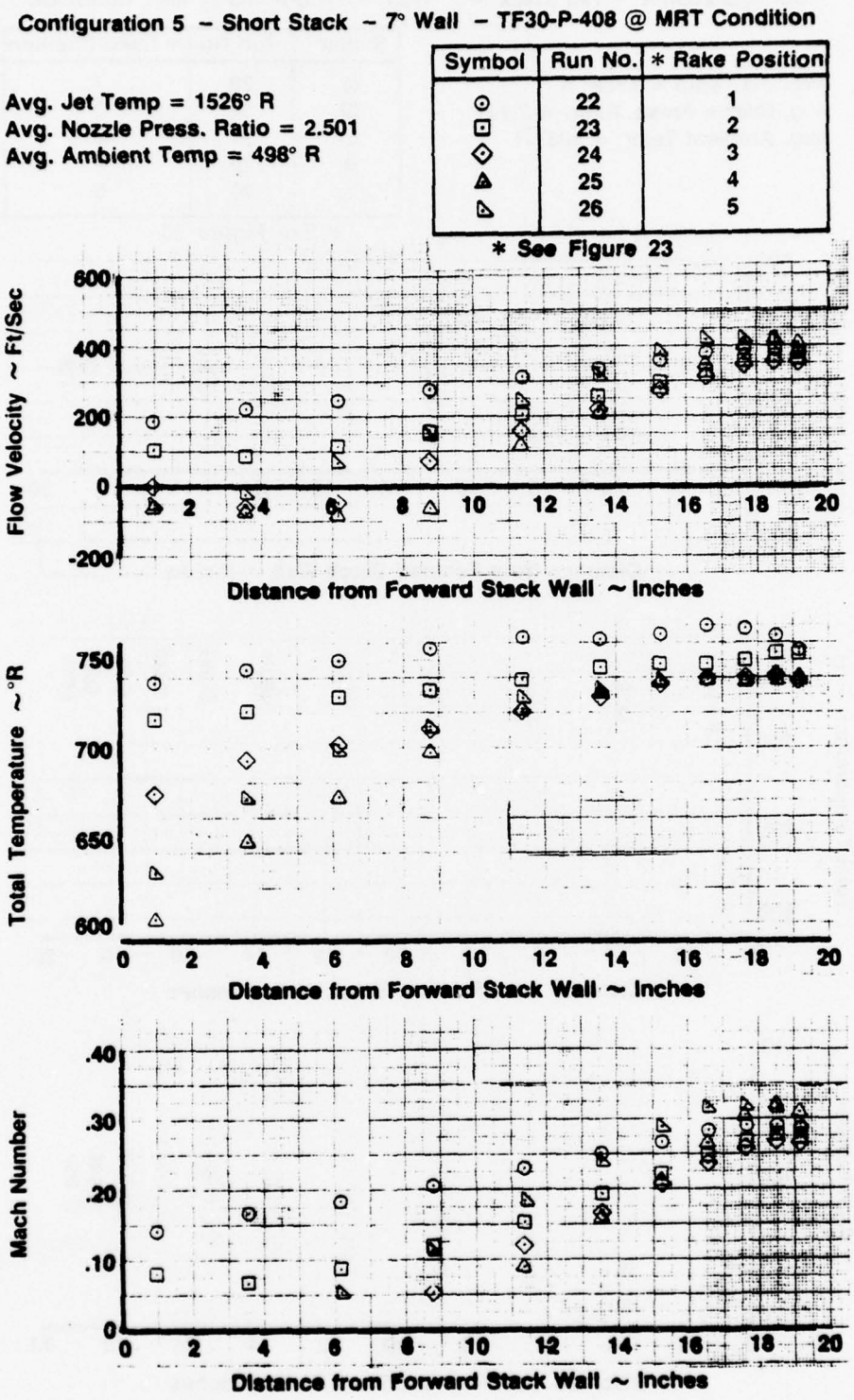

FIGURE 50: EXIT FLOW VELOCITY, TOTAL TEMPERATURE AND MACH NUMBER PROFILES, CONFIGURATION 5, TALL STACK, 7° WALL ANGLE, TF30-P-408 AT MRT CONDITION

Configuration 6 – Short Stack – 3.5° Wall – TF30-P-408 @ MRT Condition

Avg. Jet Temp. = 1529°R
Avg. Nozzle Press. Ratio = 2.492
Avg. Ambient Temp = 493° R

Symbol	Run No.	* Rake Position
○	21	1
□	20	2
◇	19	3
△	18	4
◺	17	5

* See Figure 23

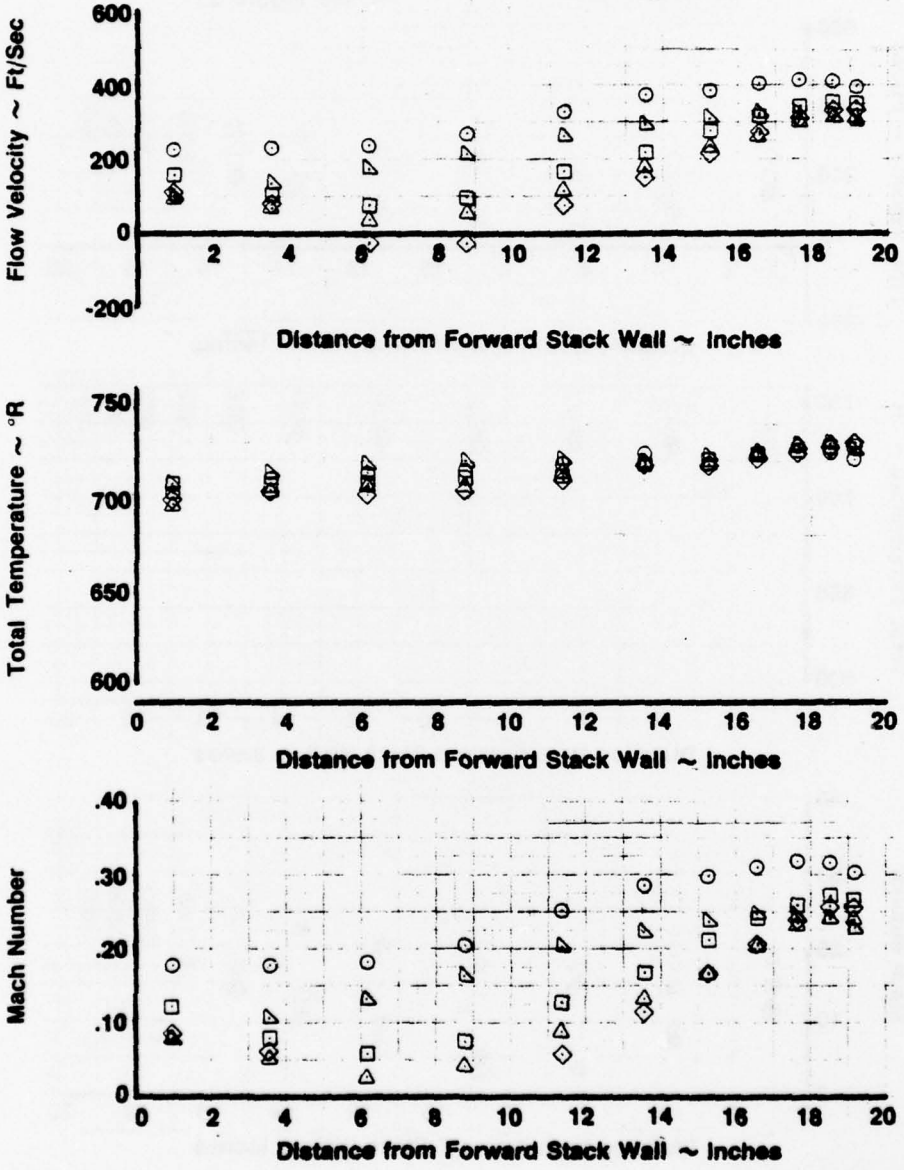

FIGURE 51: EXIT FLOW VELOCITY, TOTAL TEMPERATURE AND MACH NUMBER PROFILES, CONFIGURATION 6, TALL STACK, 3.5° WALL ANGLE, TF30-P-408 AT MRT CONDITION

Configuration 7 – Short Stack – 0° Wall – TF30-P-408 @ MRT Condition

Avg. Jet Temp = 1527° R
Avg. Nozzle Press. Ratio = 2.490
Avg. Ambient Temp = 510° R

Symbol	Run No.	* Rake Position
⊙	43	1
⊡	42	2
◇	41	3
△	40	4
◺	39	5

* See Figure 23

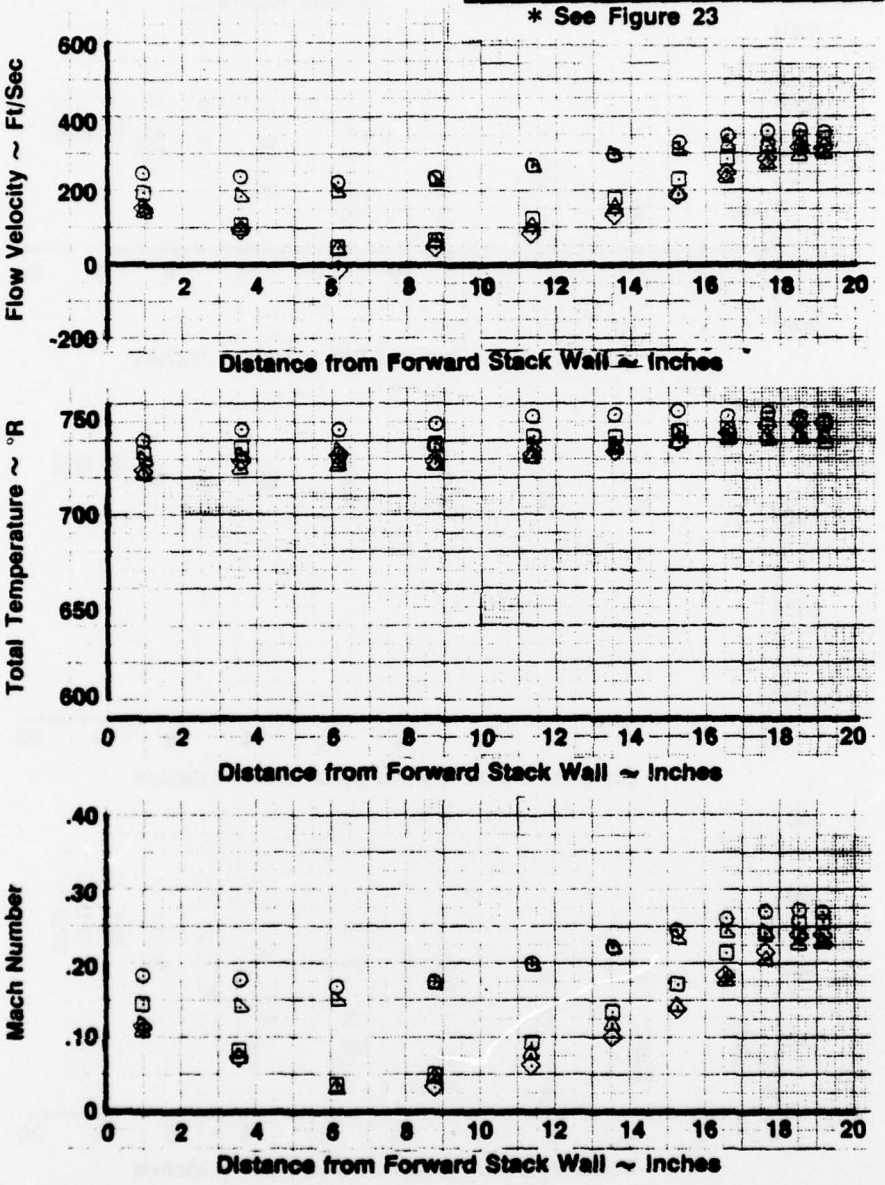

FIGURE 52: EXIT FLOW VELOCITY, TOTAL TEMPERATURE AND MACH NUMBER PROFILES CONFIGURATION 7, SHORT STACK WITH 0° WALL ANGLE, TF30-P-408 AT MRT CONDITION

Configuration 8 – Short Stack – 0° Wall – J79-GE-10/17/19 @ MRT Condition

Avg. Jet Temp = 1661° R
Avg. Nozzle Press. Ratio = 3.056
Avg. Ambient Temp = 488° R

Symbol	Run No.	* Rake Position
○	44	1
□	45	2
◇	46	3
△	47	4
▷	48	5

* See Figure 23

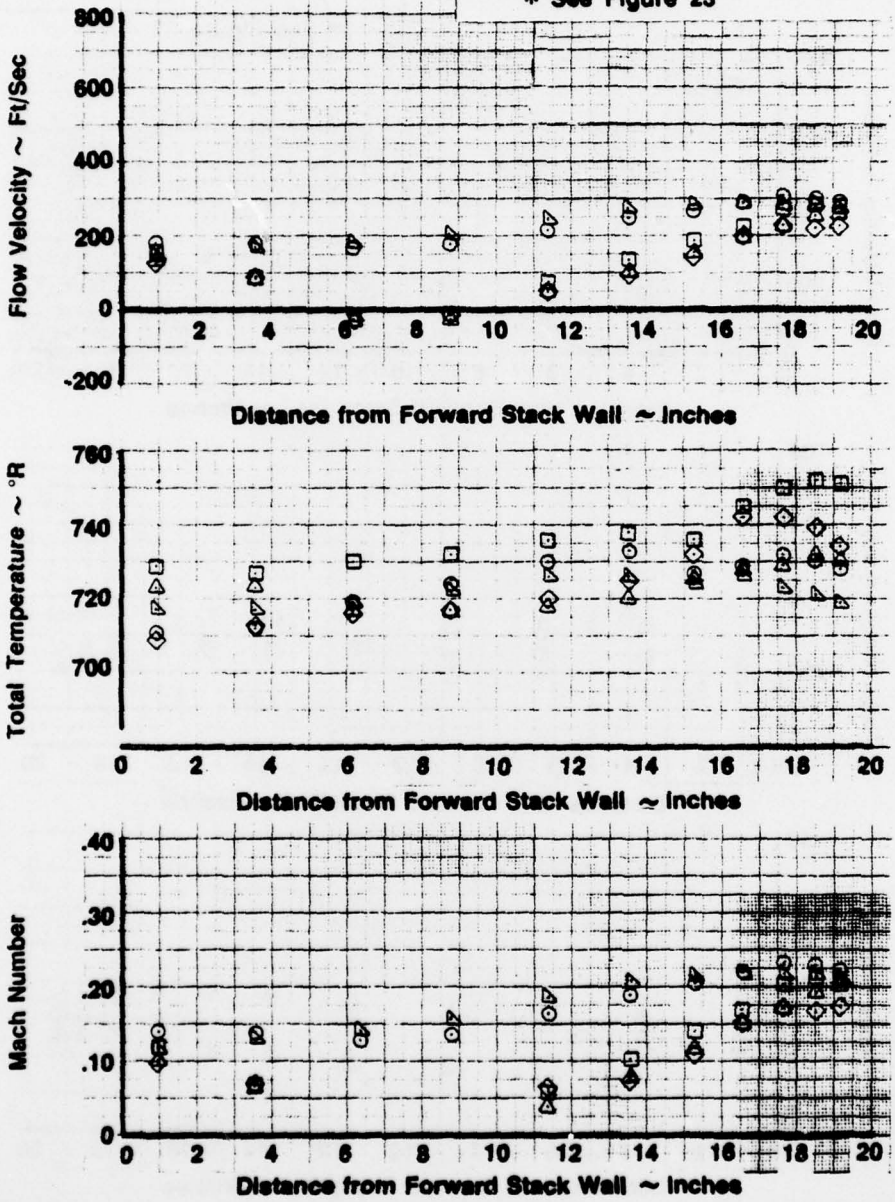

FIGURE 53: EXIT FLOW VELOCITY, TOTAL TEMPERATURE AND MACH NUMBER PROFILES, CONFIGURATION 8, SHORT STACK, 0° WALL ANGLE, J79-GE-10/17/19 AT MRT CONDITION

Configuration 9 – Tail Stack – 0° Wall – J79-GE-10/17/19 @ MRT Condition

Average Jet Temperature = 1666°R
Average Nozzle Pressure Ratio = 3.038
Average Ambient Temperature = 489°R

Symbol	Run No.	* Rake Position
⊙	53	1
⊡	52	2
◇	51	3
△	50	4
▷	49	5

* See Figure 23

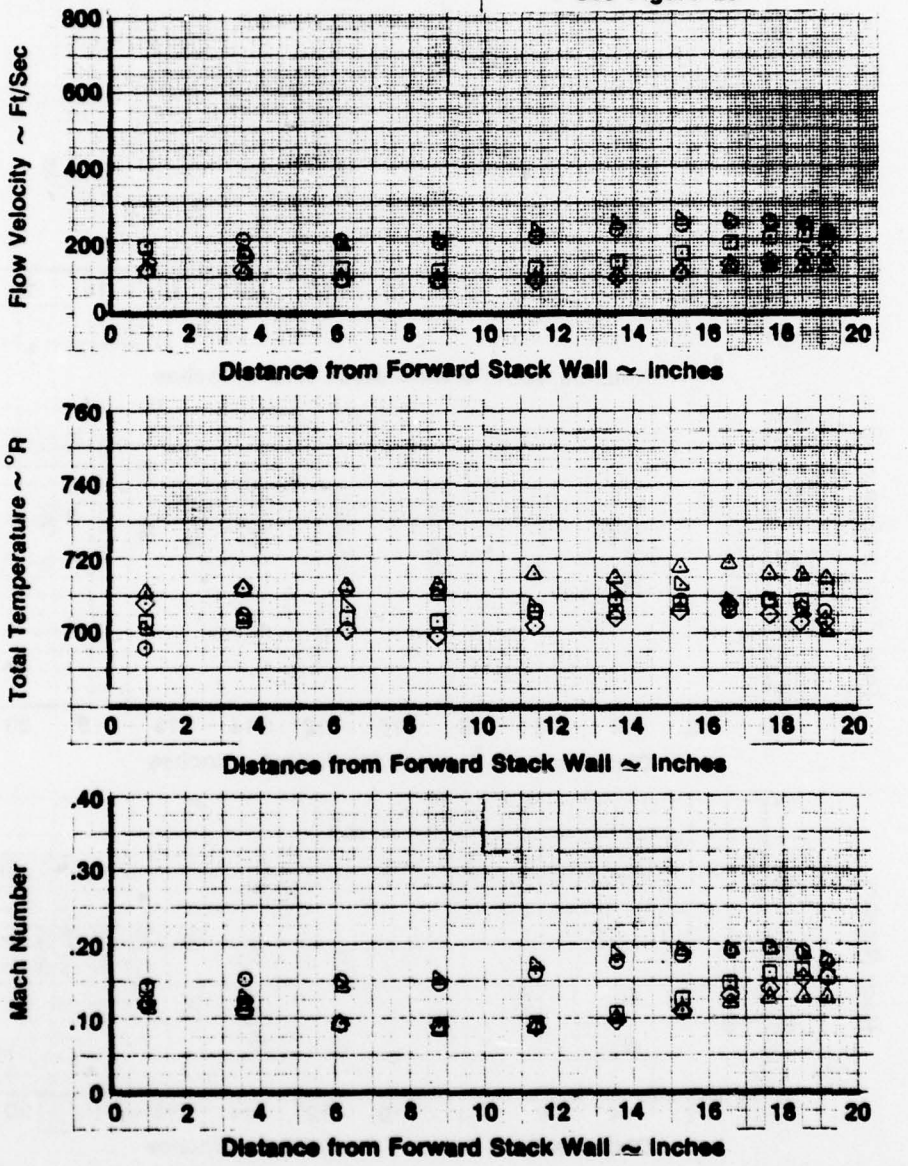

FIGURE 54: EXIT FLOW VELOCITY, TOTAL TEMPERATURE AND MACH NUMBER PROFILES, CONFIGURATION 9, TALL STACK WITH 0° WALL ANGLE, J79-GE-101719 AT MRT CONDITION

Configuration 10 – Tall Stack – 7° Wall – J79-GE-10/17/19 @ A/B Condition

Average Jet Temperature = 3725°R
Average Nozzle Pressure Ratio = 2.872
Average Ambient Temperature = 479°R

Symbol	Run No.	* Rake Position
○	80	1
□	81	2
◇	82	3
△	83	4
◁	84	5

* See Figure 23

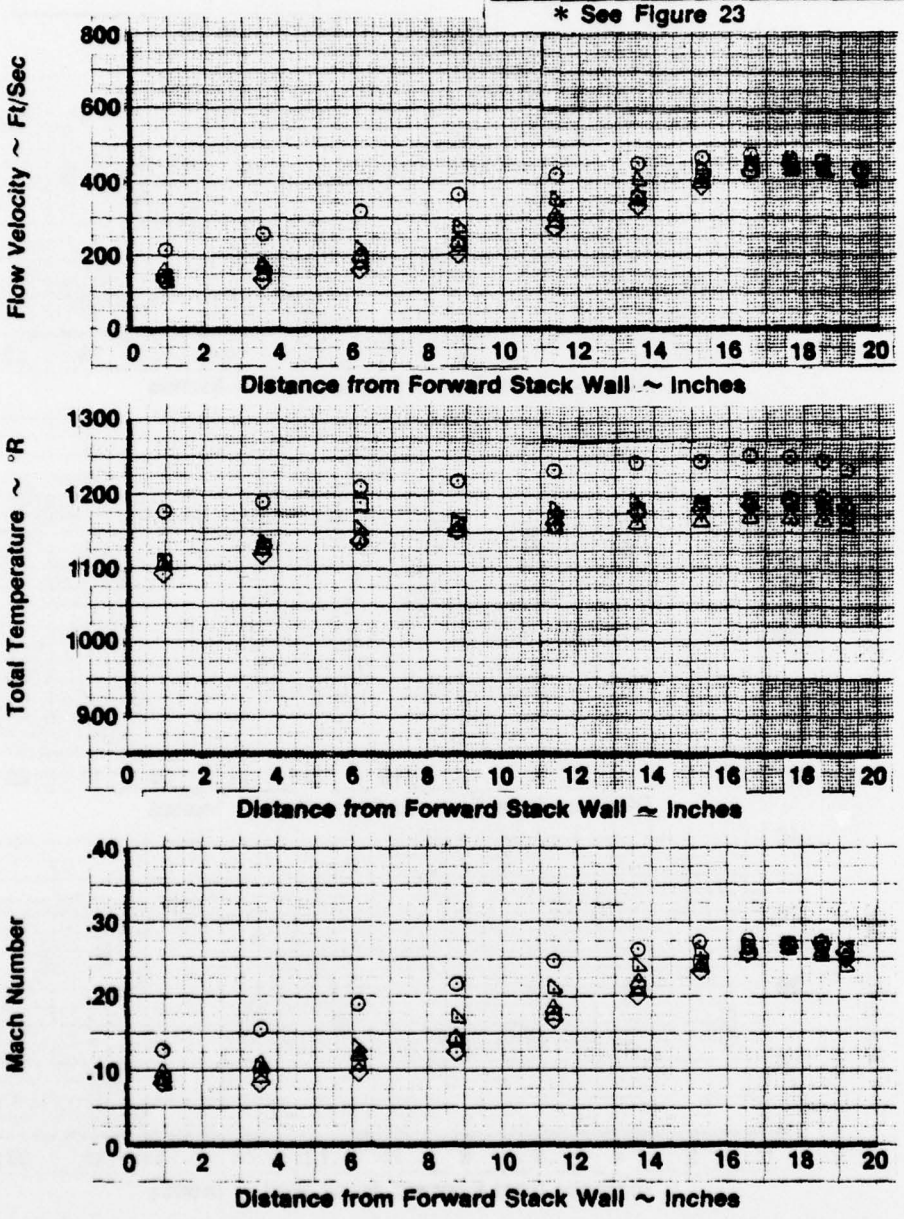

FIGURE 55: EXIT FLOW VELOCITY, TOTAL TEMPERATURE AND MACH NUMBER PROFILES, CONFIGURATION 10, TALL STACK, 7° WALL ANGLE, J79-GE-10/17/19 AT A/B CONDITION

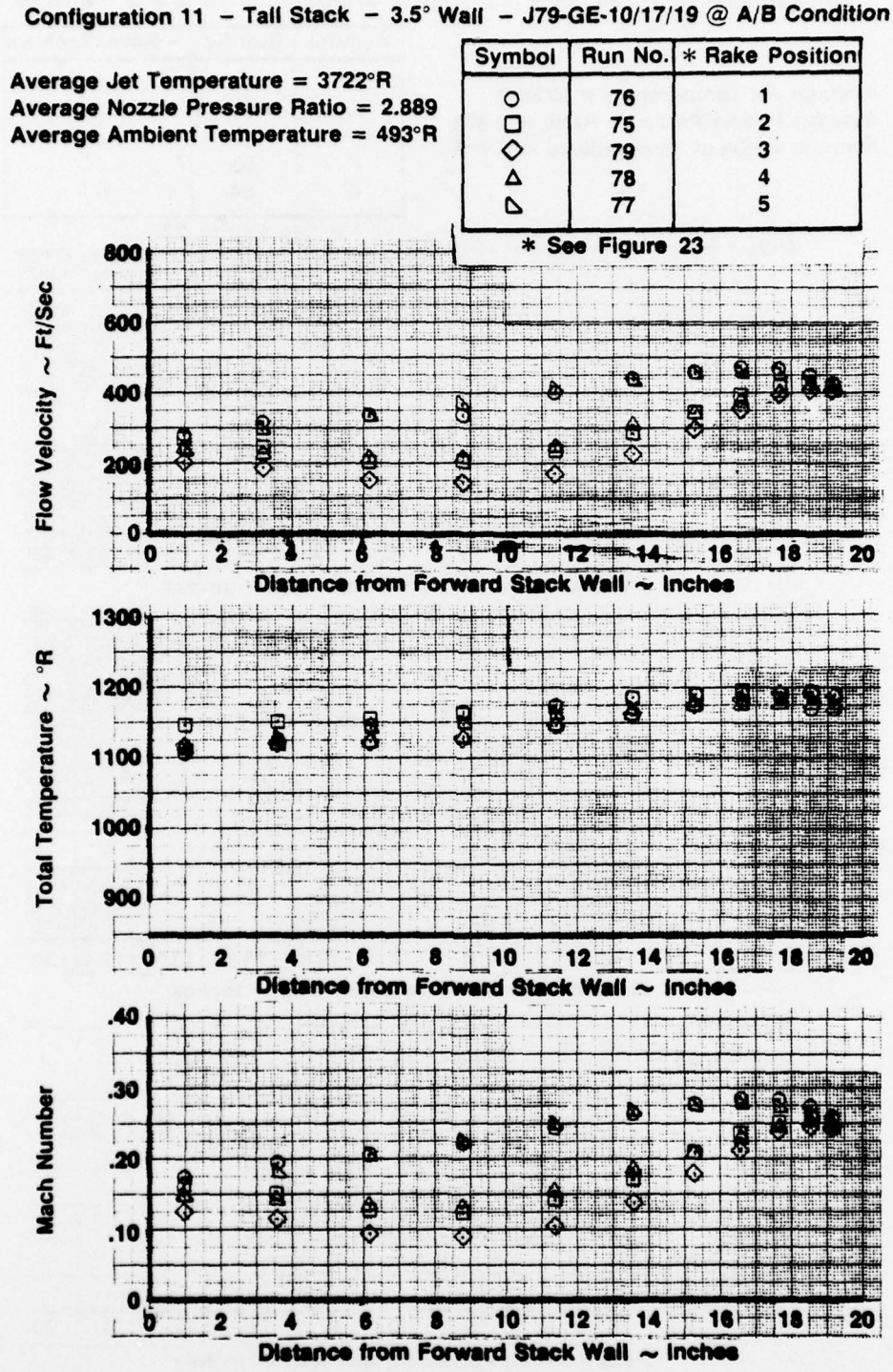

FIGURE 56: EXIT FLOW VELOCITY, TOTAL TEMPERATURE AND MACH NUMBER PROFILES, CONFIGURATION 11, TALL STACK WITH 3.5° WALL ANGLE, J79-GE-10/17/19 AT A/B CONDITION

Configuration 12 – Tall Stack – 0° Wall – J79-GE-10/17/19 @ A/B Condition

Average Jet Temperature = 3721°R
Average Nozzle Pressure Ratio = 2.848
Average Ambient Temperature = 491°R

Symbol	Run No.	* Rake Position
○	56	1
□	57	2
◇	58	3
△	59	4
◺	60	5

* See Figure 23

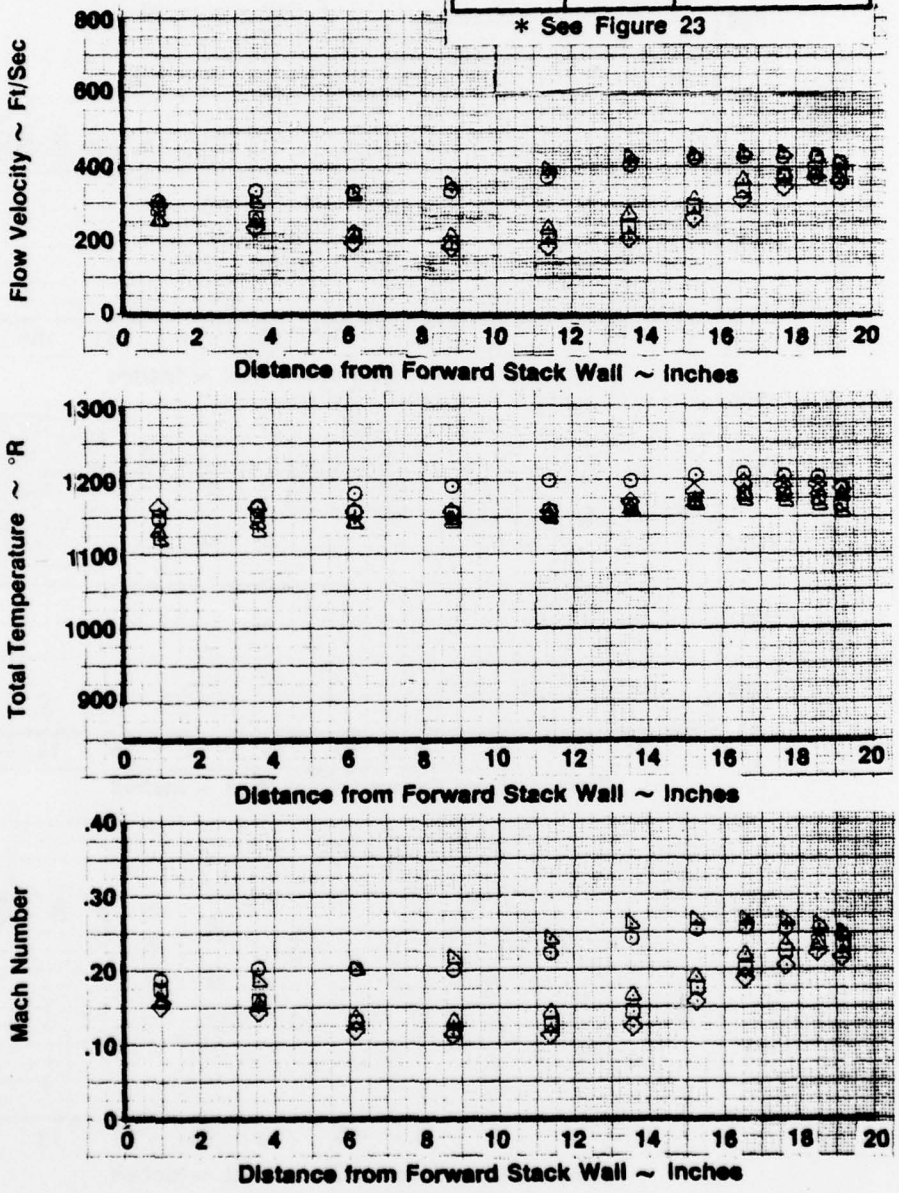

FIGURE 57: EXIT FLOW VELOCITY, TOTAL TEMPERATURE AND MACH NUMBER PROFILES, CONFIGURATION 12, TALL STACK, 0° WALL ANGLE, J79-GE-10/17/19 AT A/B CONDITION

Configuration 13 – Short Stack – 0° Wall Angle – J79-GE-10/17/19 @ A/B Condition

Average Jet Temperature = 3723°R
Average Nozzle Pressure Ratio = 2.879
Average Ambient Temperature = 482°R

Symbol	Run No.	* Rake Position
○	65	1
□	64	2
◇	63	3
△	62	4
◺	61	5

* See Figure 23

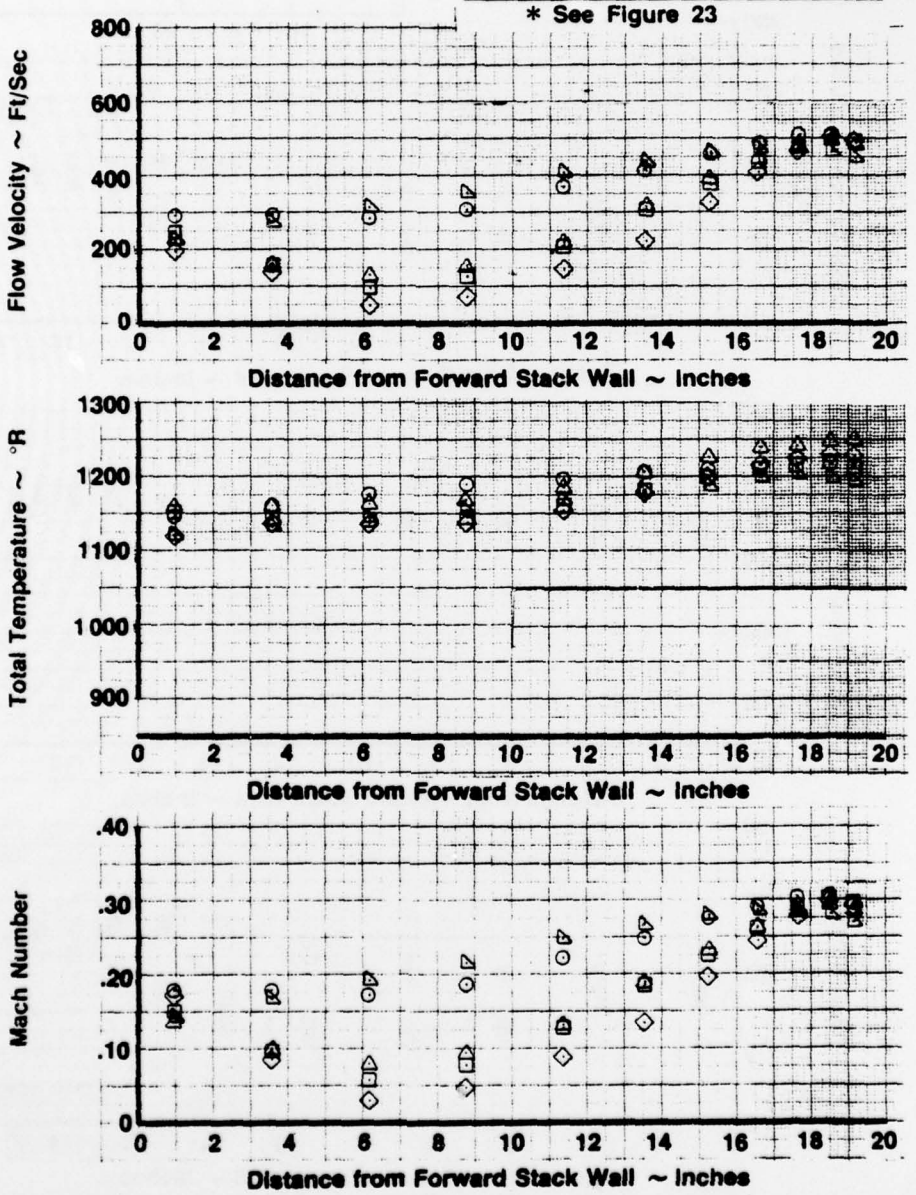

FIGURE 58: EXIT FLOW VELOCITY, TOTAL TEMPERATURE AND MACH NUMBER PROFILES, CONFIGURATION 13, SHORT STACK, WITH 0° WALL ANGLE, J79-GE-10/17/19 AT A/B CONDITION

Configuration 14 – Short Stack – 3.5° Wall Angle – J79-GE-10/17/19 @ A/B Condition

Average Jet Temperature = 3718°R
Average Nozzle Pressure Ratio = 2.880
Average Ambient Temperature = 484°R

Symbol	Run No.	* Rake Position
○	66	1
□	67	2
◇	68	3
△	69	4
◺	70	5

* See Figure 23

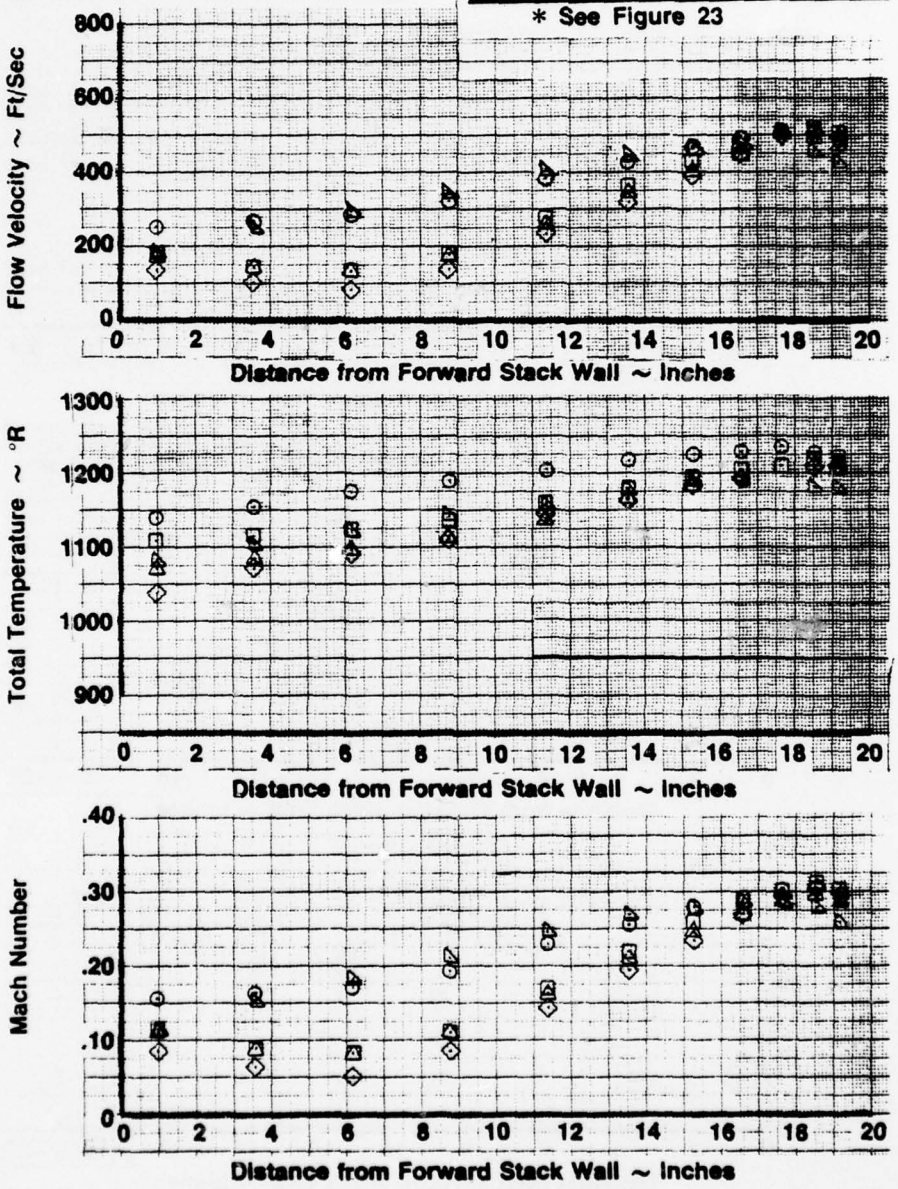

FIGURE 59: EXIT FLOW VELOCITY, TOTAL TEMPERATURE AND MACH NUMBER PROFILES, CONFIGURATION 14, SHORT STACK WITH 3.5° SIDEWALL ANGLE, J79-GE-10/17/19 AT A/B CONDITION

Configuration 15 – Short Stack – 7° Wall – J79-GE-10/17/19 @ A/B Condition

Average Jet Temperature = 3723°R
Average Nozzle Pressure Ratio = 2.882
Average Ambient Temperature = 479°R

Symbol	Run No.	* Rake Position
○	90	1
□	86	2
◇	87	3
△	88	4
◺	89	5

* See Figure 23

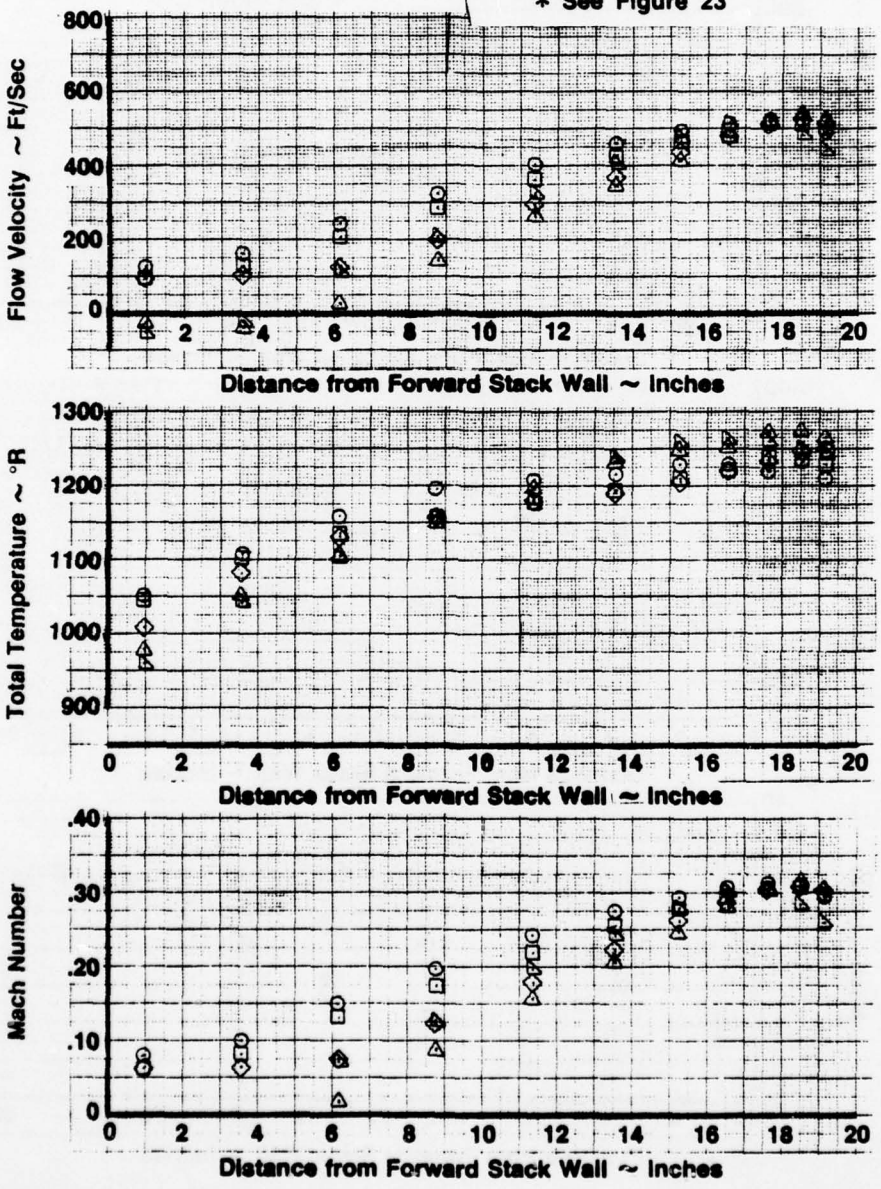

FIGURE 60: EXIT FLOW VELOCITY, TOTAL TEMPERATURE AND MACH NUMBER PROFILES, CONFIGURATION 15, SHORT STACK, 7° WALL ANGLE, J79-GE-10/17/19 AT A/B CONDITION

V. CONCLUSIONS

The following conclusions are drawn from the model scale tests of the proposed "C" cell retrofit configuration:

- The presence of the partition (wall with nine- by nine-foot opening) between the old spray chamber and exhaust chamber was shown to cause no detrimental flow problems and need not be removed to install and use the Coanda retrofit configuration (Paragraph IV.A). The presence of the wall creates flow patterns that actually provide additional Coanda surface and ejector cooling (Paragraphs IV.A.2. and IV.A.3.).

- The addition of the exhaust stack extension (tall stack) produced no undesirable results in the test data; in fact, it causes an increase in secondary airflow entrainment over the short stack configurations (Paragraph IV.B.1.).

- Variations of the exhaust stack inner sidewall angle from vertical to produce a diffuser effect produced no appreciable benefit. At the highest angle of 7 degrees from vertical, the secondary airflow was decreased, probably due to the reduction of flow area at the entrance to the exhaust stack with that configuration (Paragraph IV.B.2). Ejector and Coanda surface temperatures are not appreciably affected by either changes in stack height or stack sidewall angle (Paragraph IV.C.1. and IV.C.2.). However, they may be a slight advantage in flow attachment with the 0 degree angle stack sidewall (Paragraph IV.D.3.).

- Lower enclosure sidewall temperatues indicate no treatment would be required on those walls. The aft wall, however, due to higher temperatures near the exhaust stack entrance (top), will require thermal cover plates (Paragraph IV.C.3.) such as those required on the forward and aft inner walls of the exhaust stack (Paragraph IV.C.4.).

VI. RECOMMENDATIONS

The following recommendations are made based on the results of the testing described in this report and the primary goals of the Navy Coanda ground noise suppressor program:

- Model testing should be accomplished with the goal of improving the mixing in the ejectors and Coanda flow turning. The result of improved mixing would be lower temperature and lower velocity flow through the exhaust muffler (stack). This could possibly be accomplished by widening the ejectors and Coanda surface thereby increasing the area of flow available for mixing, reducing the height of the sheet of hot flow entering the Coanda surface which, in turn, would reduce the mixing length. The wider Coanda surface would also deliver flow to the exhaust stack that resembles the exhaust stack cross section (narrow fore-to-aft and wide side-to-side).

- The recommended production configuration is basically that which is shown on the Reference (h). Configuration control drawing and described in Section II of this report, with the exception that the exhaust muffler sidewalls are to be vertical. It is recommended that the tall stack configuration be used because of acoustic requirements.

- The concrete partition (wall with nine- by nine-foot opening) between the two secondary air chambers should not be removed. This means the Coanda surface will have to be fabricated in sections for installation in the existing concrete structure.

VII. LIST OF REFERENCES

a. Ballard, R.E., Brees, D.W., and Sawdy, D.T., "Feasibility and Initial Model Studies of a Coanda/Refraction Type Noise Suppressor System," The Boeing Company, Wichita, Kansas, D3-9068, January 1973.

b. Ballard, R.E., and Armstrong, D.L., "Configuration Scale Model Studies of a Coanda/Refraction Type Noise Suppressor System," The Boeing Company, Wichita, Kansas, D3-9258, October 1973.

c. "Test Cell Experimental Program *Coanda/Refraction Noise Suppression Concept* – Advanced Development," Final Technical Report for Navy Contract N00156-74-C-1710, Navy Document Number NAEC-GSED-97, The Boeing Company, Wichita, Kansas, March 1976.

d. "Aircraft System One-Sixth Scale Model Studies, Coanda/Refraction Noise Suppression Concept – Advanced Development," Final Technical Report for Scale Model Portion of Navy Contract N00156-74-C-1710, Navy Document Number NAEC-GSED-98, The Boeing Company, Wichita, Kansas, March 1976.

e. "Jet Engine Demountable Test Cell Exhaust System Phase, Coanda/Refraction Noise Suppression Concept – Advanced Development," Technical Report for a portion of Navy Contract N00140-76-C-1229, Navy Document Number NAEC-92-112, the Boeing Wichita Company, Wichita, Kansas, April 1979.

f. "Aircraft Hush-House Exhaust System Phase, Coanda/Refraction Noise Suppression Concept – Advanced Development, Final Technical Report for Navy Contract N00140-76-C-1229, Navy Document Number NAEC-92-114, the Boeing Wichita Company, Wichita, Kansas, June 1979.

g. "Design Configuration Handbook, *Test Cell System, Coanda/Refraction Noise Suppression* Concept," Navy Document Number NAEC Design Data 92-136, April 1979.

h. NAEC-GSED Drawing 690AS200, "'C' Cell Installation Noise Suppressor System – Coanda/Refraction," dated January 20, 1977.

VIII. LIST OF ABBREVIATIONS, ACRONYMS AND SYMBOLS

A/B	Afterburning
Amb.	Ambient
A.R.	Ejector area ratio – Ratio of ejector minimum flow area to primary exhaust nozzle area.
CPU	Central processing unit
EGT	Primary jet exhaust gas total temperature
gpm	Gallons per minute
H_2O	Water
MRT	Military rated thrust
NPR	Primary nozzle pressure ratio – Ratio of primary jet total pressure to ambient pressure
P	Pressure
P_a	Ambient pressure
P_s	Static pressure
P_t	Total pressure
psia	Pounds per square inch – absolute
psid	Pounds per square inch – differential
psig	Pounds per square inch – gauge
T	Temperature
T_a	Ambient temperature
T_{jet}	Primary jet exhaust gas total temperature
w/o	Without
Ws	Secondary airflow – lbs/sec
ΔP	Differential pressure
δa	Ambient pressure (psia)/14.696
θa	Ambient temperature (°R)/518.67

DISTRIBUTION LIST

REVISION LIST

REVISION	PAGES AFFECTED	DATE OF REVISION